GRI-96/0014

Topical Report

Analysis of Microscopic Leaks in Polyethylene Gas Distribution Piping

Prepared by:
S. M. Pimputkar
J. A. Stets
D. Mangaraj
G. Clark
D. Rider
Battelle

Gas Research Institute

Distribution Business Unit
September 1996

GRI-96/0014

Analysis of Microscopic Leaks in Polyethylene Gas Distribution Piping

Topical Report

(January 1993 to January 1996)

by

Sudheer M. Pimputkar, Joseph A. Stets,
Duryodhan Mangaraj, Glenn Clark, and Dennis Rider

BATTELLE
505 King Avenue
Columbus, Ohio 43201-2693

to

GAS RESEARCH INSTITUTE
8600 West Bryn Mawr Avenue
Chicago, Illinois 60631

GRI Contract No.
5091-271-2351

GRI Project Monitor
Michael M. Mamoun
Principal Technology Manager
Distribution Business Unit

September 1996

LEGAL NOTICE

This report was prepared by Battelle as an account of work sponsored by the Gas Research Institute (GRI). Neither GRI, members of GRI, Battelle, officers, trustees, or staff of Battelle, nor any person acting on behalf of either:

a. Makes any warranty or representation, expressed or implied, with respect to the accuracy, completeness, or usefulness of the information contained in this report, or that the use of any information, apparatus, software, method, or process disclosed in this report may not infringe privately owned rights; or

b. Assumes any liability with respect to the use of, or for damages resulting from the use of, any information, apparatus, software, method, or process disclosed in this report.

Reference to trade names or specific commercial products, commodities, or services in this report does not represent nor constitute an endorsement, recommendation, or favoring by GRI or Battelle of the specific commercial product, commodity, or service.

50272-101

REPORT DOCUMENTATION PAGE	1. REPORT NO. GRI-96/0014	2.	3. Recipient's Accession No.

4. Title and Subtitle

Analysis of Microscopic Leaks in Polyethylene Gas Distribution Piping

5. Report Date
September 1996

6.

7. Authors

S.M. Pimputkar, J.A. Stets, D. Mangaraj, G. Clark, D. Rider

8. Performing Organization Rept. No.

9. Performing Organization Name and Address

Battelle
505 King Avenue
Columbus, Ohio 43201-2693

10. Project/Task/Work Unit No.
N5742-7020

11. Contr. (C) or Grant (G) No.
(C) 5091-271-2351
(G)

12. Sponsoring Organization Name and Address

Gas Research Institute
8600 West Bryn Mawr Avenue
Chicago, Illinois 60631

13. Type of Report & Period Covered
Topical
Jan 1993 to Sep 1996

14.

15. Supplementary Notes

16. Abstract (Limit 200 Words)

The objective was to determine the cause of tiny holes (5 μm to 50 μm) found in polyethylene (PE) gas distribution piping in service, with the intent of reducing the number of leaks and thereby the operational costs. Since 1993, United Cities Gas Co. (UCG) in Tennessee has discovered gas leaks that were traced to small holes that traversed the pipe wall approximately radially. These holes are smaller by an order of magnitude than other small holes known to occur in PE tubing because of electrostatic discharge. The pinholes were examined and characterized both physically and chemically, followed by experimental attempts to reproduce the pinholes. The causes of the pinholes could not be proven statistically, and the occurrence could not be reproduced in a controlled environment. However, evidence suggests that the pinholes occur because of a progressive breakdown in the electric resistance of the PE under a static electric field which is smaller than that necessary for instantaneous discharge to occur.

17. Document Analysis a. Descriptors

Gas pipes, Pipes, Piping systems, Gas industry, Natural gas

b. Identifiers/Open-Ended Terms

Gas distribution, Pipelines, Gas flow, Polyethylene, Leaks, Field experience, Repair, Electrostatic, Chemical analysis, Soil testing

c. COSATI Field/Group

18. Availability Statement	19. Security Class (This Report)	21. No. of Pages
Availability Unlimited	Unclassified	143
	20. Security Class (This Page) Unclassified	22. Price

(See ANSI-Z39.18) *See Instructions on Reverse*

OPTIONAL FORM 272 (4-77)
(Formerly NTIS-35)
Department of Commerce

RESEARCH SUMMARY

Title	**Analysis of Microscopic Leaks in Polyethylene Gas Distribution Piping**
Contractors	Battelle Contract 5091-271-2351
Principal Investigator	S. M. Pimputkar
Report Period	January 1993 to September 1996 Topical Report GRI-96/0014
Objective	To determine the cause of tiny holes (typically 5 μm to 50 μm) found in polyethylene (PE) gas distribution piping in service, with the intent of reducing the number of leaks and thereby the operational costs.
Technical Perspective	Since 1993, United Cities Gas Co. (UCG) in Tennessee has discovered gas leaks that were traced to small holes (about 5 to 50 μm) that traversed the pipe wall approximately radially. These holes are smaller by an order of magnitude than other small holes known to occur in PE tubing because of electrostatic discharge. Although the length of pipe with pinholes is a tiny fraction of the length of installed pipe, the proliferating number of holes and the absence of a known cause concerned UCG, which contacted Gas Research Institute (GRI) for assistance. The study that resulted was funded by GRI, and Plexco provided some cofunding. In 1996, two such pinholes were found in tubing in Virginia.
Approach	Battelle and its subcontractors used two approaches to identify the origin of the small leaks, termed "pinholes": (1) the pinholes were examined and characterized both physically and chemically, followed by tests to determine their likely origin, and (2) experiments were conducted, based on a knowledge of manufacturing and service procedures, in an attempt to reproduce the pinholes. Research was aimed at determining whether the holes occurred instantaneously or through a growth phenomenon, and whether the holes occurred during manufacture or in service.
Results	The reason for the existence of the pinholes could not be proven statistically. However, an evaluation of the accumulated information suggests that the pinholes occur because of a progressive breakdown in the electric resistance of the PE under a static electric field which is smaller than the electric field that would cause an instantaneous discharge. It is not clear whether this occurs prior to the pipe being put in service or while the pipe is in service.

Project Implications

GRI sponsored this research to assist United Cities Gas Company in identifying the probable cause of the microscopic holes, and in instituting remedial measures.

GRI Project Monitor

Michael M. Mamoun
Principal Technology Manager
Distribution Business Unit

RESULTS AND CONCLUSIONS

Gas Research Institute (GRI) sponsors research at Battelle to analyze leaks, failures, and other incidents related to polyethylene (PE) gas distribution piping with the objective of reducing the number of leaks and failures, thereby reducing the cost of operations for U.S. gas companies.

Since 1993, United Cities Gas Co. (UCG) has discovered leaks in polyethylene (PE) gas distribution piping that were traced to small holes (about 5 μm to 50 μm) that traversed the pipe wall approximately radially. These small holes were termed "pinholes." These holes are smaller (by an order of magnitude) than other small holes known to occur in PE tubing because of electrostatic discharge. Although the length of pipe in which pinholes have been found is a tiny fraction of tubing in service, the proliferating number of holes and the absence of a known cause concerned UCG. UCG contacted GRI for assistance, and GRI requested Battelle to analyze the leaks. Plexco cofunded the work at Battelle. Since then, the number of new pinhole discoveries has stabilized, and in 1996, there are indications that the rate of discovery may be declining. In 1996, two pipe samples from Virginia were determined to contain pinhole leaks similar to the Tennessee pinhole leaks.

There has been a sustained effort, involving many resources in research and industry, to conclusively identify the origin of the pinholes. This is the final report on the analysis of the pinholes. The reason for the existence of the pinholes could not be proven statistically. However, an evaluation of the accumulated information and data suggests that the pinholes occur because of a progressive breakdown in the electric resistance of the PE under a static electric field. Published literature indicates that such breakdowns tend to occur preferentially at locations where the wall has a void or some other nonuniformity. It is not clear whether the progressive breakdown and the formation of pinholes occur prior to the pipe being put in service, or whether these events happen while the pipe is in service.

The specific results that were obtained are as follows:

- No convincing explanation was found for the fact that most of the pinhole leaks have been found in Central Tennessee. Although it is true that the UCG personnel use detection equipment which have rubber "boots" that serve to trap the gas, and UCG personnel are exceptionally thorough in their inspection procedure, by itself these factors are insufficient to explain the discovery of most of the pinholes in Central Tennessee. It is possible that pinhole leaks have been found elsewhere and repaired without undue scrutiny. This, however, is conjectural. It is noted that at least one pinhole leak occurred in Missouri in the 1980s, and two pinholes were discovered in Virginia in 1996.

- Physical and chemical nonuniformities were found in the gas distribution piping material that was tested. The scale of these nonuniformities was on the order of 10 μm to 100 μm. However, these nonuniformities existed both in the proximity of the pinholes and away from the pinholes. Therefore, there is no reason to believe that these nonuniformities cause, or are associated with, the pinholes.

- Extended thermal cycling of pressurized tubing containing a pinhole, a suspect length of tubing, and virgin tubing, did not cause the formation of a pinhole or an additional pinhole. This, combined with the absence of evidence of classical service failure mechanisms such as slow crack growth, suggests that mechanical and thermal factors are not primarily responsible for the formation of the pinholes.

- The pinholes do not appear to be the result of high-voltage instantaneous discharge, which generally produces holes that are characterized by:
  - Branching of the discharge path
  - A size that is typically larger (greater than 100 μm) than that of pinholes
  - Traces of carbon
  - Absence of clogging fibrils in the discharge path.

Typically, for defect-free PE material, it takes about 1000 V/mil to cause an instantaneous discharge.

- A visible pinhole may have incomplete pinholes in its vicinity. These incomplete pinholes are radially aligned, but do not emerge at both the inside and outside surface of the pipe. It is not clear whether these incomplete or "baby" pinholes grow into visible pinholes, or whether they were present at extrusion. The difficulty in answering this question is that the "baby" pinholes are so small that they cannot be detected except by destructive microtoming. The presence of a "baby" pinhole reduces the voltage necessary to cause discharge through the pipe wall at that location.

- Voltages lower than that required for instantaneous discharge can cause dielectric breakdown of PE when the voltages are applied for a long enough time. These are termed partial discharges. The presence of imperfections in the pipe wall reduce the voltage level, or the time required, for partial discharge. Increased temperatures may hasten the discharge. The amount of data collected was not sufficient to quantify these statements.

- From the fact that the presence of "baby" pinholes reduces the instantaneous discharge voltage, and from the fact that partial discharges occur, it may be conjectured that partial discharges are likely to occur in the proximity of "baby" pinholes, thereby converting them into visible pinholes. The data collected were insufficient to validate this conjecture.

- The reason for the existence of the pinholes could not be proven statistically. However, an evaluation of the accumulated information suggests that the pinholes occur because of a progressive breakdown in the electric resistance of the PE under a static electric field which is smaller than the electric field that would cause an instantaneous discharge. It is not clear whether this progressive breakdown and

pinhole formation occur prior to the pipe being put in service, or while the pipe is in service.

CONTENTS

TABLES

FIGURES

FIGURES (Continued)

FIGURES (Continued)

FIGURES (Continued)

Analysis of Microscopic Leaks in Polyethylene Gas Distribution Piping

by

Sudheer M. Pimputkar, Joseph A. Stets, Duryodhan Mangaraj, Glenn Clark, Dennis Rider

INTRODUCTION

Gas Research Institute (GRI) has sponsored a long-term program of research and development at Battelle to analyze leaks, failures, and other incidents related to polyethylene (PE) gas distribution piping. The intent of this program is to provide guidelines to U.S. gas companies so that frequency of occurrence of similar incidents is minimized, and operational costs are reduced.

United Cities Gas (UCG) is a gas company that supplies gas to customers in several states including Tennessee. UCG surveys its distribution system every five years using flame ionization techniques. Starting in 1993, such surveys have uncovered several leaks of an unusual kind. The gas leaks were through small holes, typically 5 μm to 50 μm in "diameter" (a substantial length of most of the holes is approximately circular), that extended through the wall of the pipe. Such holes were termed "pinholes." Most of the leaks were found in ½-inch service medium density polyethylene (MDPE) pipe made by Plexco, which also supplies a majority of MDPE tubing used in that service area. Some pinholes have also been reported in pipe from Poly Pipe and Phillips. The holes varied in size from 5 μm to 40 μm. No third party damage or stress cracks were evident. The environment of the leaks was not similar, other than the fact that they all occurred in the central part of Tennessee. Four cities are located in that area. Therefore, the work crews were different. Some of the pipes in which the leaks were found were located at a shallower depth (14 to 18 inches) than usual, but the majority were discovered in pipe buried at the usual depth of 18 to 24 inches. Tracer wire was buried with the pipe but was not taped to it. On occasion, it may have touched the pipe, but this did not occur near the leak locations. The Middle Tennessee Utility District, which uses warming tape and does not use tracer wire, also experienced some pinholes. The leaks did not occur near transition fittings, risers, or taps. Most

pipe was installed using open trench techniques. Where horizontal boring was used, the minimum bore size was 1-1/4 inches. There was no evidence of rock impingement. The gas was supplied by three different companies and was not unusually dirty. No condensation was evident. There were no other utilities in the same trench. The leaks have occurred in orange and yellow pipe made from 1974 to 1992. UCG estimates that almost 85 percent of leaks have been in pipe manufactured between 1985 and 1993. No correlation was discovered between the pipe lots in which pinholes were detected and the extrusion conditions for those pipe lots (such as extruder, time of day, or weekday of extrusion). The leaks were detected a few weeks to a few years after the pipes were put in service. Occasionally, the yellow pipe leaks were seen to have small "icicles" on the inside surface of the pipe at the hole locations.

The leaks were examined by Broutman and Associates and by Union Carbide prior to Battelle's involvement. Neither could offer any explanations as to the cause, although the latter emphatically ruled out lightning or any sudden electrical discharge. UCG also conducted several studies in order to identify the cause of the pinholes. These studies were inconclusive.

UCG approached GRI for assistance, and GRI initiated a contract with Battelle. The objective was to identify the origin of the pinhole defects observed in pipe used by UCG.

In 1996, two in-service samples from Virginia were examined, and were found to contain pinholes. Because the pinhole specimens in Virginia were found toward the end of this study (in 1996), the vast majority of the data in this report pertains to the pinholes found in Tennessee. References to the Virginia pinholes are explicitly noted.

Technical Approach and Rationale

Two approaches are possible when identifying the origin of a leak. First, the leak can be examined, characterized physically and chemically, and from these observations, hypotheses about the origin can be formulated and tested. Second, based on a knowledge of the manufacturing procedures and of the service procedures, the mechanism of formation can be postulated, and

specific experiments can be devised to reproduce the pinholes. In either case, reproduction of the pinholes under controlled circumstances is proof that the cause has been identified.

Both approaches were used in this effort. The material in the proximity of the pinholes, the material away from the pinholes, the pinhole and its inside surface, and typical samples of the surrounding soil were examined. At the same time, experiments were devised and constructed to evaluate specific hypotheses (such as temperature cycling and electrostatic discharge) about the origin of the pinholes. Testing was also undertaken by organizations under subcontract to Battelle. These organizations included the University of Pennsylvania, Exxon, Southwest Research Institute, Miami University, and Fein Focus Laboratories. GRI shared these data and information with the Plastic Pipe Institute (PPI), which had activated a Task Force to evaluate the occurrence of the pinholes.

This report is divided into the following major sections:

- Gas Industry Collaboration
- Characterization Tests
- Specific Mechanism Tests
- Pinhole Morphology
- Partial Discharge Hypothesis
- Conclusions and Discussion.

In order to sustain the clarity of the primary data and conclusions, details of supporting technical work are relegated to the appendices.

Questions to be answered are:

- Did the pinholes occur instantaneously or did they occur through a growth phenomenon?
- If they occurred instantaneously, did they occur during manufacture or service?

If they occurred during manufacture, similar pinholes should be detectable in unused pipe of the same vintage. If it is a growth phenomenon, some of the growth must have occurred after the pipe had been put into service. In that case, samples of in-use pipe should have pinhole flaws that have not completely penetrated the wall. For a complete study, the four classes of materials that needed to be examined are:

- In-service materials near locations of known leaks
- In-service materials away from locations of known leaks
- Unused materials from the same lot
- Unused materials of the same vintage, but not necessarily from the same lot.

A systematic and complete testing effort would have been prohibitively expensive. Therefore, experience and judgment were used to minimize the number of tests and maximize the information extracted per test.

Acknowledgments

It is a pleasure to acknowledge the generous assistance of the following companies and individuals in the performance of this project:

- Mr. Robert Elam, United Cities Gas Company;
- Mr. Michael Byrne, Plexco; and
- Mr. Anthony Nicholas, Union Carbide.

In addition, we would like to thank the Plastic Pipe Institute, and particularly the members of the Task Force on this subject.

GAS INDUSTRY COLLABORATIONS

Meeting with Resin Suppliers, Pipe Extruders, and Gas Suppliers

Two meetings were held at Battelle to solicit suggestions and ideas from experienced personnel in the gas industry as to the cause of the pinholes. Both meetings were limited to invitees. The complete meetings were recorded on audio tape, while portions were recorded on videotape.

The first meeting was held on August 2, 1994, and the focus was on the suppliers of the resins used in gas pipe. The following attended:

- Bill Beaulau of Phillips Chemical Company
- Frank Galiano of Chevron
- Wayne Korall of Novacor Chemicals
- Tony Nicholas of Union Carbide
- Steve Sandstrum of Solvay Polymers.

Prior to the meeting, a copy of the agenda and a summary of the problem and progress were mailed to the attendees.

The suggestions that resulted from this meeting were to:

- Examine the composition of small particles of pipe material found at the surface of some of the pinholes to see if they are due to die buildup
- Determine how to create pinholes deliberately, and thereby deduce the natural mechanism
- Determine the effect of soil radioactivity on PE pipe
- Determine the effect of pellet size and screw design on throughput.

The second meeting was held on August 18, 1994, and the attendees were:

- Will Bezner of Poly Pipe Industries
- Bob Elam of UCG
- Gene Palermo, formerly of Uponor
- Paul Petro of Plexco.

Staff from Phillips Driscopipe were invited but could not attend. Gene Palermo made a presentation suggesting that instantaneous static discharge was the cause of the pinholes.

A visit was made by GRI and Battelle staff members to areas served by UCG. Leak detection techniques used by UCG were observed. Three additional pinhole leaks were detected and excavated during the visit. A piece of tubing which had never been in service, and which was said to have a leak, was brought back to Battelle and was subjected to temperature cycling under pressure. A visit was also made to Plexco's Knoxville plant, and to Poly Pipe's plant in Erwin, Tennessee. The manufacturing and quality control procedures at these plants were observed.

Industry Group Activities

The Plastic Pipe Institute (PPI) constituted a Task Force to analyze the pinhole leaks. In order to avoid duplication of effort and invoke the best combined resources available to the gas industry, a meeting was held at GRI to discuss collaboration between GRI and PPI. In principle, the attendees were in favor of a collaboration. The technical details of the collaboration were discussed further by Tony Nicholas of Union Carbide and Sudheer Pimputkar of Battelle at a subsequent meeting at Bound Brook, New Jersey.

Sudheer Pimputkar attended and made presentations at PPI Task Force meetings in Dallas, San Diego, and Hilton Head.

Service Line Inspections of Other Gas Companies

One of the puzzling features of the pinhole leaks was that the occurrence appeared to be confined to a small geographical region in Central Tennessee. If the pinholes were confined only to Central Tennessee, it was felt that the cause was more probably service-related, while if pinholes were occurring in other geographical regions without detection, the cause was more probably manufacturing-related. In order to examine whether pinholes have occurred in other service areas, a request was made to several gas companies. Columbia Gas of Ohio granted permission to perform service line inspections with assistance from personnel from UCG.

Leak inspection personnel from UCG visited Commonwealth Gas in Virginia in 1995 to assist with leak detection. Five leaks were detected. Battelle did not receive pipe specimens with any of these leaks for examination. Reports from the leak detection crews indicated that none of the leaks was a pinhole leak of the type under investigation. A supervisor at Commonwealth Gas recalled a pinhole leak being detected in his service area about two years earlier. That leak sample had been removed and sent to Columbia Gas of Ohio. The failure report was located but the leak sample was not found, and therefore Battelle did not have an opportunity to determine the characteristics of the reported pinhole.

It is known that pinholes have been found in distribution piping in service outside Central Tennessee on at least two occasions. In the first instance, in 1985, a gas company in Missouri found pinhole leaks in 5/8-inch PE2306 tubing. A coil of this tubing was sent to Battelle for analysis. A detailed report prepared at that time contains photographs and descriptions that are almost identical to photographs and descriptions for the current set of pinholes. No specific cause was identified for the Missouri pinholes. Another possible occurrence of a pinhole may be a PE pipe sample with microscopic holes described in the Field Failure Reference Catalog For Polyethylene Gas Piping (Lustiger et al. 1986). However, no further information is available to determine whether that sample contains conventional electrostatic discharge holes or pinholes. Therefore, this reported leak is noted for information purposes, but is not presented as an example of a known pinhole.

In the second instance, in June 1996, two pipe samples from the service area of Commonwealth Gas in Virginia were received through Columbia Gas of Ohio. Both samples were Plexco ½-inch MDPE tubing, and were in service in the Fredericksburg, Virginia service area when discovered by a leak survey. One sample (termed Hamlin) was installed in 1992, and was detected to be leaking on January 4, 1996. The other sample (termed Cornwallis) was installed in October 1991, and was detected as leaking on April 17, 1996. Figures 1 and 2 show these samples as received.

The sample ends were fused to end caps, and then each sample was pressurized and immersed in water. The Hamlin sample had several streams of bubbles from a small area. The Cornwallis sample had one stream of bubbles. The leaking areas of each sample were then examined using scanning electron microscopy (SEM).

The OD of the Hamlin sample was rough, and it was difficult to determine whether the surface features were pinhole apertures, or whether they were surface imperfections. Views of this surface at increasing magnification (10X, 50X, and 300X) are shown in Figures 3, 4, and 5 (photo ID 4438, 4439, 4442). A few layers (totaling a few mils) were microtomed, and the resulting surface was observed. About twenty small holes were seen at a low magnification (15X).

An examination of the ID of the Hamlin sample indicated several small holes as shown in Figure 6 (photo ID 4422). The number of these holes was of the same order of the holes seen in the microtomed OD section, implying that there did not appear to be any significant branching. Figure 7 (photo ID 4421) is an enlarged (350X) view of one of the holes at the ID. It appears to have a "cap" covering the hole, as has been found in several of the field leaks from Tennessee. Figure 8 (photo ID 4425) shows another of the ID holes at high magnification (1000X). The focus is on the interior of the hole and the surface is out of focus. The hole diameter appears to be about 35 to 50 microns. A view of the same hole from a different perspective and at a different magnification (750X) is shown in Figure 9 (photo ID 4423).

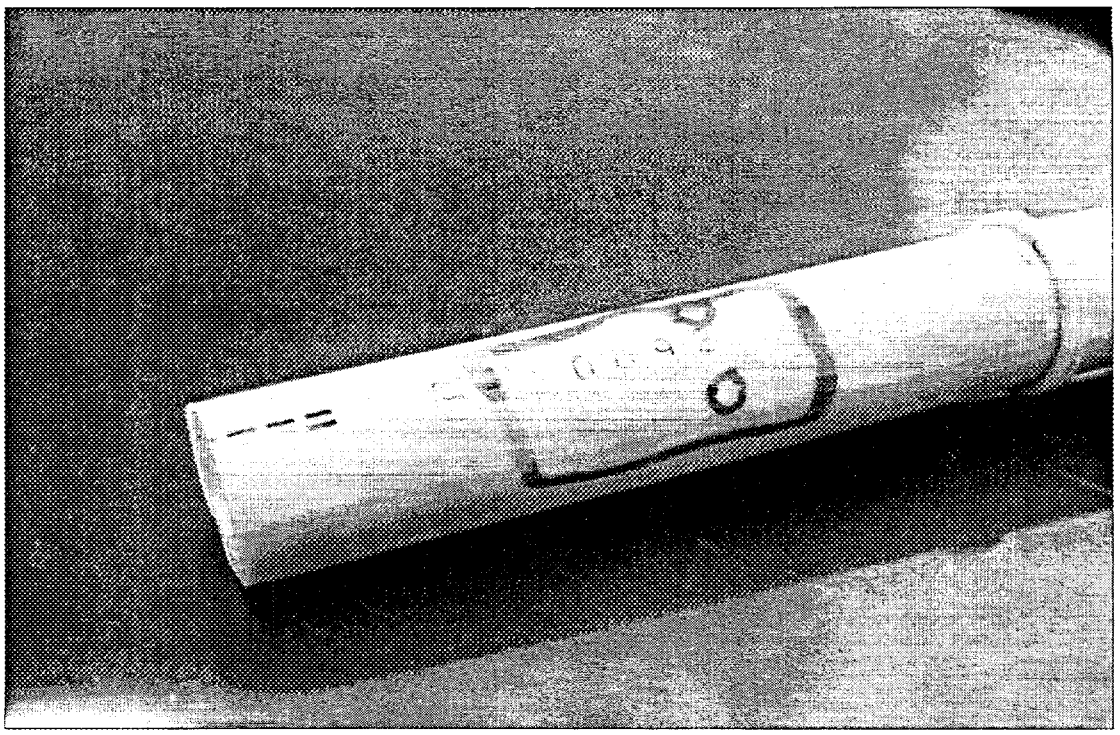

Figure 1. As-received Hamlin sample from Virginia

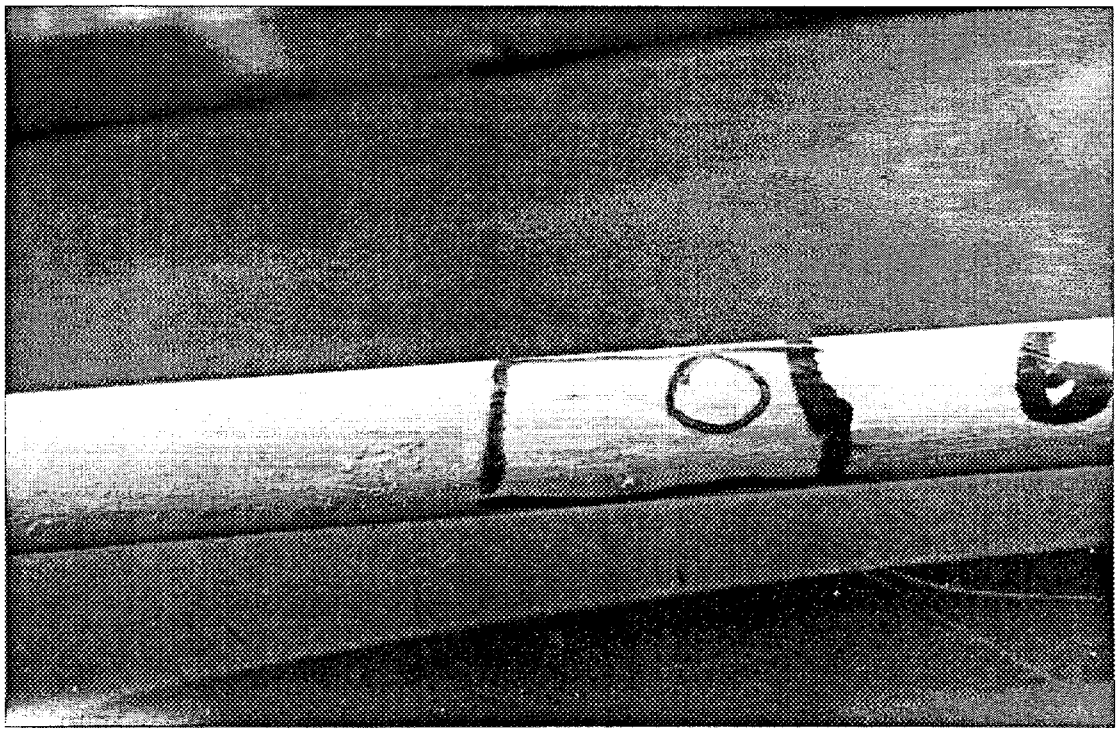

Figure 2. As-received Cornwallis sample from Virginia

Figure 3. OD of Hamlin sample (10X)

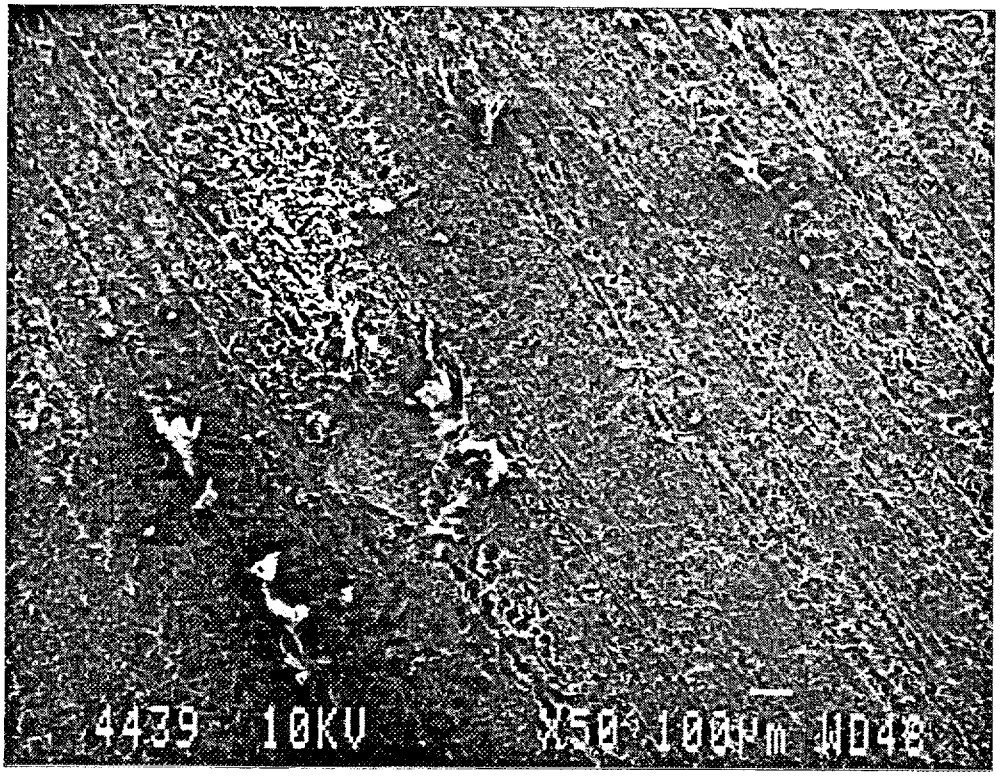

Figure 4. OD of Hamlin sample (50X)

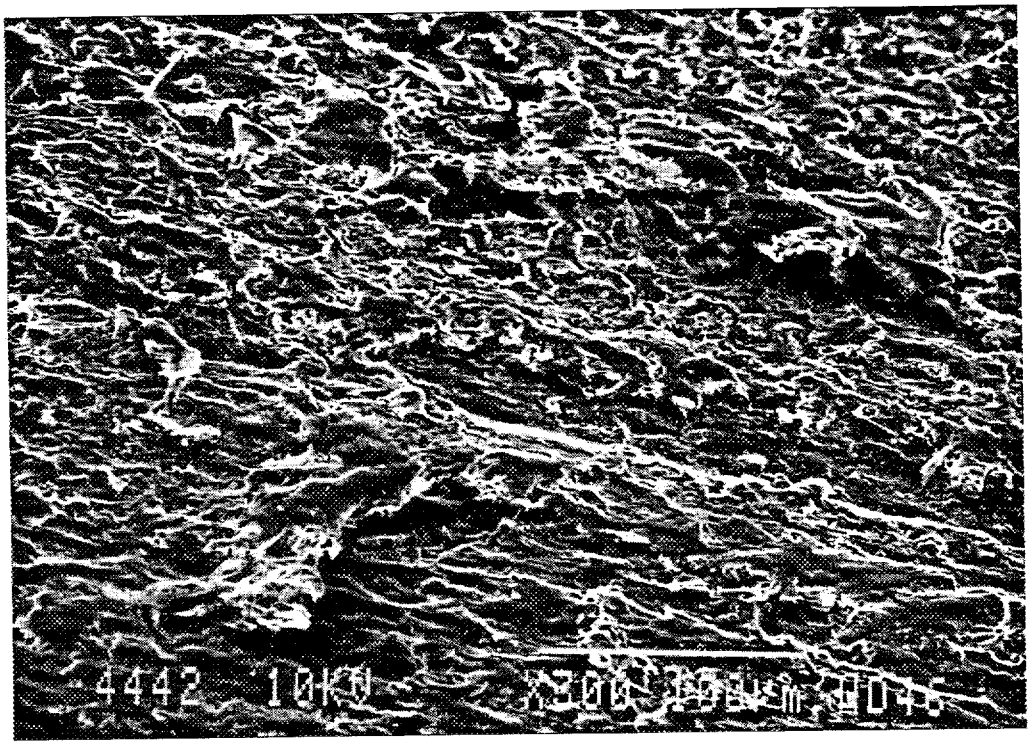

Figure 5. OD of Hamlin sample (300X)

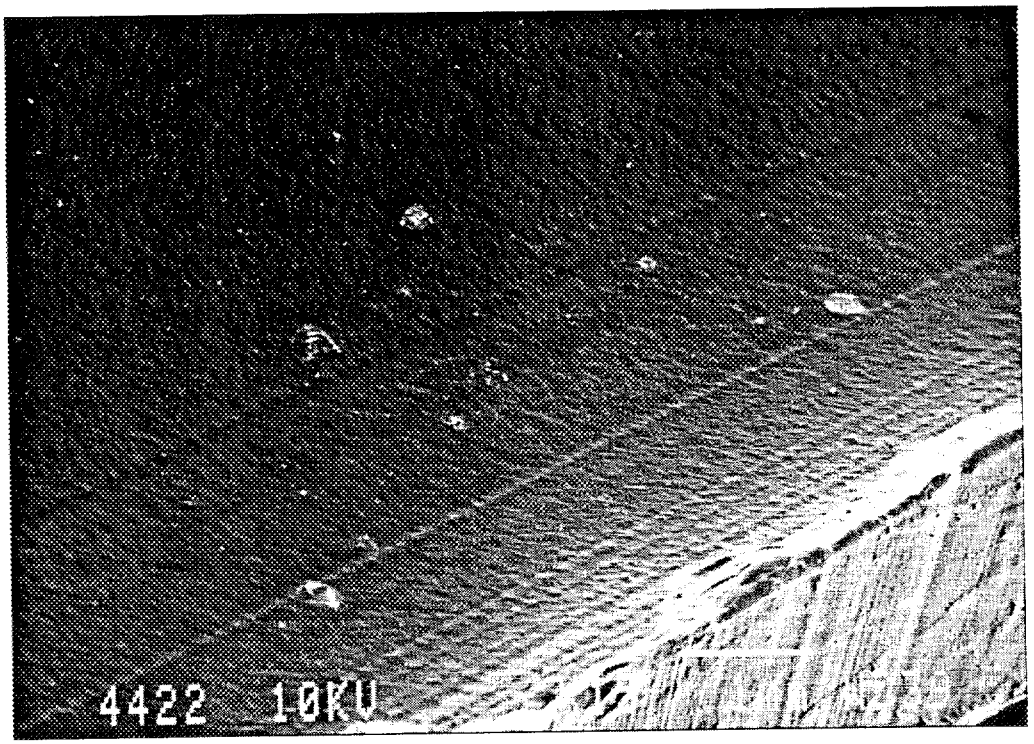

Figure 6. ID of Hamlin sample (15X)

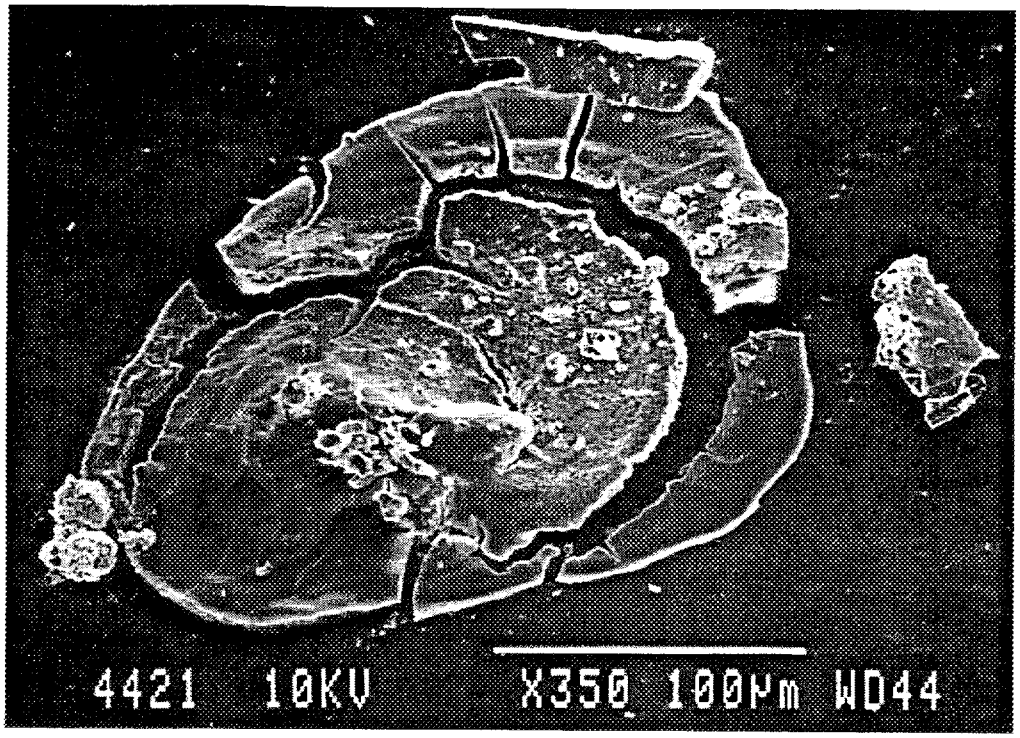

Figure 7. Enlarged view of one hole at ID (350X)

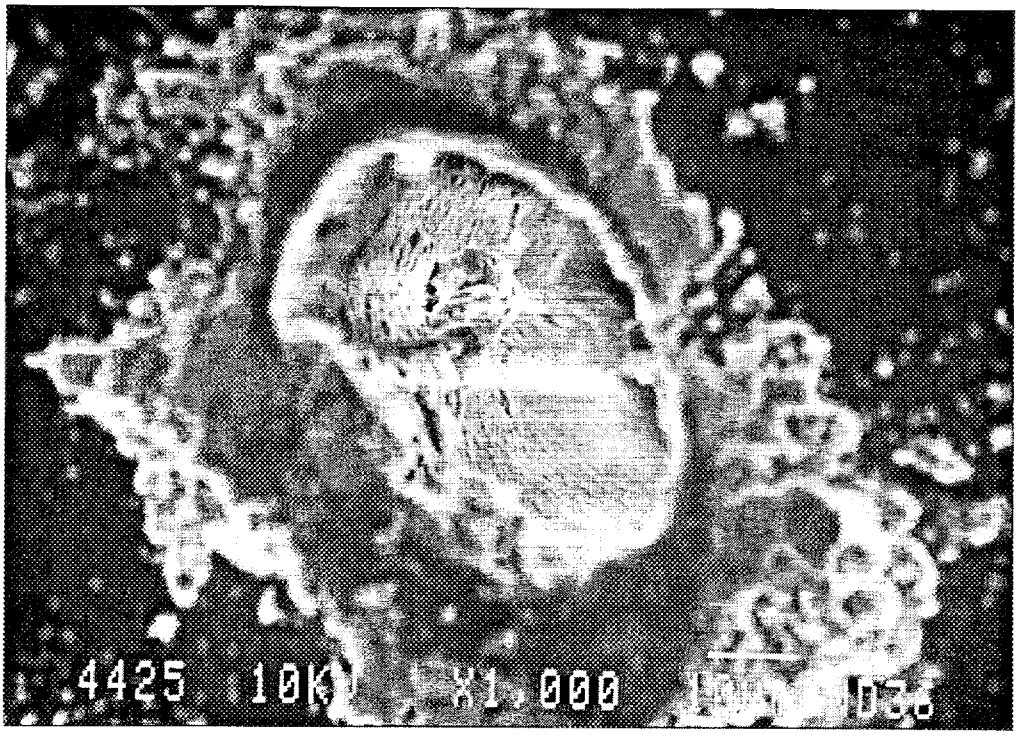

Figure 8. High-magnification view of hole at ID (1000X)

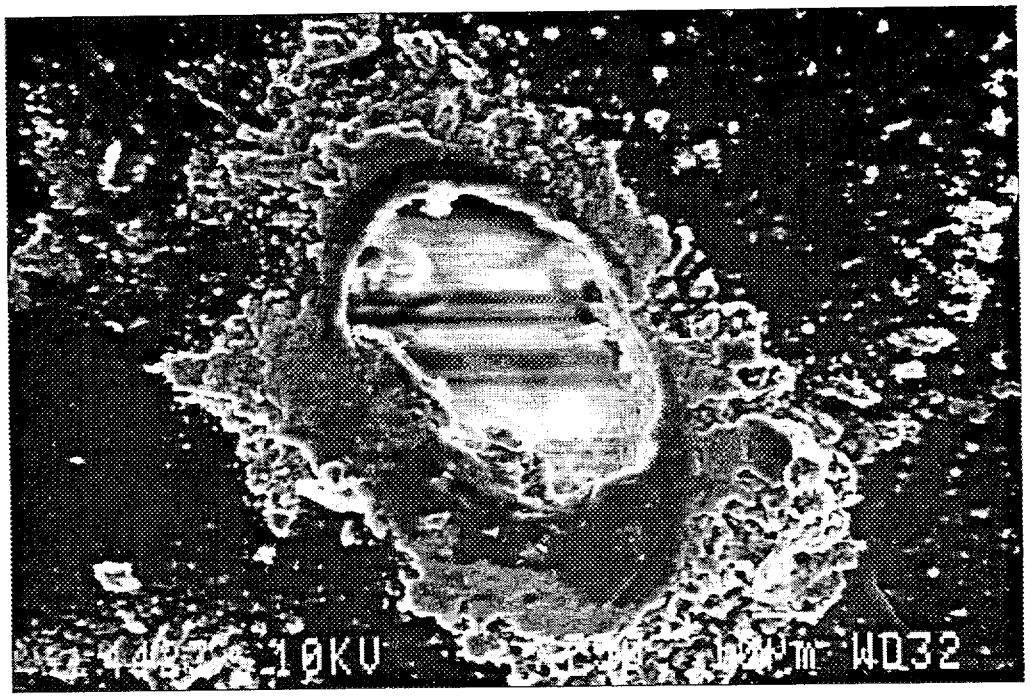

Figure 9. Different view of hole shown in Figure 8 (750X)

The OD of the Cornwallis sample at low magnification (50X) is shown in Figure 10 (photo ID 4413). The features of the leak site at greater magnifications (350X and 750X) are shown in Figures 11 (photo ID 4415) and 12 (photo ID 4416). The hole is visually similar to several of the Tennessee field leaks.

Figure 13 (photo ID 4418) shows the ID of the Cornwallis leak site at a magnification of 350X. The central region of lighter coloration houses the pinhole which is not visible at this magnification. The same area is shown at higher magnifications (1000X and 2500X) in Figures 14 and 15 (photo ID 4419 and 4420). The leak site is visible as a crater-like hole in the central foreground. The size appears to be about 5 microns.

Based on the examination of the Hamlin and Cornwallis leak samples, it appears that the leaks in both samples are "pinhole leaks" as typified by the leak samples from Central Tennessee. This is the first recent example of pinholes from outside Tennessee, and lends credence to the argument that it is not an unique combination of service conditions in Tennessee that is causing the pinholes.

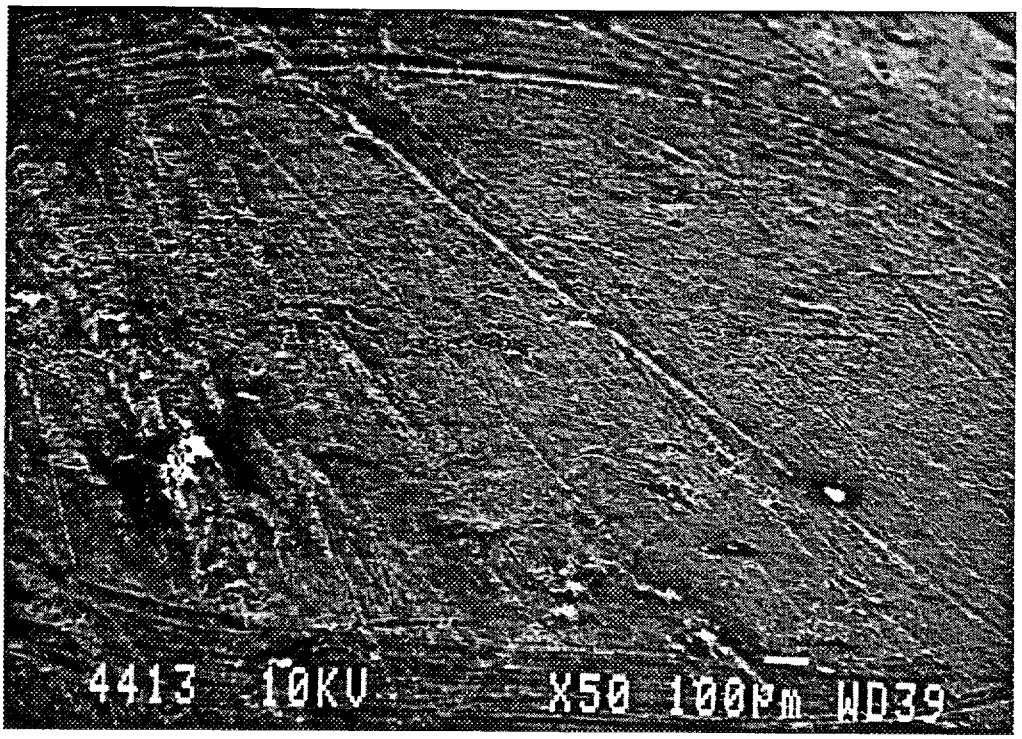

Figure 10. OD of Cornwallis sample (50X)

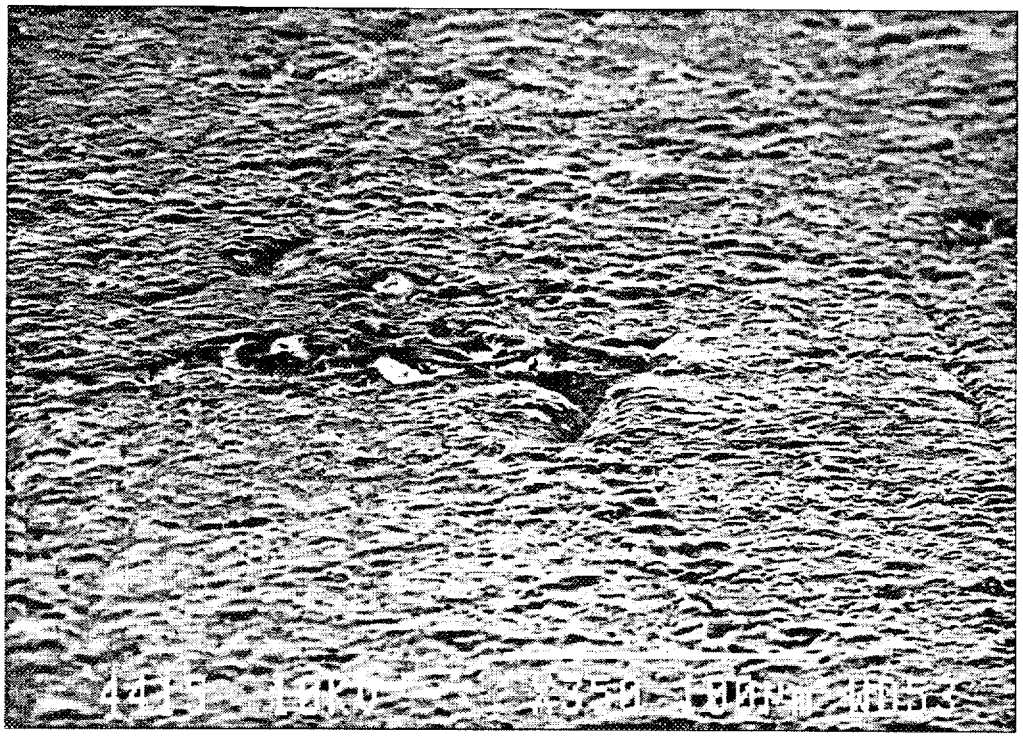

Figure 11. Leak site of Cornwallis sample (350X)

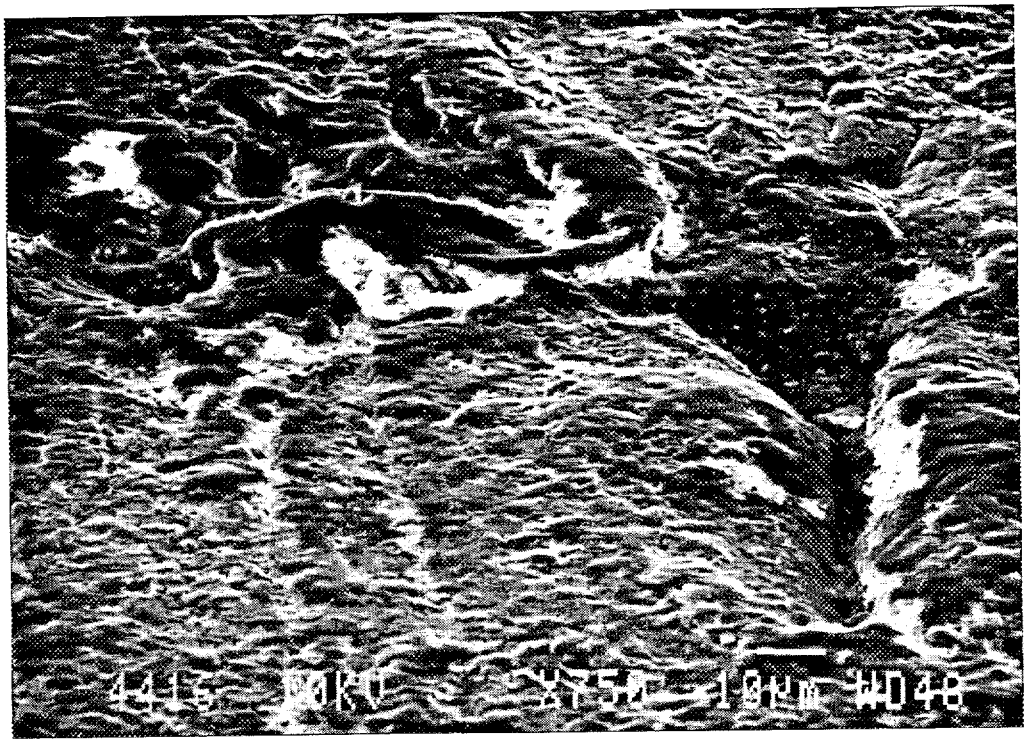

Figure 12. Leak site of Cornwallis sample (750X)

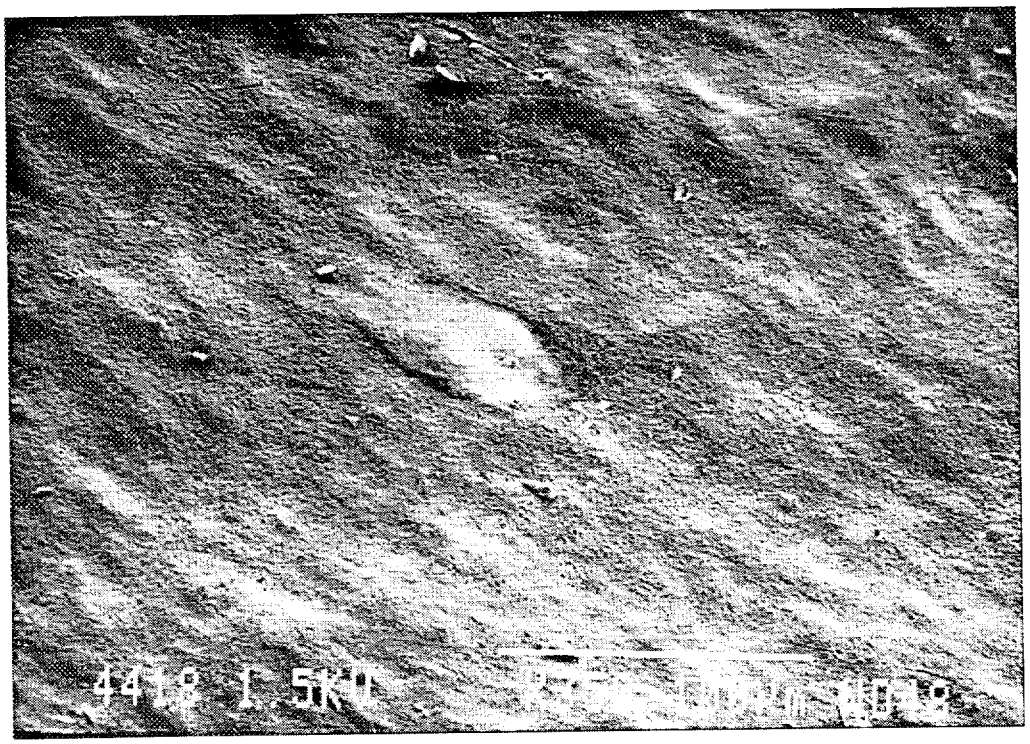

Figure 13. ID of Cornwallis sample leak site (350X)

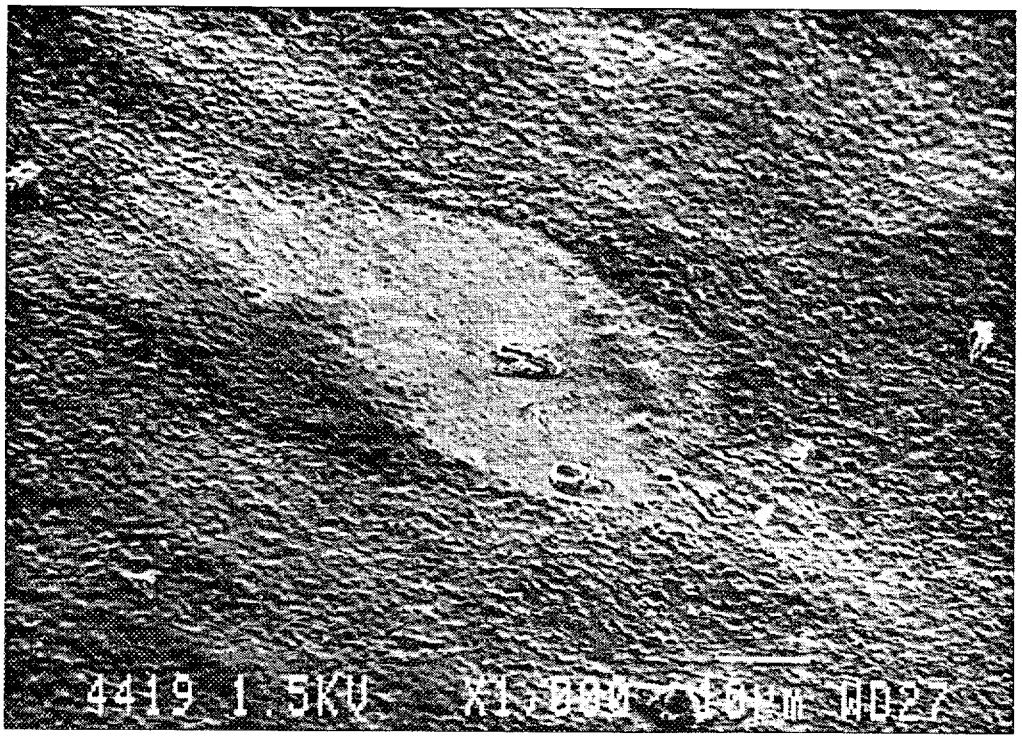

Figure 14. Enlarged view of Cornwallis sample leak site (1000X)

Figure 15. High-magnification view of leak site (2500X)

CHARACTERIZATION TESTS

The original sequence of testing that had been planned is shown in Table 1. The test plan was based on the successive performance of tests that were expected to be most productive and cost-effective.

Scanning electron microscopy was used continually throughout this study. The early microscopy was limited to a preliminary visual characterization as part of the several tests noted in Table 1.

Tests Conducted

The following tests were conducted, as detailed below and in Appendices A through D: scanning electron microscopy, electron scattering chemical analysis, infrared analysis, molecular weight and melt index measurements, Raman spectroscopy, hot-stage microscopy, and soil analysis.

Early Microscopy. Yellow and orange pipe samples were examined optically and through a scanning electron microscope (SEM). The material surrounding the pinhole (termed the "near field") appeared to be visually distinct from the material away from the pinhole (termed the "far field"), and appeared to be separated from it by a "ridge" or boundary. The pinhole path was not directly radial, but meandered in an overall radial direction. The cross-section of the earliest specimens appeared to be a flattened ellipse or a crack rather than circular. Later, after examination of additional pinholes, it was recognized that the pinholes are approximately circular over much of the internal length.

Pipe sections were submerged in liquid nitrogen and microtomed. The micrographs exhibited "pock marks," which appeared to be regions of a visually different material. The length scale of the pock marks was about 200 μm. The pock marks appeared to have distinct

Table 1. Rationale for Failure Analysis

Hypothesis	What Needs to Be Done and Why	Priority
Chemical Aspects		
Agglomeration of antioxidants, pigments, and other additives in the resin and their migration through PE	■ Conduct FTIR* and HPLC** analysis between control and failed samples. Check for local concentration of the additives and any adverse chemical change in PE due to interaction with additives	High
Unacceptable level of micro inhomogeneity in Plexco polyethylene	■ Morphology evaluation by etching technique to determine if pinhole areas have significantly different material characteristics particularly the interspherulite region	High
Some gas effluents attacking intercrystalline region or dissolving amorphous region in PE	■ Study gas make-up and conduct exposure tests with suspicious effluents and follow up with chemical evaluation (FTIR and HPLC)	High
Leaching out of amorphous regions in PE from waterborne salts. Moisture induced degradation (intercrystalline region in PE)	■ Conduct thermal cycling in moist and dry conditions to evaluate moisture/waterborne salt interaction with PE ■ Assess Tennessee soil environment	High
Physical Aspects		
Pinholes created by water pressure or air pressure during pipe manufacturing. Flaws around knit line.	■ Review die design and sizing procedure for tube ■ Review processing conditions	Medium
Defect grows in service and not in production	■ service. Provides information on PE degradation	High
Electrical Aspects		
Pinholes are created due to low voltage electric discharge.	■ Evaluate damage under polarized light. Check for melting and other stress fields associated with slow or fast progression of damage. Check for electrical characteristics in the damage area.	Medium

* FTIR — Fourier transform infrared spectroscopy
** HPLC — High-pressure liquid chromatography

boundaries, and appeared to be loosely connected to the rest of the polyethylene matrix. Most of the pock marks were aligned along the axis of the pipe. No unique relationship was established between the existence of the pock marks and the existence of the pinholes.

Occasionally for pipe material that contained a hard inclusion, microtoming sheared the inclusion, leaving a hole that could be seen at higher magnification. Analysis of the inclusion using energy dispersion spectroscopy (EDS) indicated that the inclusion contained mainly Si, Al, Ti, and Na.

Additional details on this preliminary electron microscopy investigation is given in the Monthly Progress Report dated April 8, 1994, included as Appendix A.

Electron Scattering Chemical Analysis (ESCA). The inner and outer surfaces of the pipe at the pinhole contained several inorganic species including Na, K, Al, Si, P, S, and Cl. These species were absent away from the pinhole. These may have originated in the leak detection liquid used by the UCG field crew. Inclusions within the pinhole were found to contain Na, Al, Si, S, Cl, K, and Ca, while inclusions within the material but away from the pinhole contained mainly Si.

Infrared Analysis. The more recently extruded pipe samples contained metal carboxylates, unlike the earlier material. However, the metal carboxylates were found in pipe with and without pinholes and were deemed to be irrelevant to the occurrence of pinholes.

Infrared spectra showed a depletion of paraffinic material near the pinhole, and a large increase in the methyl to methylene group ratio in the same area.

Molecular Weight Measurements. Gel permeation chromatography (GPC) was used to analyze the near field and the far field materials in yellow and orange pipe. It was found that the high molecular weight polyethylene components were substantially lower in the pipe material near the pinhole for yellow pipe. However, insignificant differences were found in the orange

pipe. The implication was that there was no unique relationship between the local molecular weight and the occurrence of the pinholes. Details on the testing are given in Appendix B.

Melt Index Measurements. The melt index provides an approximate measurement of the flow characteristics of the polymeric material. Because flow characteristics of the extruded product are an important property, melt indices of PE samples taken from the orange and yellow pipes containing pinholes, and those taken from the virgin pipe extruded in 1993, were measured following ASTM Standard D1238. Approximately 15 grams of the material was used in each case. The flow behavior was measured under two different loads, E and N. The ratio

$$Flow\ Rate\ Ratio\ (FRR) = \frac{weight\ extruded\ under\ load\ N}{weight\ extruded\ under\ load\ E}$$

provides an insight into the shear thinning characteristics of the material. Under condition E, the extruded weight is measured after 6 minutes of extrusion, whereas under condition N, the extruded weight is measured after 30 seconds. Five measurements were carried out under each condition, and the average was used for calculating the melt index and FRR. The melt index of another resin, TR 418, used for making gas pipes, was also measured for comparison with the melt index of extruded material. The results are presented in Table 2.

The melt indices (weight of PE extruded in 10 minutes under load E) of the four materials do not show any significant difference. They are close to the melt index of polyethylene material used for gas pipe extrusion (PE2406) of 0.2 gm/10 minutes. The FRRs for the new pipe and the two old pipes with pinholes are close to each other showing no difference in shear thinning behavior. They are slightly different from the FRR of the reference material (TR 418 resin).

The melt indices of the pipe with pinholes were found to be in a range typical of gas distribution piping. Therefore, the melt index is not an indicator of pinhole occurrence.

Table 2. Melt Index of PE Materials

Sample	Extruded Weight, gms		Extruded Weight, gms/10 min		Melt Index, gms/10 min	Extruded Weight under N, gms/10 min	N/E
	E	N	E	N			
New 11/93 Yellow Pipe	.1078	.1472	.1797	2.944			
	.1159	.1506	.1932	3.012			
	.1023	.1467	.1705	2.934			
	.1041	.1480	.1735	2.96			
	.1059	.1444	.1765	3.53	.1787±.008	3.08±.26	17.2
Orange Pipe	.1258	.1578	.2097	3.156			
	.1158	.1610	.1930	3.22			
	.1185	.1620	.1975	3.24			
	.1165	.1549	.1942	3.098			
	.1158	.1590	.1930	3.86	.1975±.007	3.32±.31	16.8
Yellow Pipe	.1174	.1579	.1957	3.158			
	.111	.1558	.1852	3.116			
	.1088	.1591	.1813	3.626			
	.1100	.1556	.1833	3.112			
	.1094	.1595	.1823	3.190	.1856±.006	3.24±.22	17.5
Reference TR418 Resin	.1079	.2015	.1798	4.03			
	.1103	.2076	.1838	4.152			
	.1028	.2047	.1713	4.094			
	.1040	.2025	.1733	4.05			
	.1106	.2156	.1843	4.312	.2042±0.003	4.12±.22	21.2

Raman Spectroscopy. Raman spectroscopy has a high resolution and can determine compositional differences over a few microns. This work was carried out at Miami University in Oxford, Ohio. No crystallinity differences were detected in the polyethylene through the defect areas. Only compositional differences that could be attributed to the lead chromate pigment were observed. This type of compositional gradient was also observed away from the pinhole. Additional details of the testing are in Appendix C.

Hot-Stage Microscopy. Hot-stage microscopy was used to assess the nature of the pock marks. The interior of the pock marks did not melt at the same temperature as the rest of the matrix, implying the presence of gel particles. This work was carried out at Exxon Research Laboratories.

Soil Analyses. Several samples of soil sent by UCG were subjected to organic and inorganic testing at Battelle. Although traces of organics were detected, they did not appear to be present in quantities substantial enough to be significant. Details of the soil testing are in Appendix D.

Conclusions from Characterization Tests

The characterization measurements did not lead to a definite conclusion regarding pinhole formation.

In one case (yellow pipe), the material near the pinhole area was depleted of its high molecular weight fractions, whereas the material away from the pinhole area retained them. The polydispersity of the material near the pinhole was much smaller (3.3) compared to that of the material away from the pinhole. This could indicate polymer degradation leading to chain scission. This would agree with the results of an IR study at Battelle in which the ratio of CH_2/CH_3 in the defect area was very high. However, the materials close to and away from the pinhole in the orange pipe did not show such a trend. Either the test sample of the orange pipe was not close enough to the pinhole, or it did not undergo degradation and chain scission in the same way as the material in the yellow pipe. The presence of lead chromate in the yellow pipe

could contribute to thermal oxidative degradation. Absence of degradation in the orange pipe may be attributed to the absence of transition metals in the pipe composition. On the other hand, it is quite possible that the test sample was not close enough to the pinhole. A pinhole typically extends over a small range, 5 to 20 μm, and does not follow a straight path. Hence, it is difficult to ensure that the test material from the pinhole area actually contains material at the pinhole. The only way this can be resolved is by examining a statistically large number of test specimens, each of a size smaller than the specimen size used in the current measurement.

The absence of an anomaly in the melt index suggests that the occurrence of pinholes is not reflected in the macroscopic (flow) properties of the material.

The Raman spectroscopy study also did not produce any conclusive evidence of the mechanics of pinhole formation. The variation of lead chromate concentration as a function of distance may indicate that the pock marks are due to higher lead chromate concentration in the periphery of the pock mark compared to that in the center.

SPECIFIC MECHANISM TESTS

Two separate experiments were conducted at Battelle. The first experiment tested the hypothesis that the pinholes exist before the pipe is put into service, and service conditions merely cause the pinholes to become detectable leaks. The second experiment tested the hypothesis that instantaneous static discharge caused by charge buildup on the inside of the pipe is the cause of the pinholes.

Temperature Cycling Experiments

There is anecdotal evidence that leaks have been experienced in pipe that has not been in service. The implication is that the pinholes occur during manufacture. However, there are no reliable data supporting this assertion. An experiment was designed to check this possibility. A schematic of the experimental setup is shown in Figure 16. In the experiment lengths of PE tubing were subjected to continual changes in temperature between city water temperature and 175 F while under a pressure of about 60 to 90 psi. Initially, a 20-foot length of ½-inch CTS Plexco yellow medium density PE tubing was put on test. Subsequently, other tubing samples were added. The tubing was pressurized using air, and the air pressure was monitored by a pressure transducer, P, as shown in Figure 16. A thermocouple, T, monitored the air temperature in the tubing. The city water supply through valve V1 was alternately passed through valves V2 and V3 so that either unheated, or heated, city water flooded the tubing exterior. The water level in the immersion tank was sensed by a float valve, F, that actuated the pan level solenoid valve V4. A recirculation pump, Pu, was used to maintain good heat transfer between the tubing and the water, and the water temperature was also monitored.

The process sequence was as follows:

1. Close drain when pan is empty
2. Fill pan with cold water
3. Start circulating pump

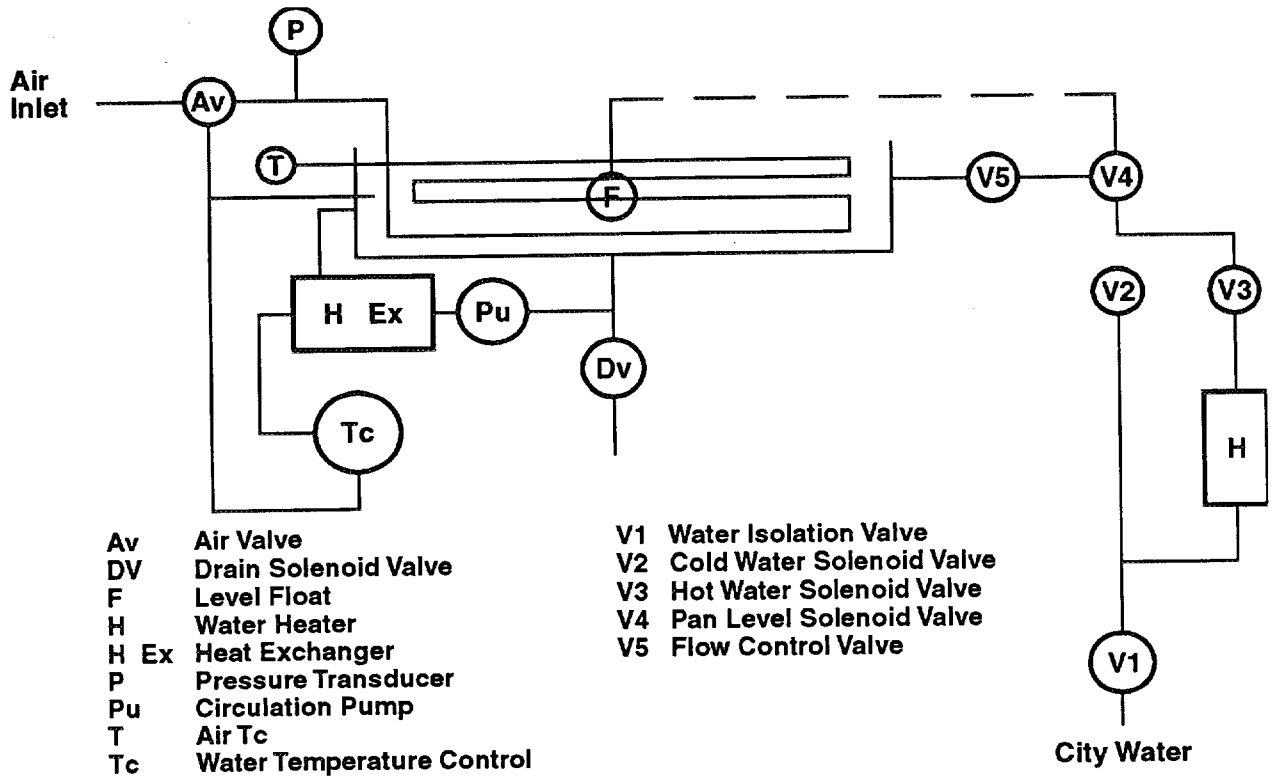

Figure 16. Schematic of test setup for temperature cycling experiment

4. Hold for 2 minutes
5. Open valve and drain cold water
6. Close valve when pan is empty
7. Fill with hot water
8. Start circulation pump
9. Heat circulating water to 80 C
10. When water temperature is 80 C, hold for 2 minutes
11. Stop circulation pump, and turn off heater
12. Open drain till pan empties
13. Loop to beginning of process sequence

The first set of data was taken June 21, 1994. Information obtained from those data was used to fine tune the process system to produce the final cycle profile.

The initial test ran for about 30 hours before the recirculation pump failed. Failure of the pump also caused the heater to fail. The recirculation pump was replaced with a hydronic

heating pump with better temperature specifications. The heater was also replaced and the testing was resumed. A steady leak in the air system leading to a pressure drop of about 2 in. water per hour existed. This was rectified by bringing the tube up to 60 psi every few days. Such a pressure drop corresponds to a leak size of about 1 micron. Initially, several days were expended in trying to detect this leak. Valve manufacturers were contacted and various valves were tried. Leak detection systems, including those based on helium, were tried. The precise location of the leak could not be located. However, based on the fact that repeated scrutiny of the tubing did not reveal the presence of any air bubbles, it was assumed that the pressure loss was due to a small leak in the system, but the leak was not in the tubing.

Testing continued until August 4, 1994, when an abnormal loss of pipe pressure was noted. Both ends of the pipe were leaking. Some bubbles were also noted in the central area of the pipe. The pipe was removed from testing. The pipe was filled with natural gas and checked for leakage using a Beckman 400 hydrocarbon analyzer set to detect gas presence at 10 ppm full scale. No leakage was noted in the 20-foot length. The fused end was then replaced with a Dresser coupling. The testing was restarted August 8, 1994, and continued until August 22, 1994. At the suggestion of UCG that a higher pressure may be necessary to observe leakage, the pressure was raised to about 90 psi. No bubbles were observed. Testing was restarted and continued through September 2, 1994, when testing was stopped to replace a Dresser fitting. Testing continued until September 6, 1994, when leakage was noted from the other Dresser fitting. The fitting was repaired and testing continued until September 9, 1994, when the heater failed. The heater was replaced and testing was continued until June 1995.

The pipe samples (one which had never been in service, one containing a pinhole, and one from the same lot as pipe exhibiting pinholes) subjected to thermal cycling did not show the formation of additional pinholes. To further accelerate the aging process, the average temperature was raised to 160 F with a cycling amplitude of ± 10 F. No new pinholes were observed. This suggests that thermal cycles do not directly cause pinholes.

Static Discharge Buildup Experiments

The second experiment was begun after the second meeting with gas industry representatives at Battelle wherein instantaneous static discharge was suggested as a potential cause. Static discharge was one of the first mechanisms that was postulated by Broutman and Associates and by Union Carbide, and was then rejected by both. The pinholes that were originally examined did not exhibit the classic features of high-voltage discharge such as "treeing" and carbon deposition. Further, the holes made by static discharge were thought to be larger than the typical size of the pinholes under consideration. However, to assess all possibilities, an experiment recirculating air containing particulate through PE tubing was begun. The intent was to simulate, under accelerated conditions, the formation of static charge on PE pipe. The charge was to be measured as a function of time to obtain quantitative data on voltage build-up and discharge. The discharge was to be parametrically facilitated using needle electrodes in the pipe wall and external squeeze tools. Although the experiment was initiated and different particulates were used, no through-wall discharges were observed. A schematic of the test setup is shown in Figure 17.

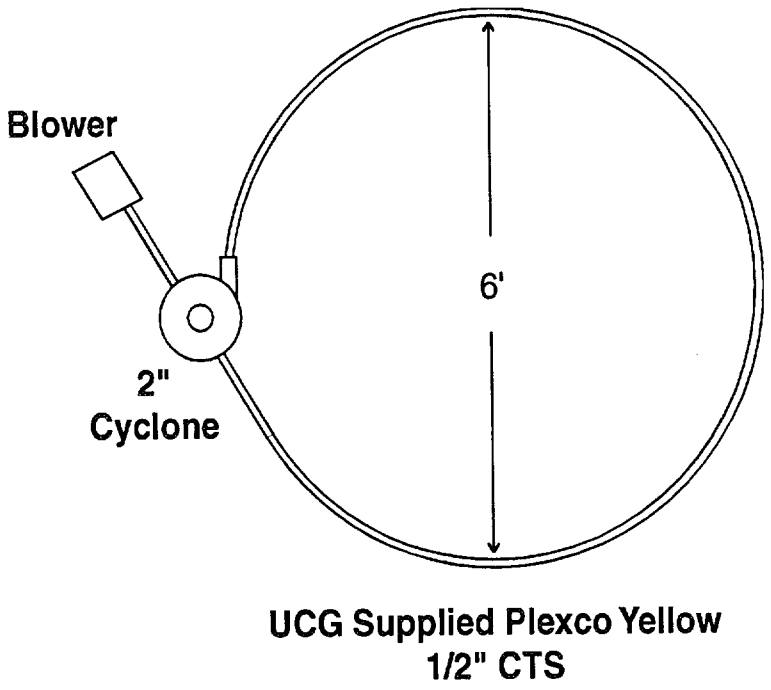

Figure 17. Schematic of test setup for static discharge buildup experiment

PINHOLE MORPHOLOGY

X-Ray Microscopy

It became evident that one of the obstacles in analyzing the pinholes was a lack of adequate characterization of a sufficient number of pinholes. Some pinholes contained inclusions, while others appeared to be relatively clean. Some pinholes appeared in trios while most appeared singly. The total number of pinholes that was studied is a small fraction of the total number discovered. One reason for this was the expense in examining a pinhole. In an effort to reduce this expense and map the existence and paths of pinholes relatively quickly, use of x-ray microscopy was attempted. Two tube samples were taken to a company, Fein Focus, in Columbus, Ohio. Fein Focus has a system that provides image magnification up to a factor of 200, while providing good contrast resolution and brightness. A 5-axis robot system allows easy and flexible manipulation of the specimen so that it can be viewed from various angles in real time. All the examined images can be stored continuously on videotape, and specific images can be frozen, computer-enhanced, and printed as still photographs.

The magnification available with the Fein Focus system proved to be inadequate to examine pinholes. However, while examining the tubing samples, dark spots were observed within the pipe wall. These particles were within the walls and were not surface features, as ascertained by rotating the pipe. Because the spots were darker than the PE matrix, it was concluded that their density was higher than that of PE. Typically the particles were of the order of 5 to 7 mils in size. Several tubing samples from two different manufacturers were examined in this manner. The frequency and size of the spots varied. One tubing sample in which the dark spot was very near two known pinholes was microtomed and analyzed. This is discussed in greater detail in the section titled, "SEM Studies at Battelle."

SEM Studies at the University of Pennsylvania

Professor Norman Brown of the University of Pennsylvania examined a tubing sample that was sent to him by Battelle at GRI's request and a sample sent to him directly by UCG. The resulting photographs are shown in Figures 18 through 27. Figures 18 through 21 and Figures 25 through 27 refer to the sample from UCG, while Figures 22 through 24 refer to the sample from Battelle. Figure 18 shows the outside of the pipe with a cluster of three holes. A matching cluster of three holes was found on the inside surface, indicating that there was no "branching" of the holes. Figure 19 shows the inside surface of one of the pinholes. Figure 20 shows a fibrilla surface of the inside wall of the hole at a magnification of 3000X. Figure 21 shows the outside surface of the same hole. Figure 22 shows a pinhole at the inside diameter. Figure 23 is an enlargement of Figure 22. Figure 24 is the same view using backscattered electrons. Figures 25 through 27 are views of a possible leak about 6 inches away from the cluster of three holes.

SEM Studies at Battelle

A tubing sample containing two pinholes and an inclusion as seen using x-ray microscopy was studied. Figure 28 (photo ID 1065) shows the two pinholes identified as "1" and "2" looking at the outside diameter (OD) of the pipe. The mark identified as "A" is not a pinhole but only a triangular surface indentation. At the lower edge of Figure 28 are notches made by a razor marking the locations where the pinholes were known to be located from the leak tests. Another view of "1" and "A" at greater magnification is shown in Figure 29 (photo ID 1066). A magnified view of the surface indentation "A" is shown in Figure 30 (photo ID 1064). Magnified views of pinhole "1," at magnifications of 200X and 500X, are shown in Figures 31 (photo ID 1062) and 32 (photo ID 1063) respectively. Figure 32 has been tilted 50 degrees to obtain a better perspective. Pinhole "1" has an exit that resembles circularity but a close examination (Figure 32) indicates that this is somewhat illusory and the opening is at least partially blocked. Enlarged views of pinhole "2," at magnifications of 75X, 150X, and 750X, are shown in Figures 33 through 35 (photo IDs 1067, 1068, and 1069) respectively. Pinhole "2" has an exit that is far from circular. Both the pinholes at the OD display rough edges.

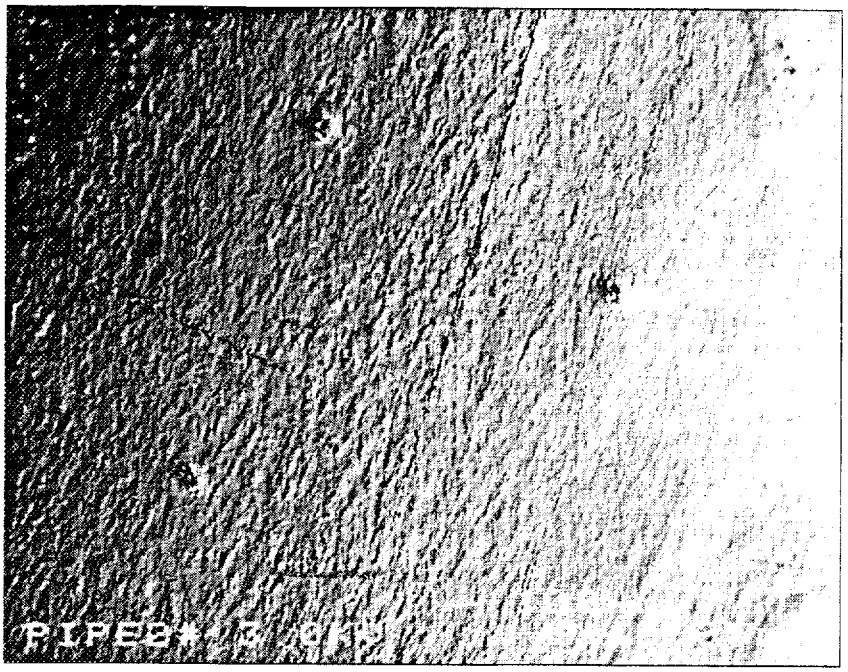

Figure 18. Three pinholes on outside surface (U. of Pennsylvania)

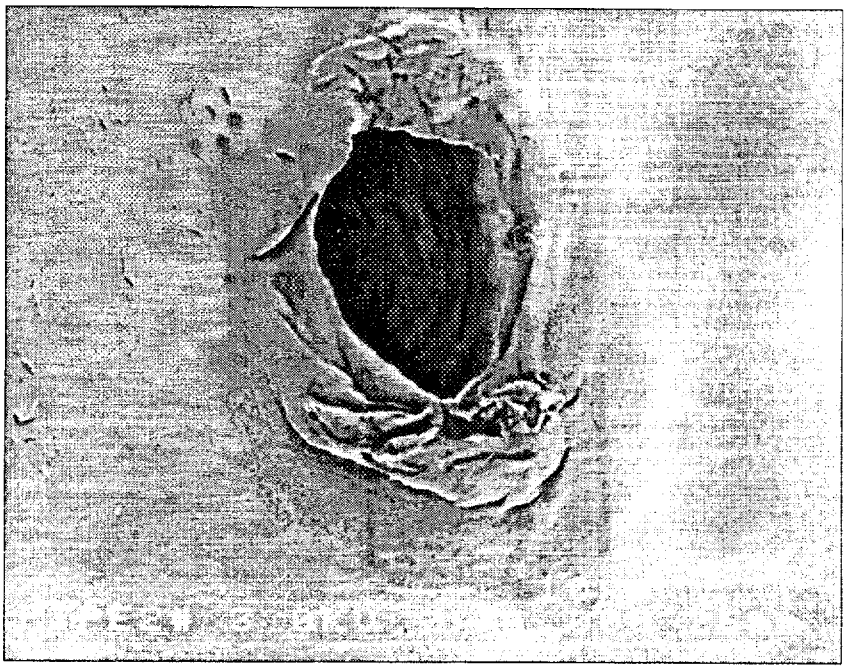

Figure 19. Inside surface of one of the pinholes (U. of Pennsylvania)

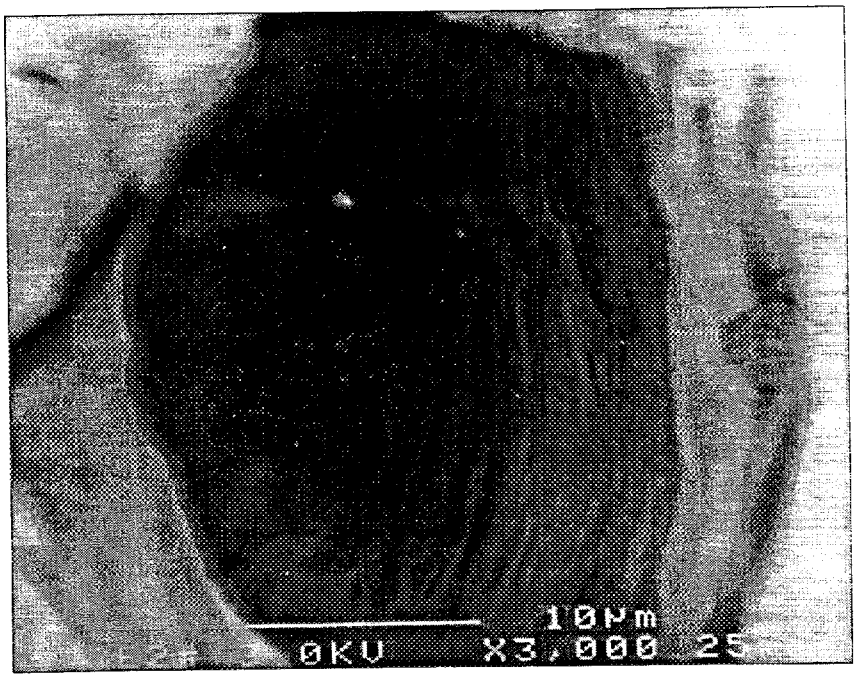

Figure 20. Fibrilla surface of inside wall of hole (U. of Pennsylvania)

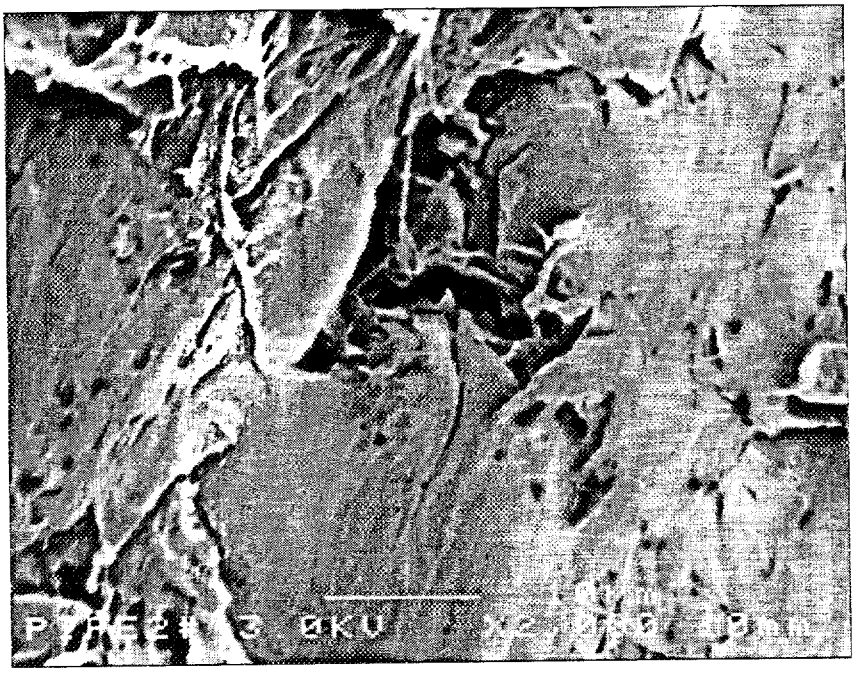

Figure 21. View of a pinhole at outside surface (U. of Pennsylvania)

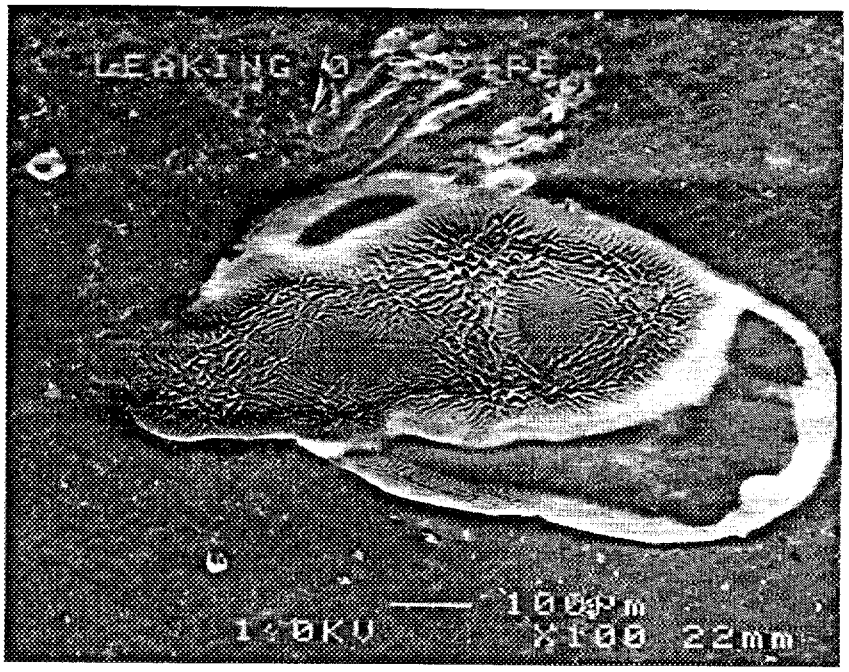

Figure 22. View of a pinhole at inside surface (U. of Pennsylvania)

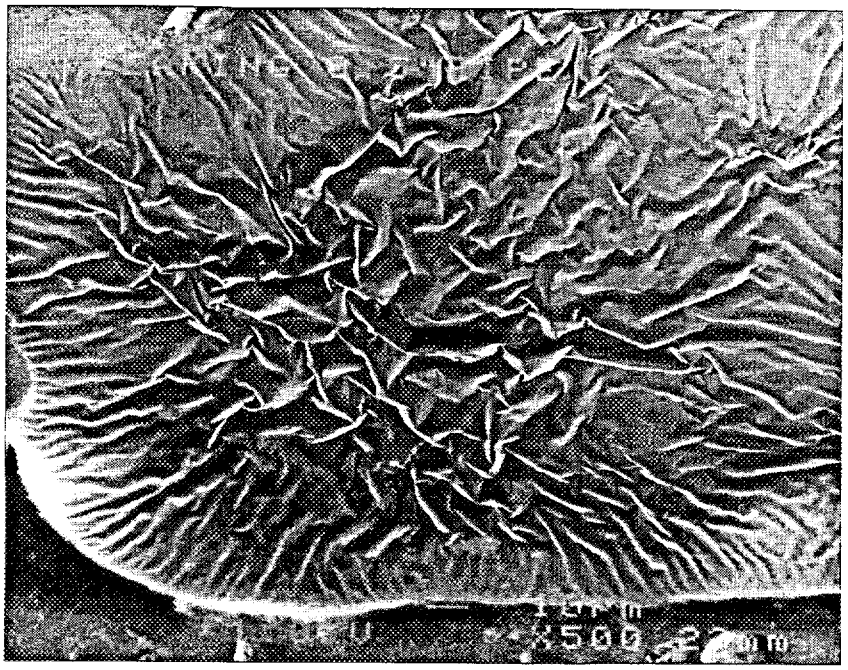

Figure 23. Enlarged view of Figure 22 (U. of Pennsylvania)

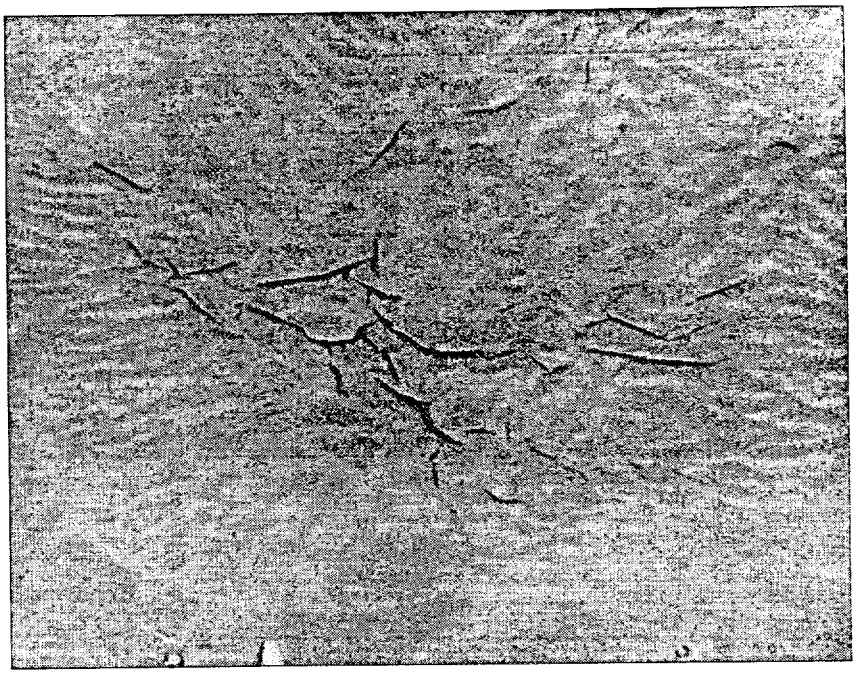

Figure 24. View of Figure 22 using backscattered electrons (U. of Pennsylvania)

Figure 25. View of a small probable leak on outside of pipe (U. of Pennsylvania)

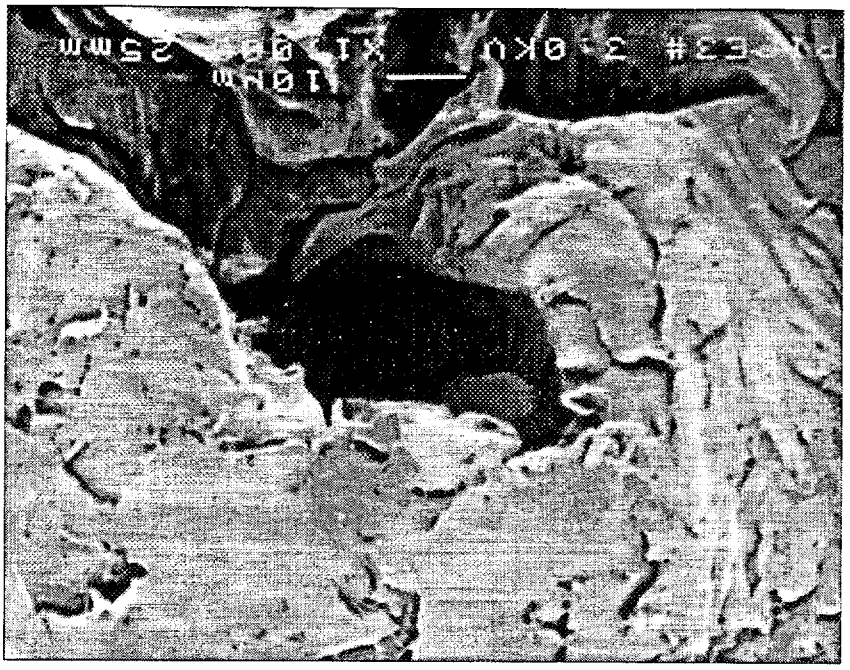

Figure 26. Enlarged view of Figure 25

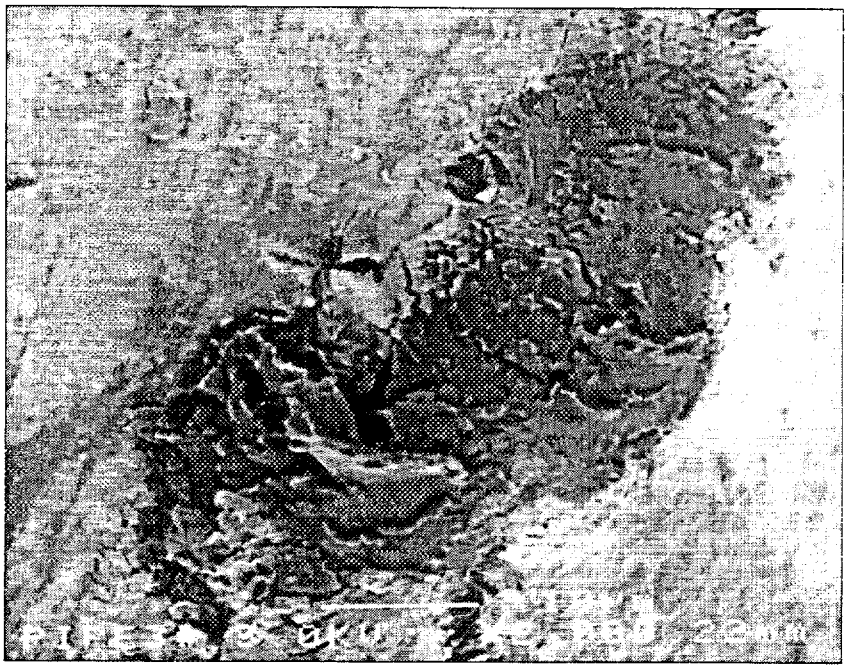

Figure 27. View of the pinhole in Figure 25 at inside surface of pipe

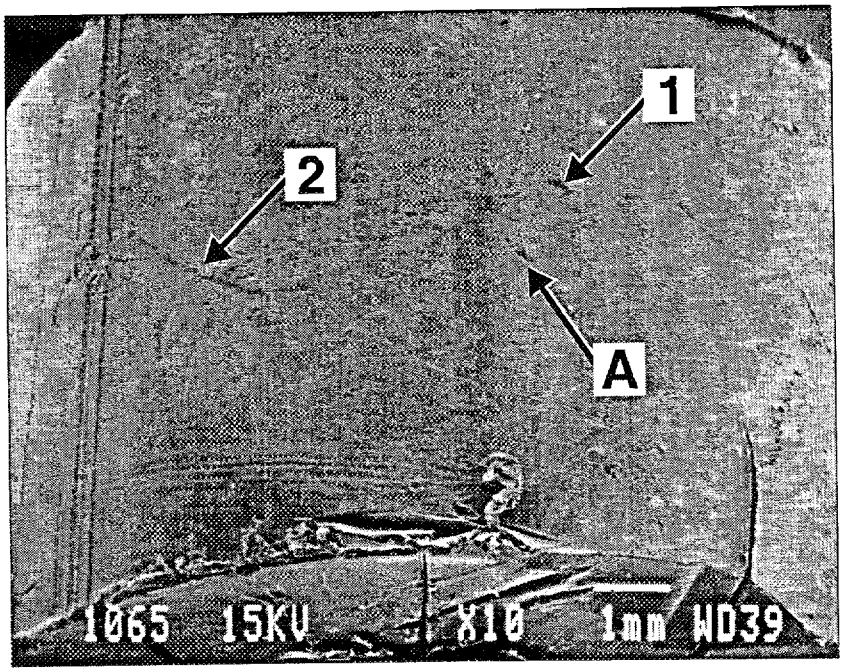

Figure 28. Two pinholes, "1" and "2," at outside diameter; "A" is a surface indentation

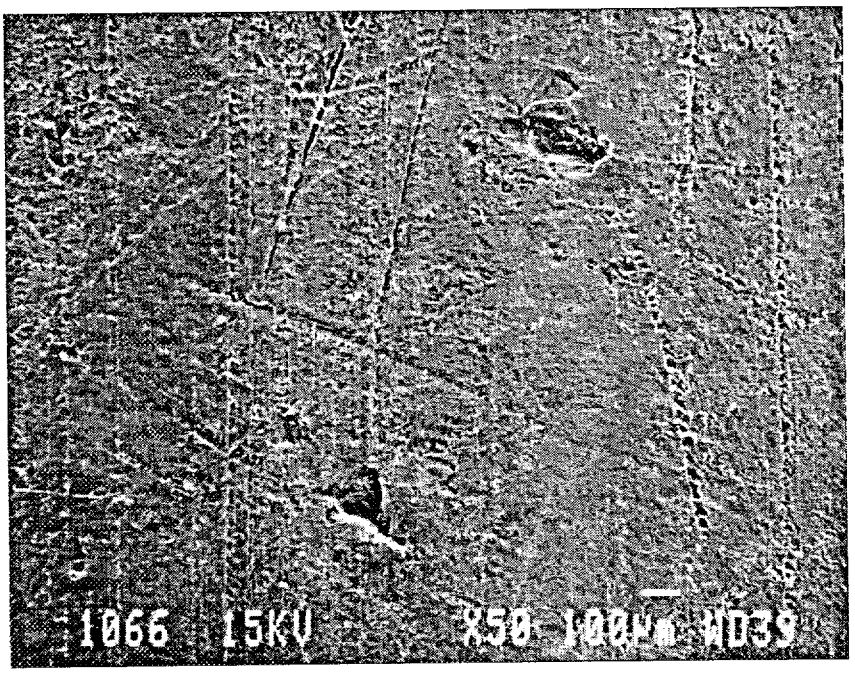

Figure 29. Magnified view of "1" and "A" in Figure 28

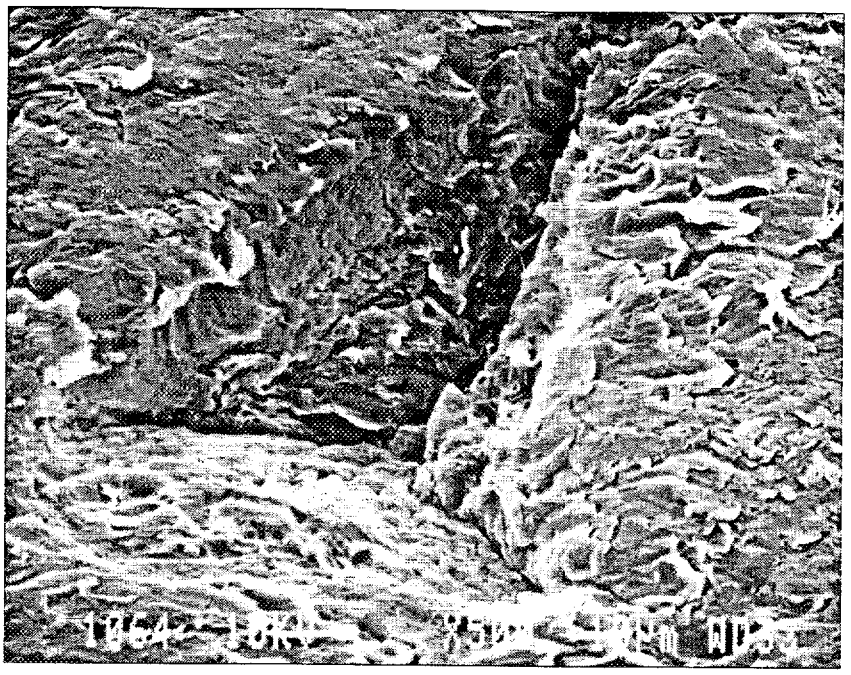

Figure 30. Further magnified view of "A" in Figure 28

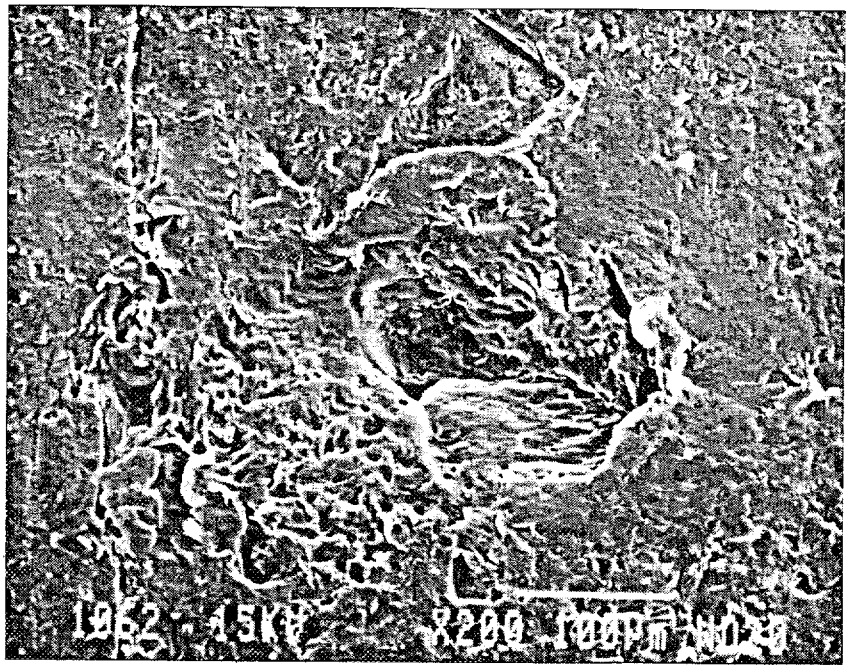

Figure 31. 200X view of Pinhole "1"

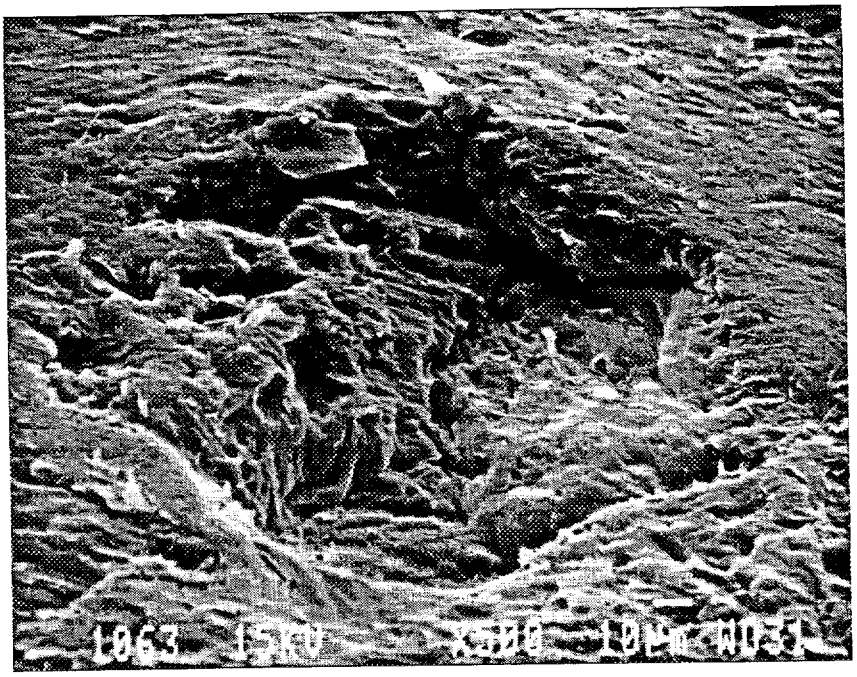

Figure 32. 500X view of Pinhole "1"

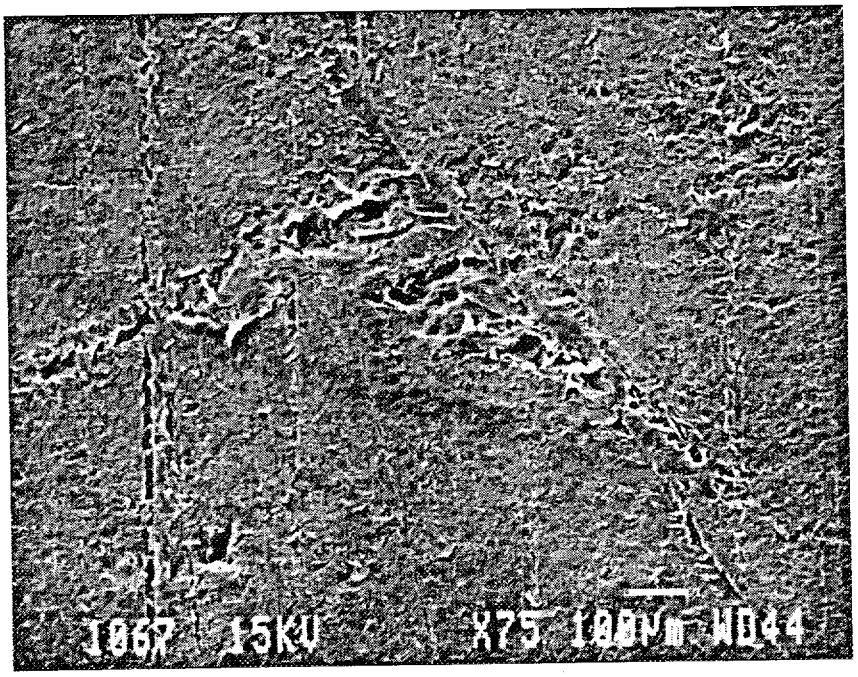

Figure 33. 75X view of Pinhole "2"

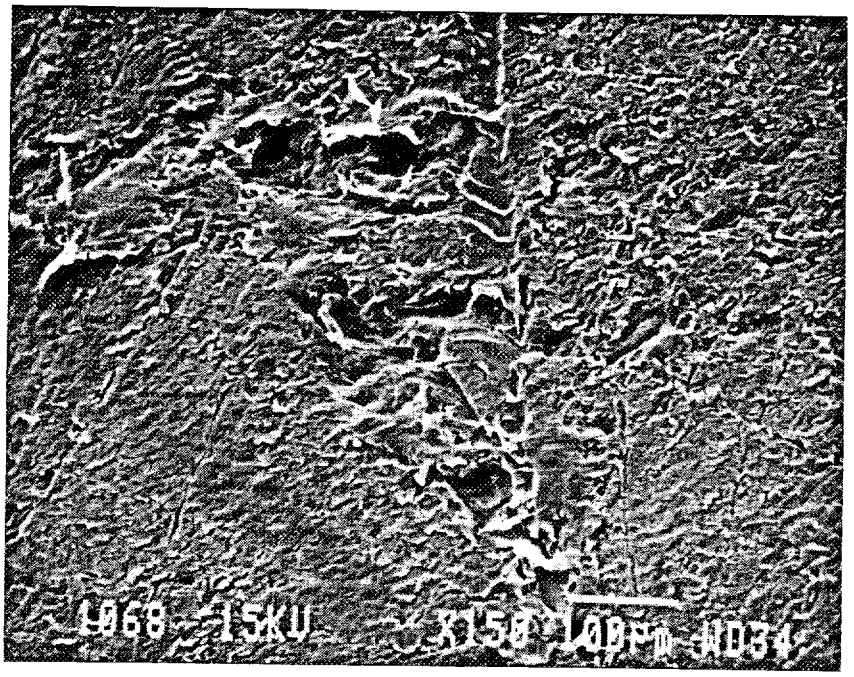

Figure 34. 150X view of Pinhole "2"

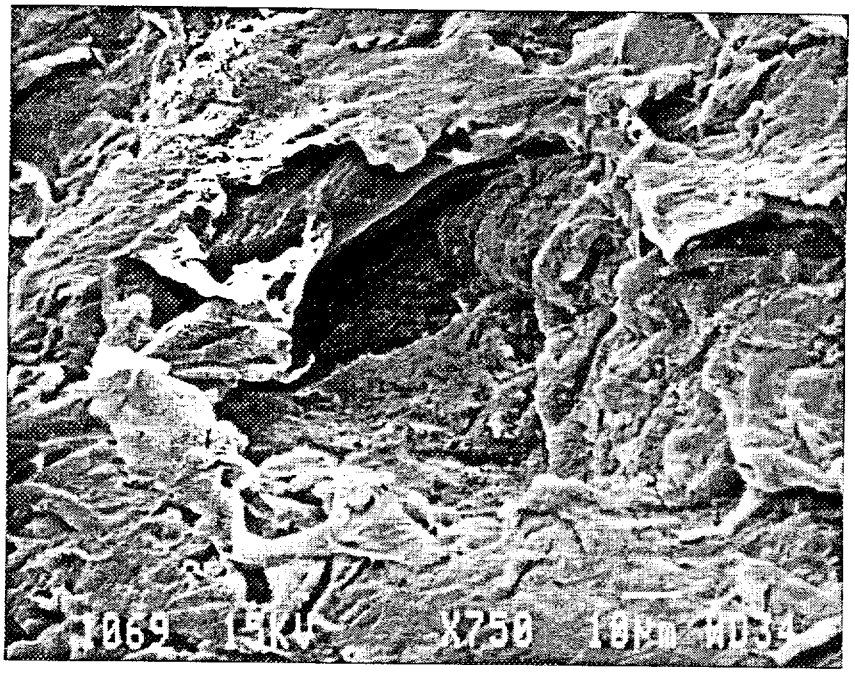

Figure 35. 750X view of Pinhole "2"

Figure 36 (photo ID 1070) shows the two pinholes at the inside diameter (ID) of the pipe. Figures 37 (photo ID 1071) and 38 (photo ID 1072) are magnified views of the pinholes at the ID. The pinholes at the ID have a dramatically different appearance than at the OD. The appearance at the ID is also similar to the appearance of pinholes at the ID in photographs taken by Professor Norman Brown (Figure 22). The material covering or filling the pinholes is visually distinctive and appears to have melted and resolidified.

After surface examination using SEM, the tubing with the two pinholes and the dark spot was immersed in liquid nitrogen for about 30 minutes to ensure that the sample was completely frozen. It was then snapped in two. The hope was that the fracture plane would pass through the material representing the dark spot, which could then be examined. A backscattered electron image of the fracture surface is shown in Figure 39 (photo ID 9133) at a magnification of 48X. A more conventional scattered electron image at 1000X is shown in Figure 40 (photo ID 9134). The line drawn on Figure 40 represents the location of the particle that appears as a dark spot on the x-ray image. It is not easy to identify it in Figure 40. However, Figure 41 (photo ID 9135) is a backscattered image of the same area and the particle can be seen distinctly. Figure 42 (photo ID 9136) shows the same view mapped for silicon, and Figure 43 (photo ID 9137) shows the same view mapped for oxygen. No carbon was detected in the particle, which appears to contain silicon and some oxygen. The spectroscopic analysis of the area containing the particle shows the presence of Si, P, S, Cl, Ti, and Cr as shown in Figure 44, but some of the elemental indications other than Si may be due to surface contamination. The particle dimensions appear to be about 60 microns by 40 microns in the plane of fracture. Because the data are drawn from different sources, it is not possible to relate the position of the particle to the position of the pinholes, or even state whether a connection exists.

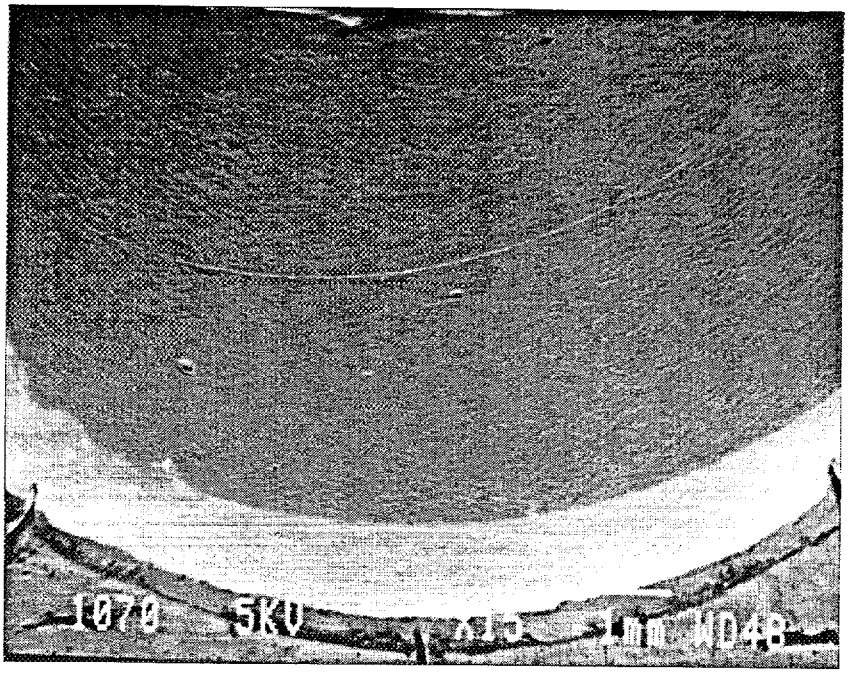

Figure 36. Two pinholes at inside diameter of pipe

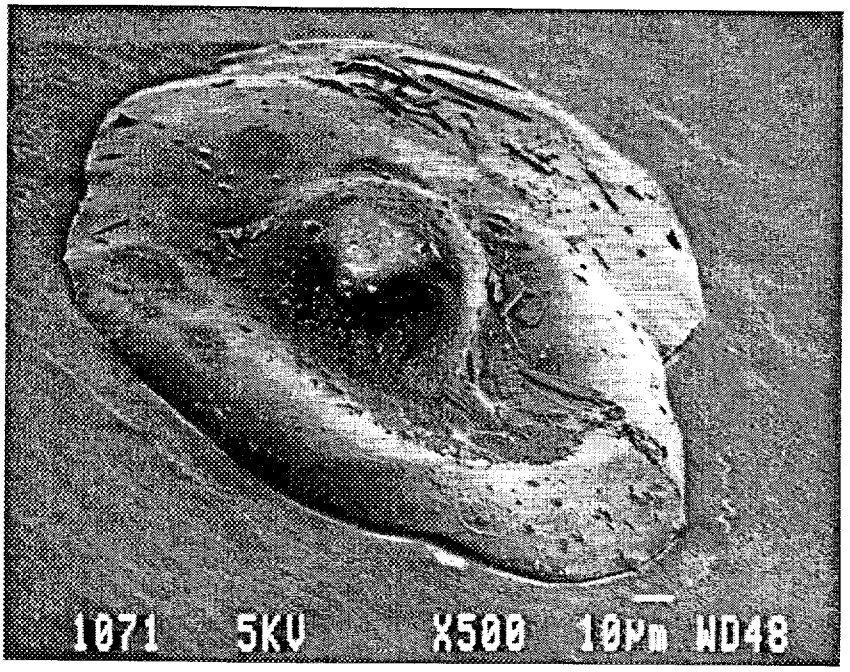

Figure 37. Magnified view of pinhole in Figure 36

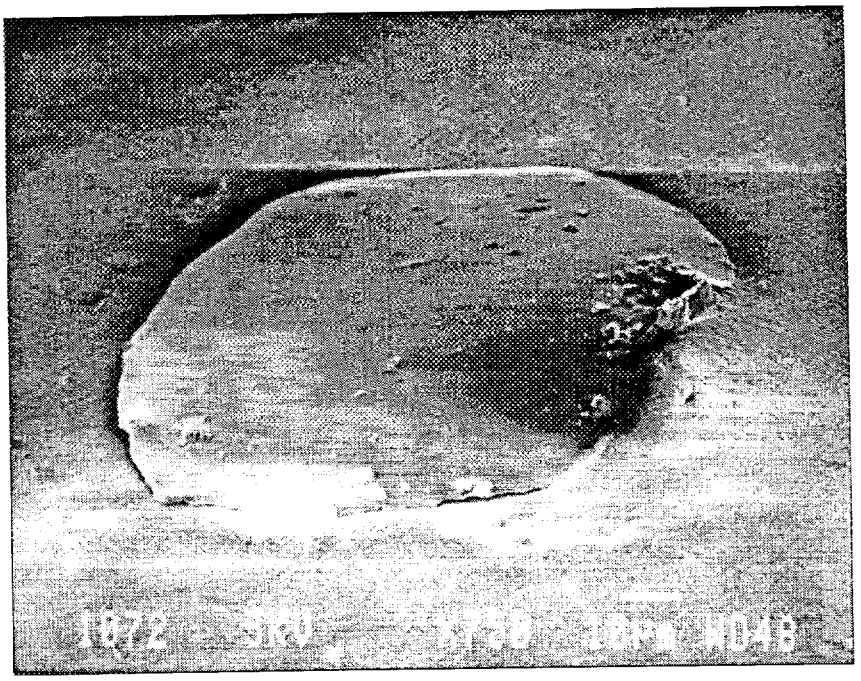

Figure 38. Magnified view of pinhole in Figure 36

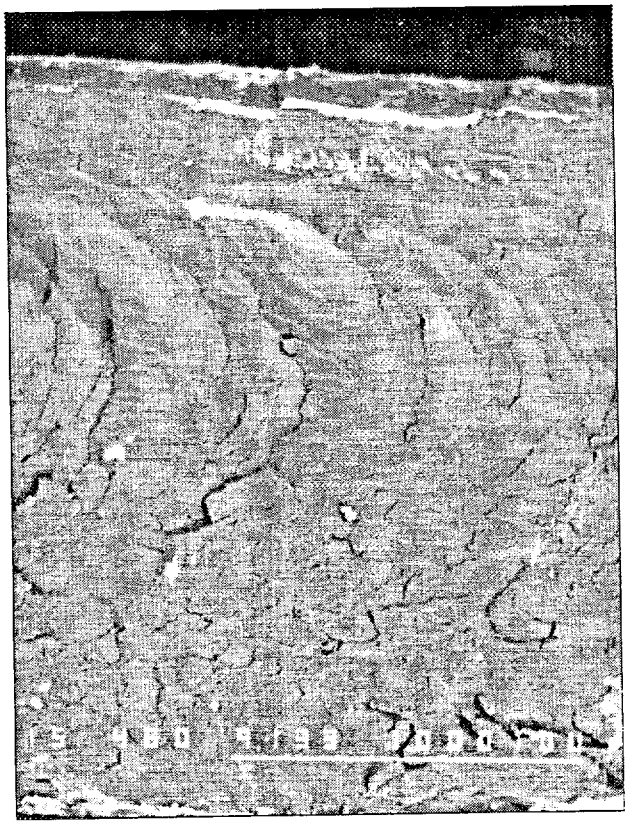

Figure 39. 48X image of fracture surface using backscattered electrons

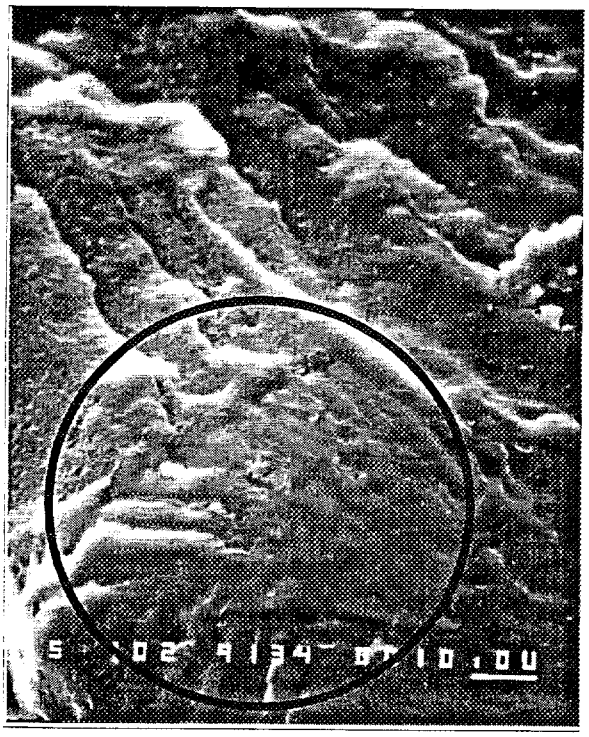

Figure 40. 1000X view of same area as in Figure 39 using conventional electron scattering

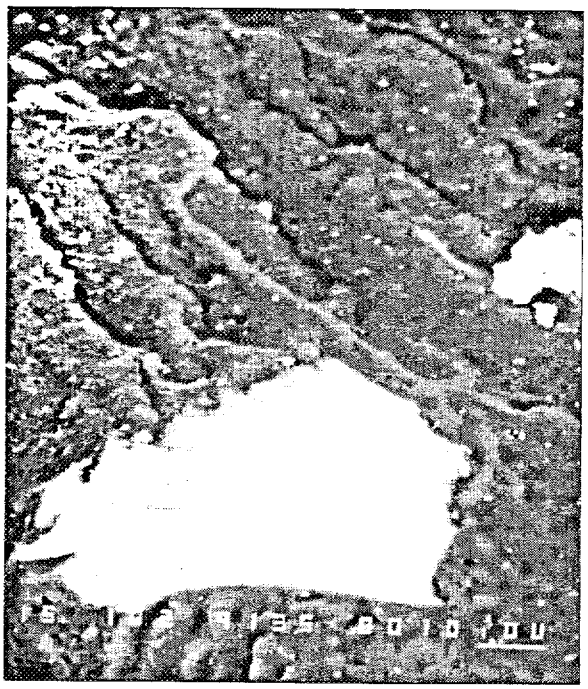

Figure 41. 1000X view of same area as in Figure 39 using backscattered electrons

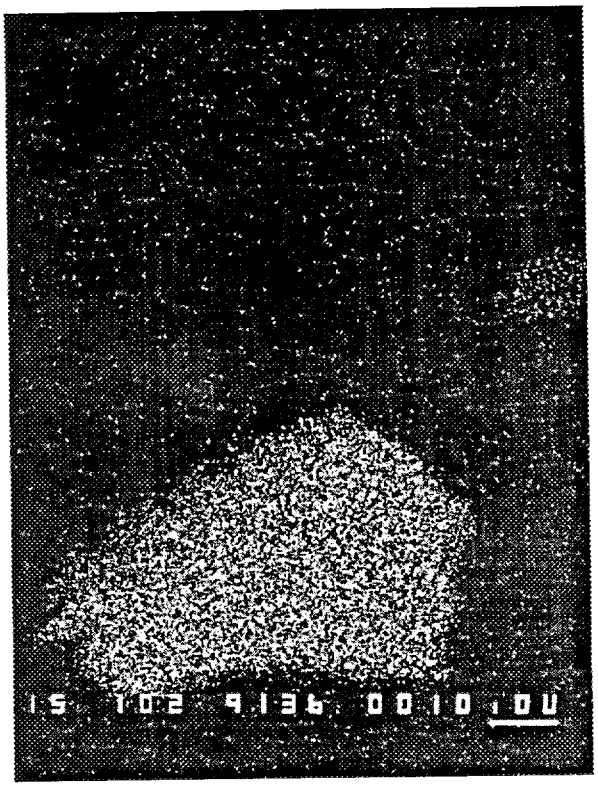

Figure 42. Same area as in Figure 41 mapped for elemental silicon

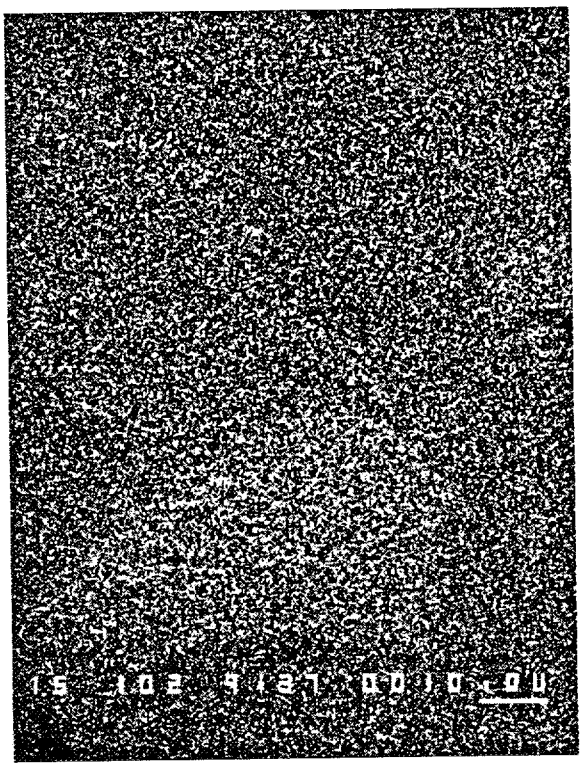

Figure 43. Same area as in Figure 41 mapped for elemental oxygen

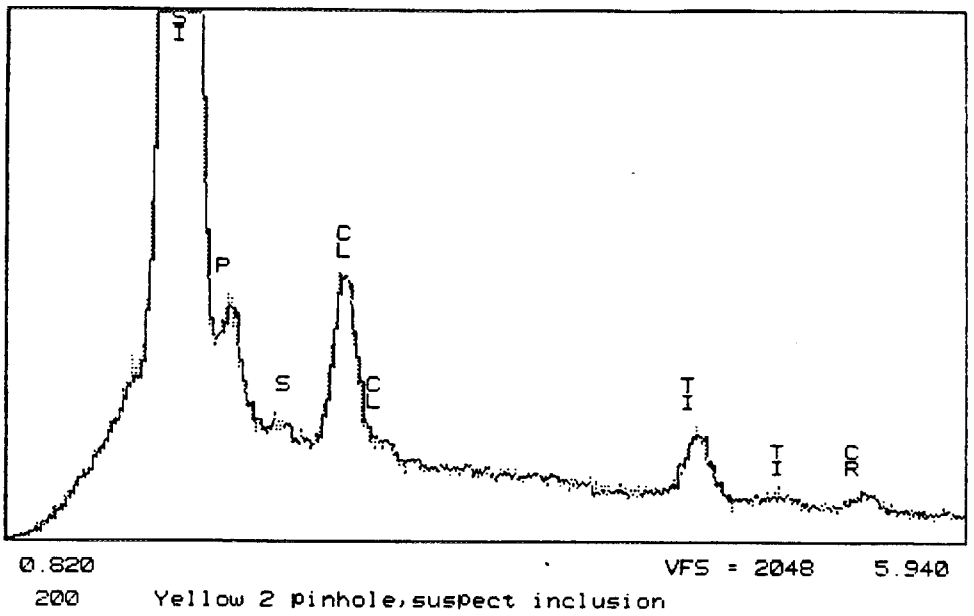

Figure 44. Spectroscopic analysis of the particle in Figure 41

Another tubing specimen containing a pinhole was found to contain an embedded surface particle. The particle could have been embedded thus in a number of ways. Nonetheless, a microscopic and chemical examination was undertaken. The particle was found to contain mainly cadmium and sulfur, and the surrounding area was rich in silicon.

Baby Pinholes

Pinhole locations in two specimens from the field were studied in order to define the morphology of the leaks along the path of the pinholes. Both leak locations occurred on the same pipe section. The first location was termed P5-A and the other was termed P5-B.

A low-magnification (12x) overview of P5-A at the OD (outer diameter) of the pipe is shown in Figure 45 (photo ID 1264). The areas marked 1, 2, and 3 are possible pinholes. The reason for the uncertainty is that the holes are not distinctive. Figures 46, 47, and 48 (photo IDs 1265, 1268, 1269) show the marked areas at greater magnifications. The composition of a particle in area 2 was analyzed and found to be mainly silicon and aluminum. This particle was on

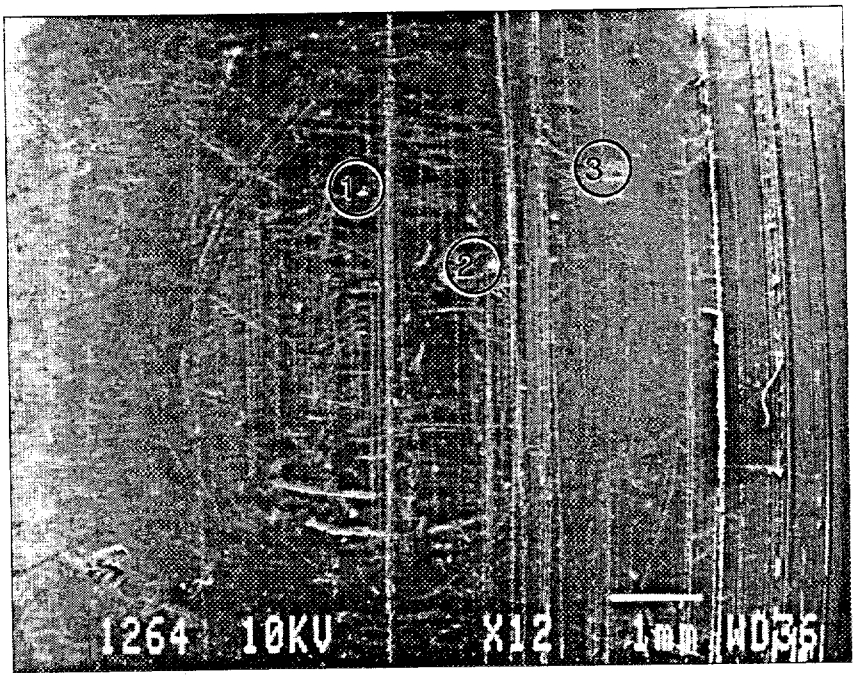

Figure 45. Overview of P5-A at OD (12X)

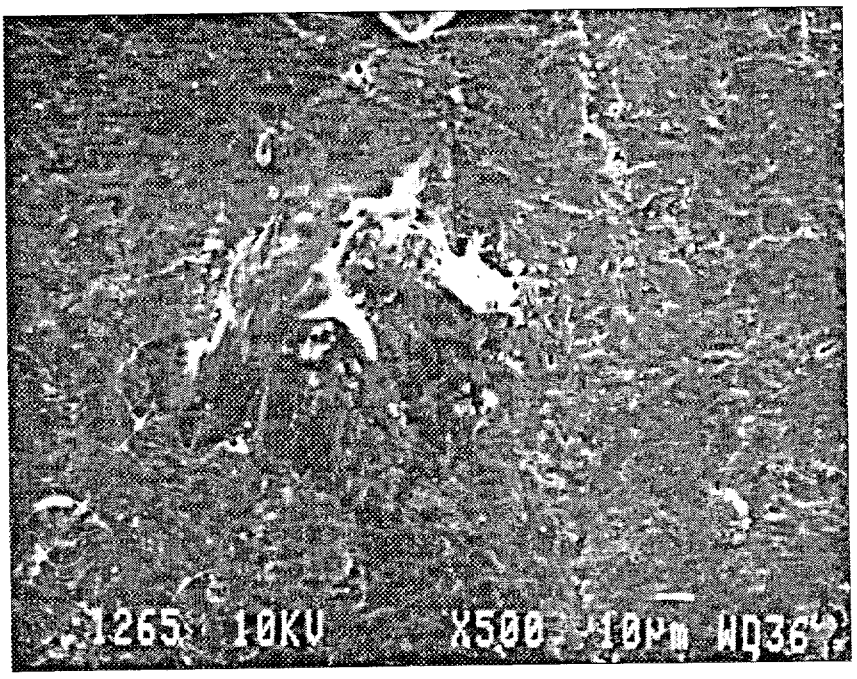

Figure 46. Enlarged view of marked area #1 (500X)

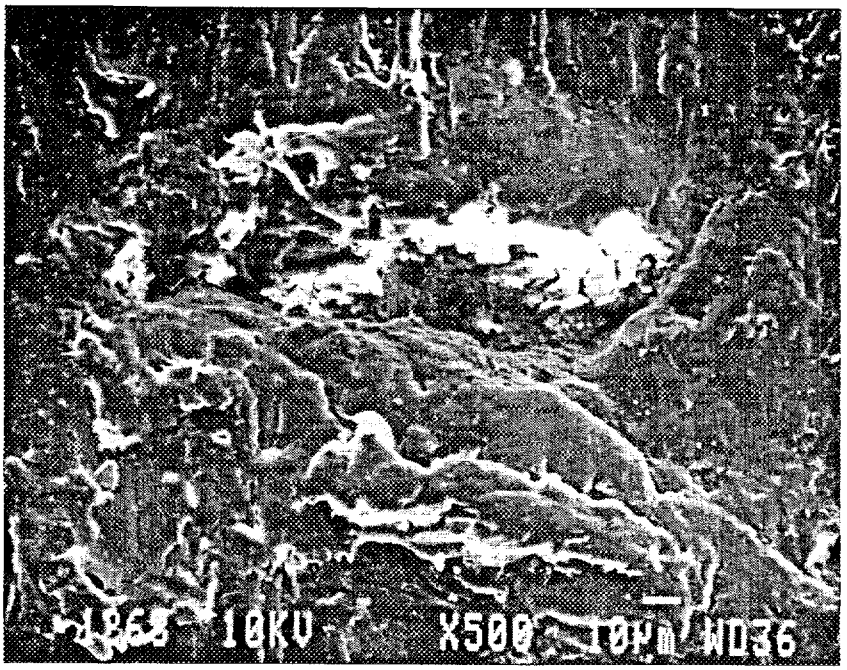

Figure 47. Enlarged view of marked area #2 (500X)

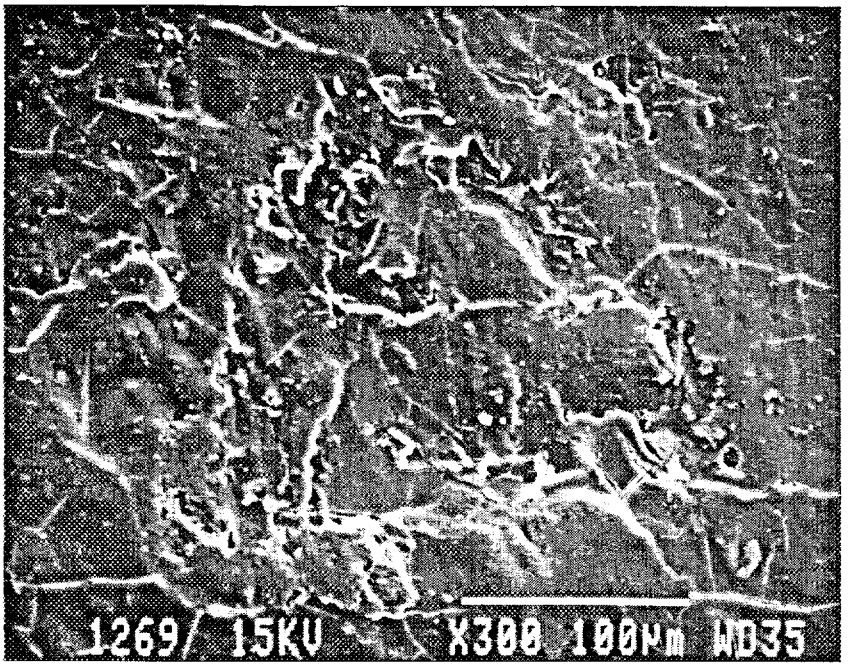

Figure 48. Enlarged view of marked area #3 (300X)

the surface and is not considered to be significant. Figure 49 (photo ID 1274) shows the two pinholes visible on the inside diameter of P5-A. This photograph clearly shows the two types of pinhole openings observed at the inside diameter. The opening on the left has material buildup around the rim, with an open (unblocked) entrance. The opening on the right cannot be seen because the opening is covered with a circular "cap" whose smooth appearance suggests the possibility of melted and resolidified material. Figures 50 (photo ID 1273) and 51 (photo ID 1275) show enlarged views of the opening on the left. Figure 52 (photo ID 1276) shows an enlarged view of the opening on the right. Figure 53 (photo ID 1277) shows the opening on the right from a point of view very close to the pipe surface. This view shows that the material blocking the opening on the right is mushroom-like, with the material along the edge hanging over the pipe surface.

Figure 54 (photo ID 1270) shows a low-magnification overview of the outer diameter of the pipe at P5-B. Figures 55 (photo ID 1271) and 56 (photo ID 1272) show enlarged views of the areas marked "1" and "2" in Figure 54, respectively. One hole was visible on the inside diameter. Three views of this hole on the inside diameter are shown in Figures 57 (photo ID 1279), 58 (photo ID 1278), and 59 (photo ID 1280) at increasing magnifications.

P5-B was microtomed in thin slices so that the plane of the slices was always perpendicular to the axis of the pinhole. Each microtomed slice was about 1 to 3 mils thick. After each slice was removed, the pinhole was examined. A reference hole in the pipe (drilled for this purpose) allows the meandering of the hole in the horizontal plane to be tracked. Although this is painstaking and time-consuming, it is the only method for determining the path and dimensions of the pinhole as it progresses through the pipe wall. The slicing was begun at the outer diameter. Figure 60 (photo ID 1336) shows the pinhole (located at the upper left) after the first few slices had removed the surface. A particle composed mainly of silicon can be seen at the lower left. Magnified views of the pinhole and particle are shown in Figures 61 (photo ID 1337) and 62 (photo ID 1338). Figure 63 (photo ID 1339) shows the view after a few more slices had been removed.

Figure 63 is at relatively low magnification (40x) in order to encompass the desired field of view. Of the three white spots (almost in a line) along the top edge, the left-most is a solid particle,

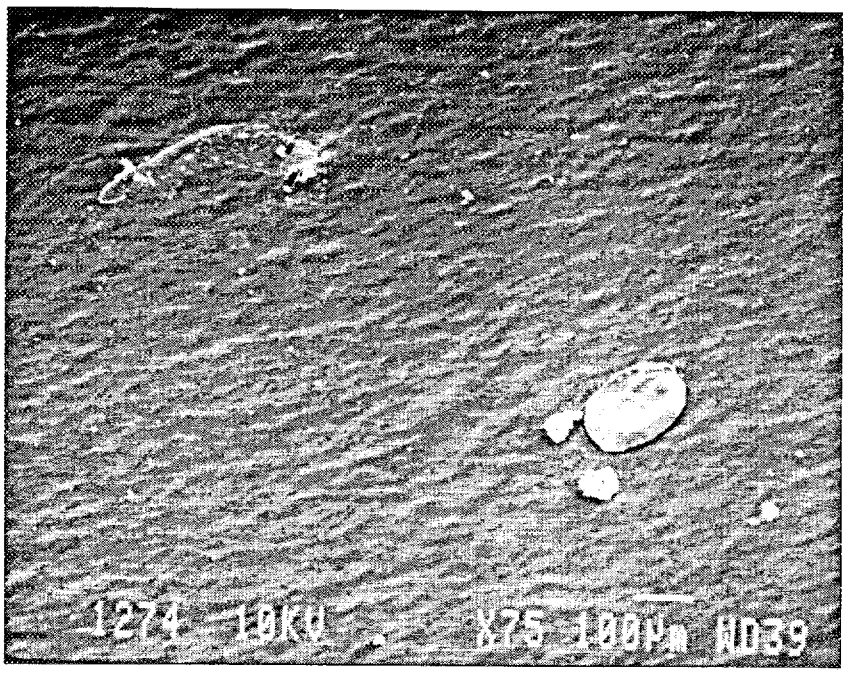

Figure 49. Two pinholes on ID of P5-A

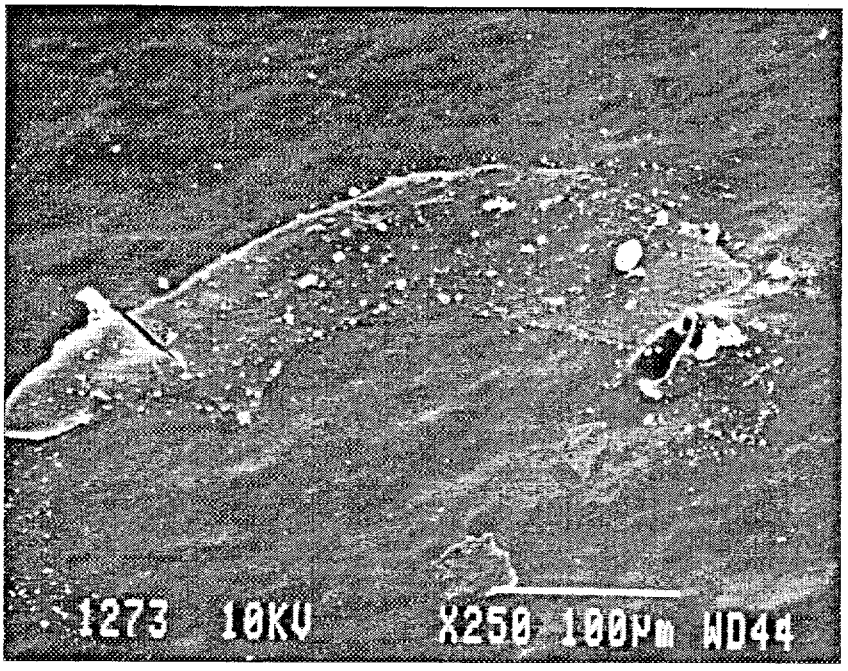

Figure 50. Enlarged view of opening on left of P5-A (250X)

Figure 51. Enlarged view of opening on left of P5-A (1000X)

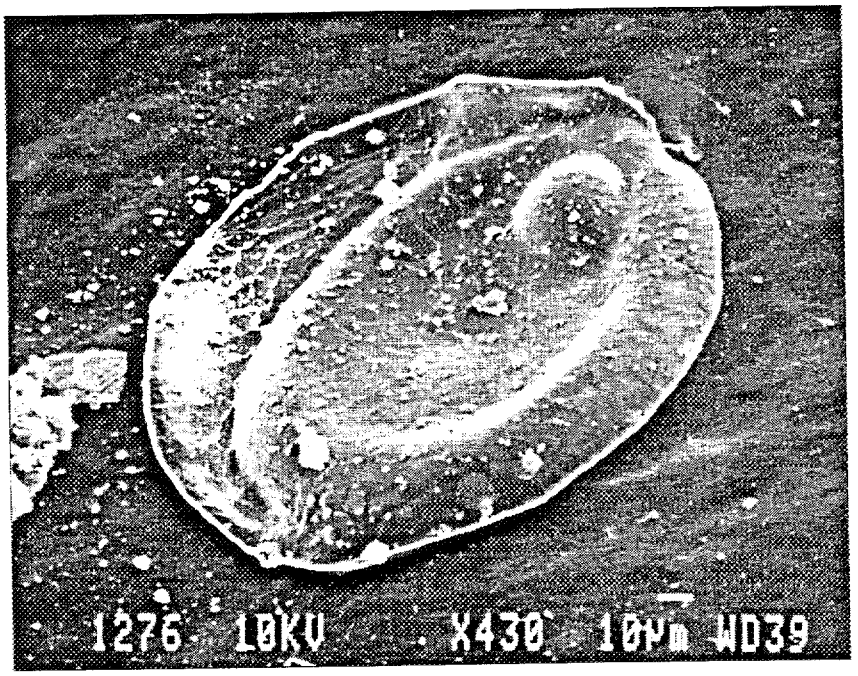

Figure 52. Enlarged view of opening on right of P5-A (430X)

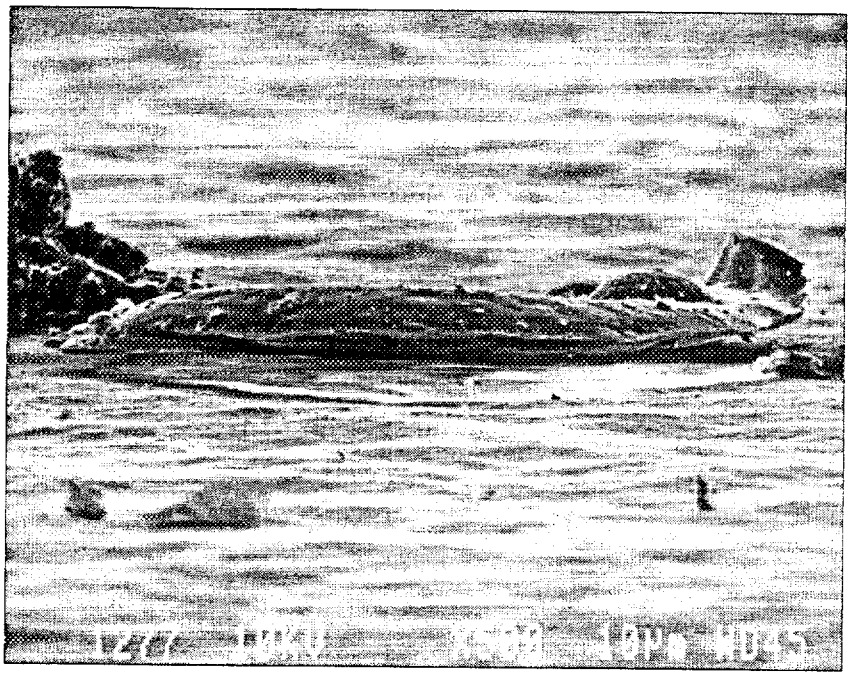

Figure 53. Opening on right from very close to surface (500X)

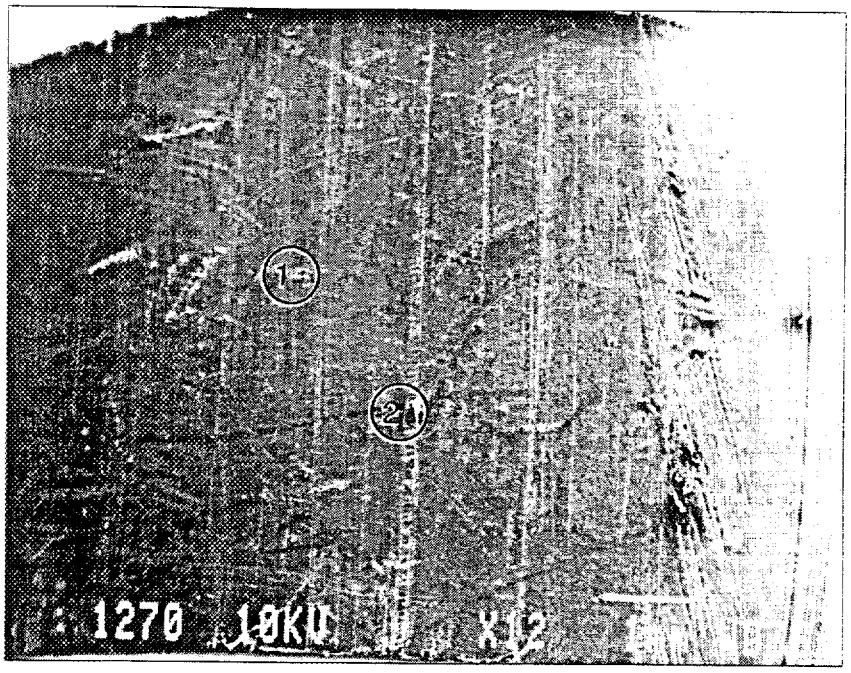

Figure 54. Overview of P5-B at OD (12X)

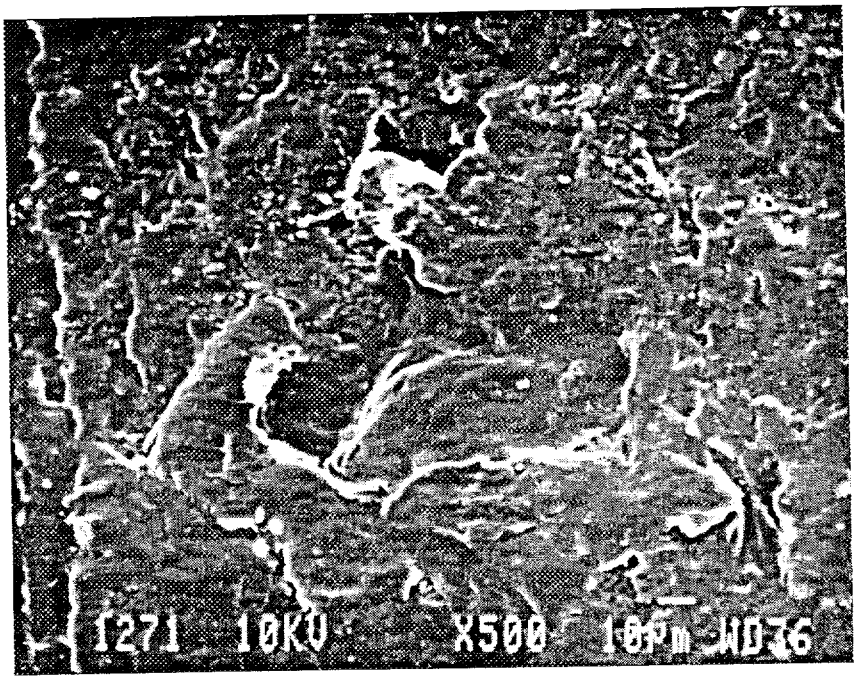

Figure 55. Enlarged view of Area 1

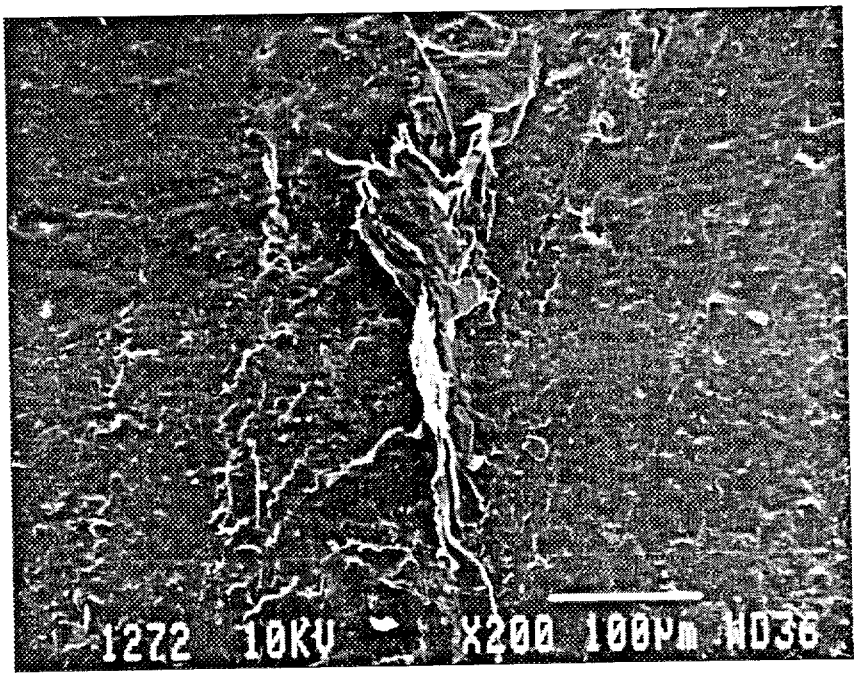

Figure 56. Enlarged view of Area 2

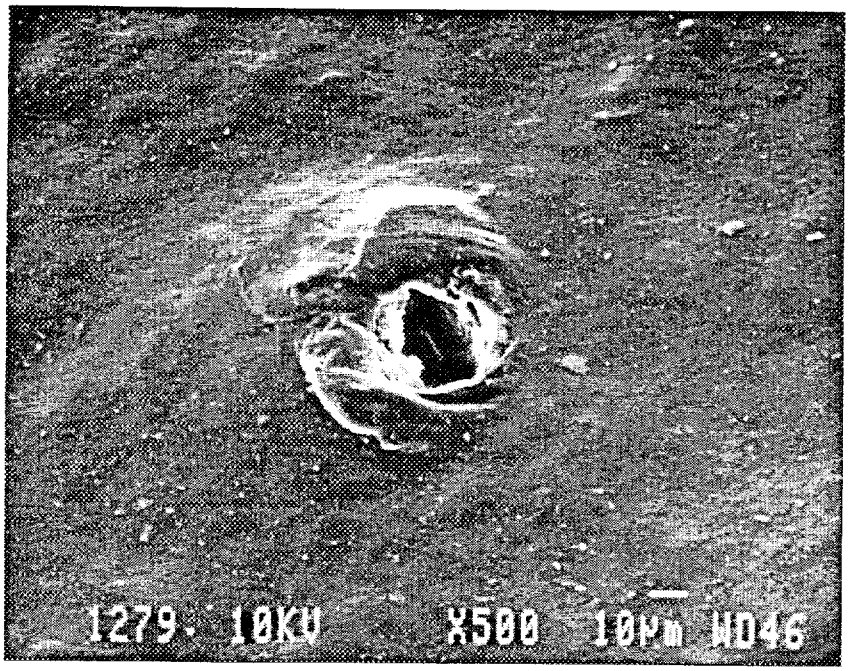

Figure 57. Hole on ID of P5-B (500X)

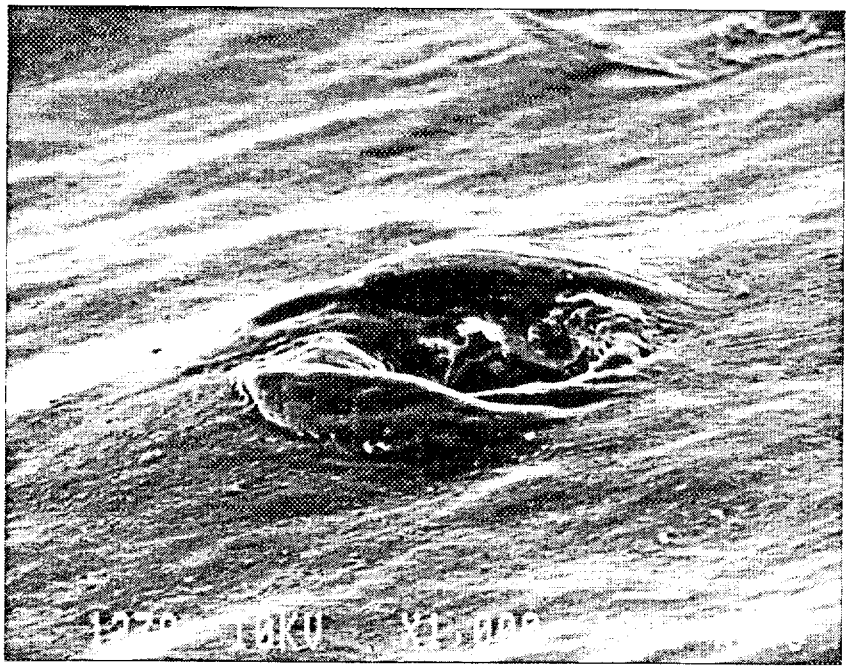

Figure 58. Hole on ID of P5-B (1000X)

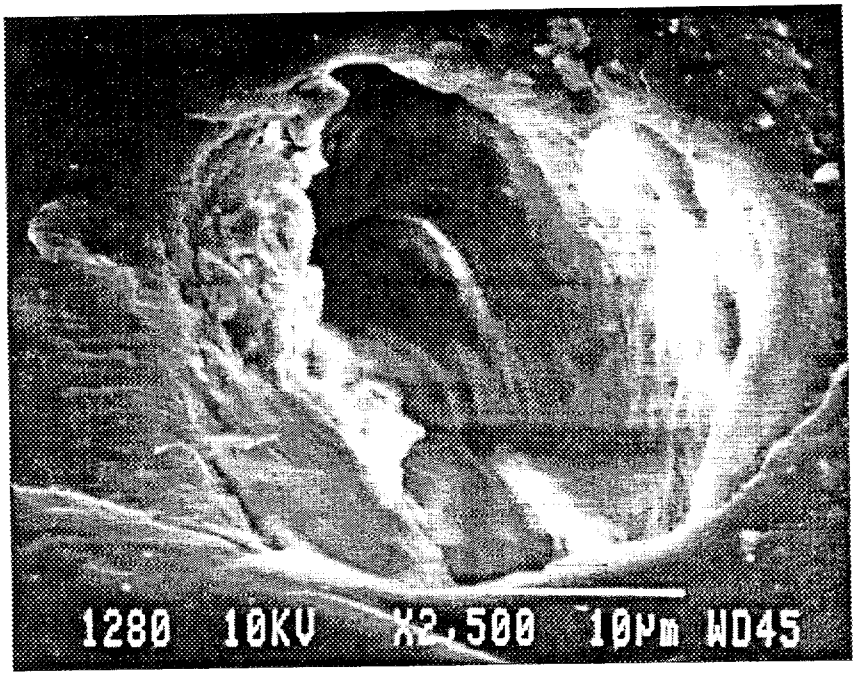

Figure 59. Hole on ID of P5-B (2500X)

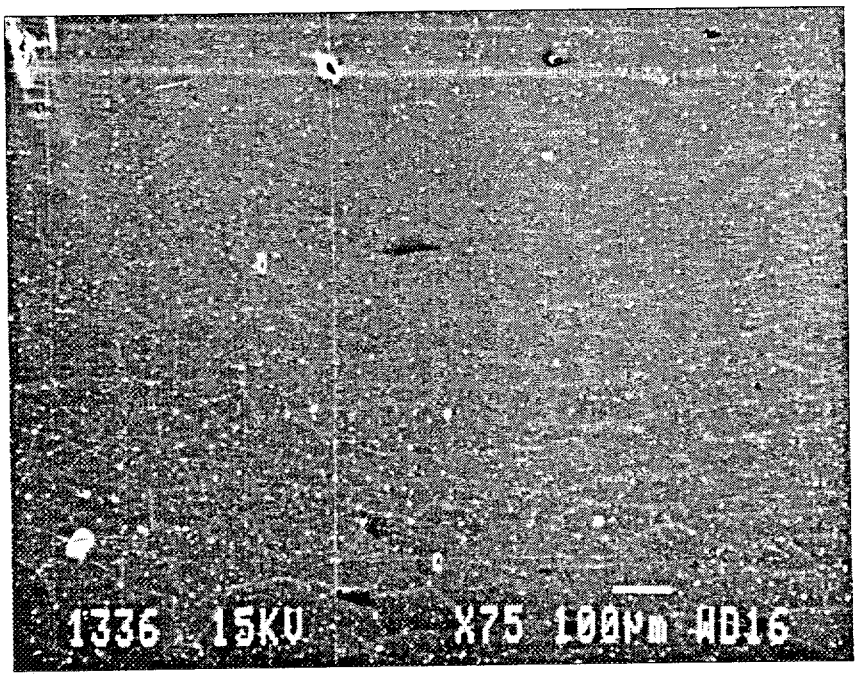

Figure 60. Pinhole after first few microtome slices

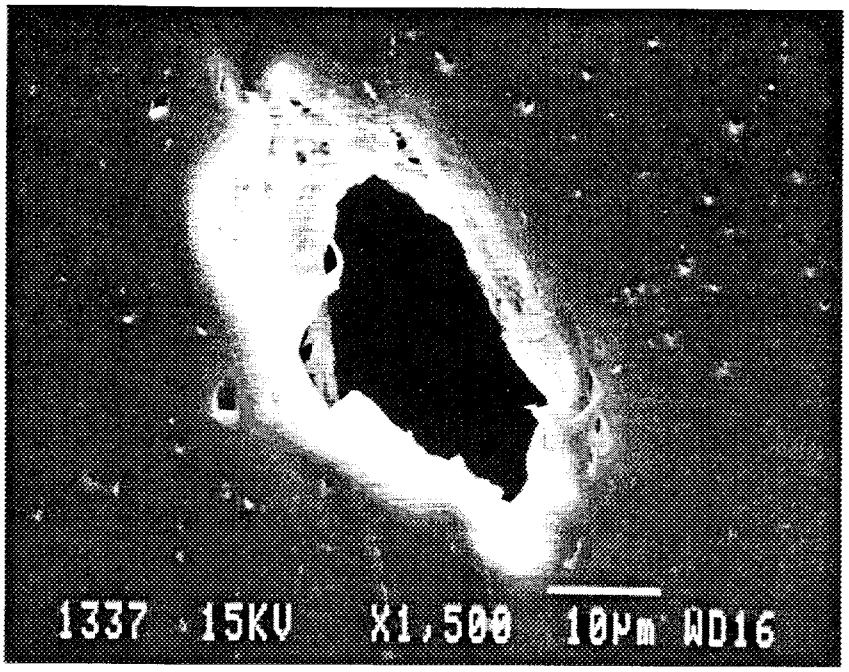

Figure 61. Magnified view of one of the pinholes in Figure 60 (1500X)

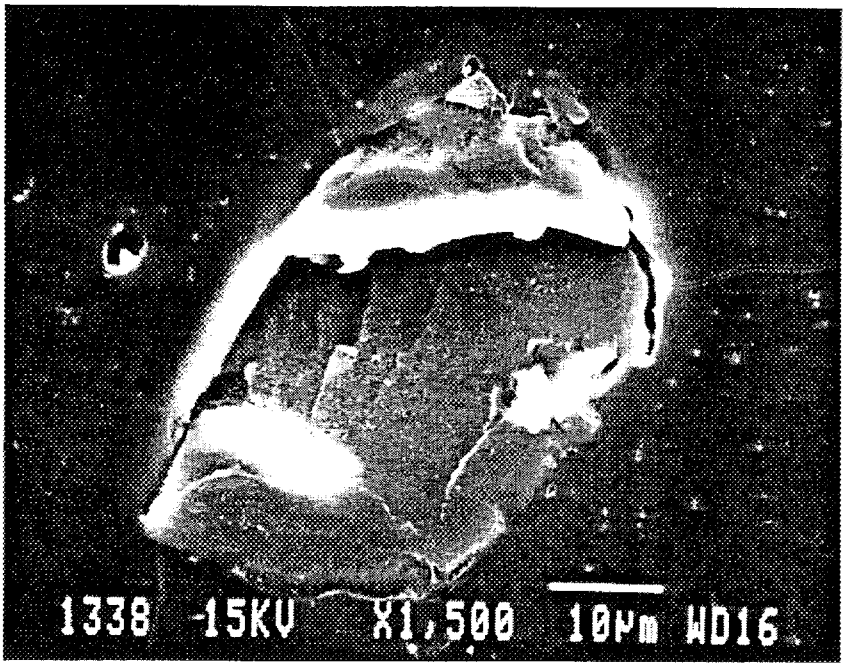

Figure 62. Magnified view of silicon particle in Figure 60 (1500X)

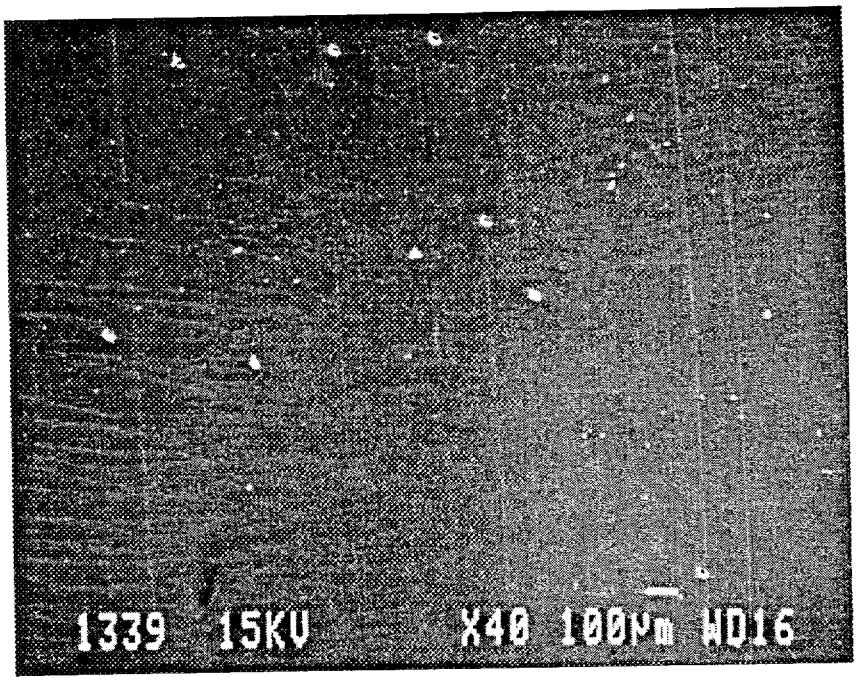

Figure 63. Pinhole after second set of microtome slices (40X)

while the other two are pinholes. The center one is designated as "1," and the one on the right as "2." The cluster of three white spots (in the shape of a triangle) at the center-right of the picture consists of two pinholes (designated "3" and "4") and a solid particle. The remaining two white spots (center-left) consist of a pinhole on the left (designated "5") and a solid particle on the right. In going from Figure 60 to Figure 63, no evidence of branching was observed. Figure 64 (photo ID 1340) shows an enlarged view of pinholes "1" and "2" in Figure 63. Figure 65 (photo ID 1342) shows enlarged views of pinholes "3" and "4" in Figure 63. Figure 66 (photo ID 1343) shows a high-magnification view of pinhole "4." Figure 67 (photo ID 1344) shows a high-magnification view of pinhole "5." Additional microtoming was continued until about one-third of the wall had been removed. The pinholes that had appeared in the interior of the pipe wall retained their identity as distinct pinholes through this depth.

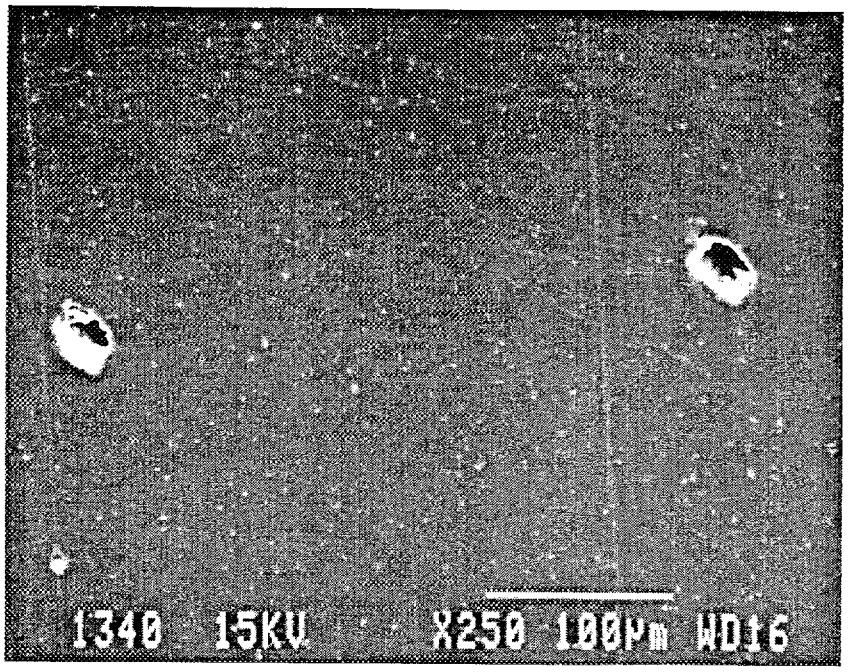

Figure 64. Enlarged view of Pinholes 1 and 2 from Figure 63

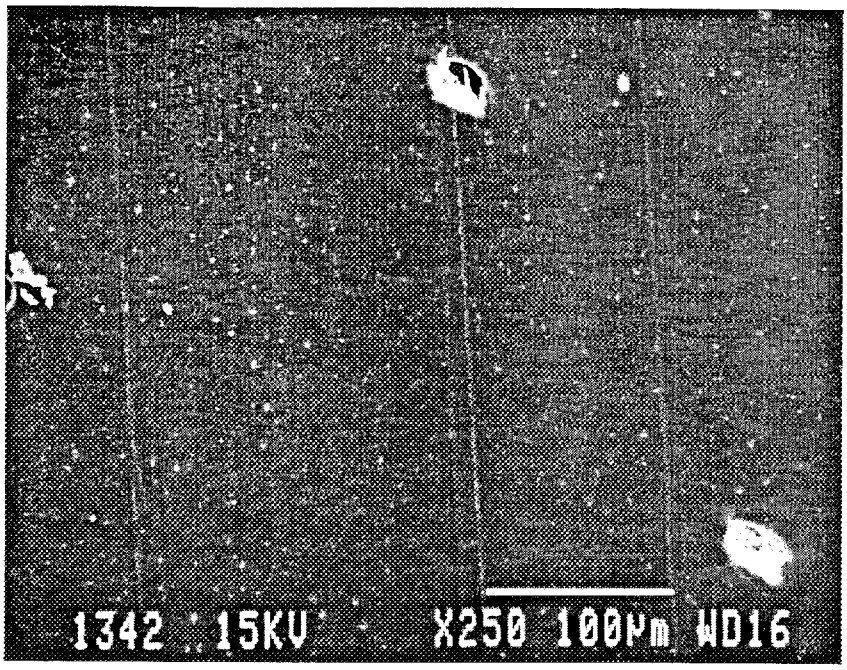

Figure 65. Enlarged view of Pinholes 3 and 4 from Figure 63

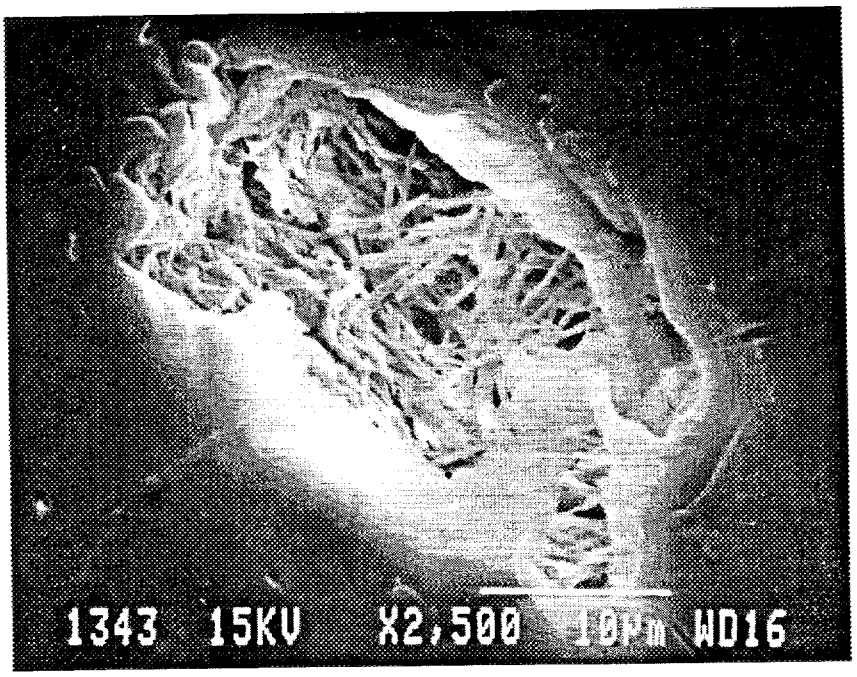

Figure 66. High-magnification view of Pinhole 4

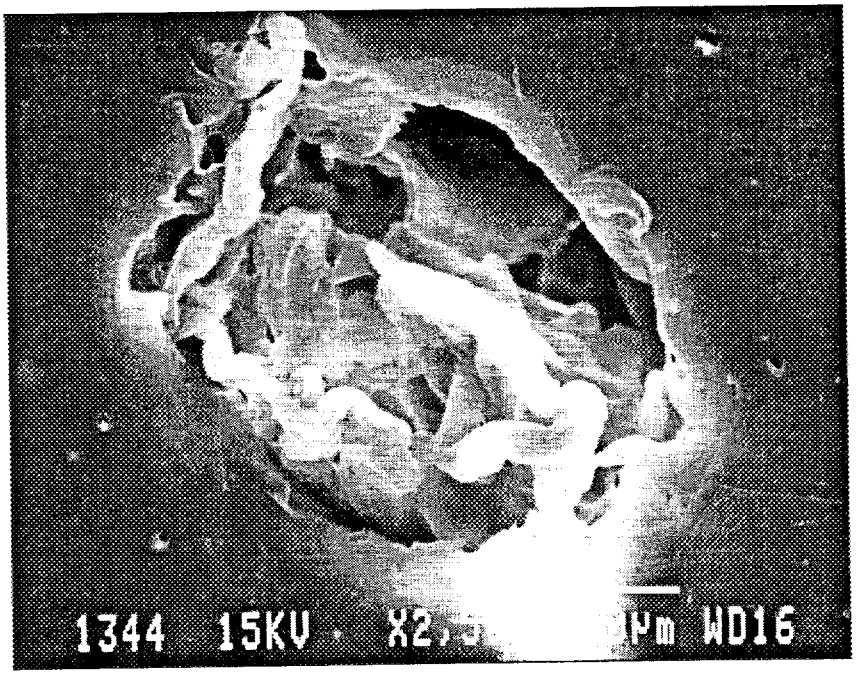

Figure 67. High-magnification view of Pinhole 5

This shows that "incomplete" or "baby" pinholes exist in the proximity of the visible pinhole.

Electrostatic Discharge Experiments at Battelle

The SEM studies showed that elongated cavities existed in the proximity of a visible pinhole. These elongated cavities were approximately parallel to the visible pinhole. In order to determine whether the effective reduction in wall thickness (and thereby a reduction in the dielectric resistance) due to the "baby" pinholes facilitated an electrical discharge, a pipe sample taken from close proximity to a visible pinhole was subjected to electrostatic discharge. It was assumed that the sample contained such "baby" pinholes.

The schematic of the test setup is shown in Figure 68. A copper plug inside the pipe was the cathode while a needle electrode on the outer surface of the pipe was the anode. The pipe was submerged in a dielectric bath to avoid short circuiting between the electrodes. Discharge occurred at a voltage difference of about 32,500 volts. This is about one-third the voltage that would be needed for a discharge through a 90 mil thick wall in the absence of the "baby" pinholes. The implication is that the presence of "baby" pinholes results in discharge at much lower voltages. Microscopic examination of the discharge path indicated that the morphology was characteristic of that of a high-voltage instantaneous discharge, and was not similar to most of the field pinholes. This means that the discharge path was "clean" and relatively large.

Figure 69 (photo ID 1632) shows the OD (outer diameter) of the pipe sample used in the discharge experiments at low magnification (20X). Two holes are visible. The larger hole is on the upper right with an adjacent circular mark. The smaller hole is on the lower left with an adjacent linear gouge. Magnified views (100X) of the larger and smaller holes are shown in Figure 70 (photo ID 1633) and Figure 71 (photo ID 1634) respectively. Figures 72 (photo ID 1635) and 73 (photo ID 1637) show the small hole in two views at 600X magnification. Figure 74 (photo ID 1638) shows the smaller hole at a magnification of 2000X. The holes are quite "clean" in

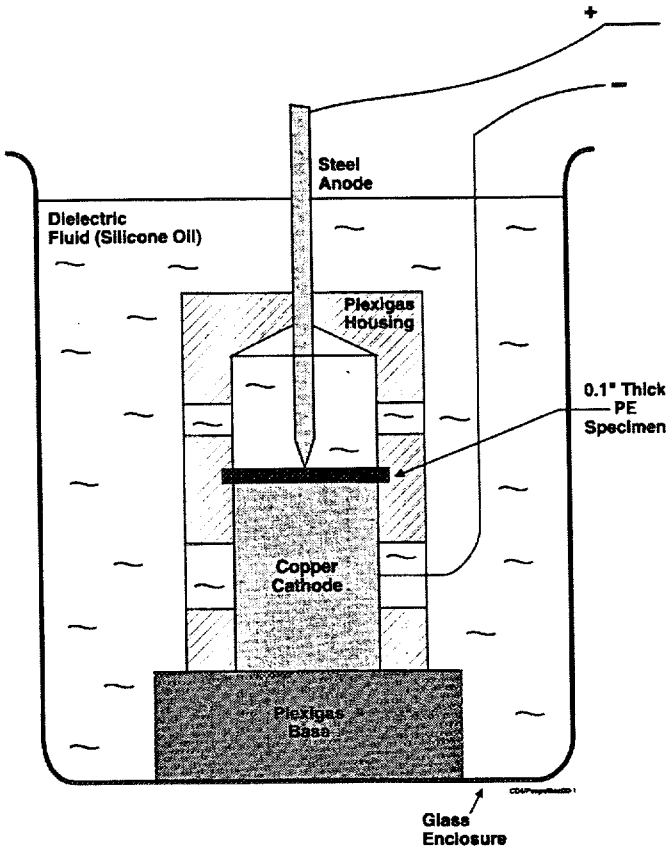

Figure 68. Schematic of electrostatic discharge test setup at Battelle

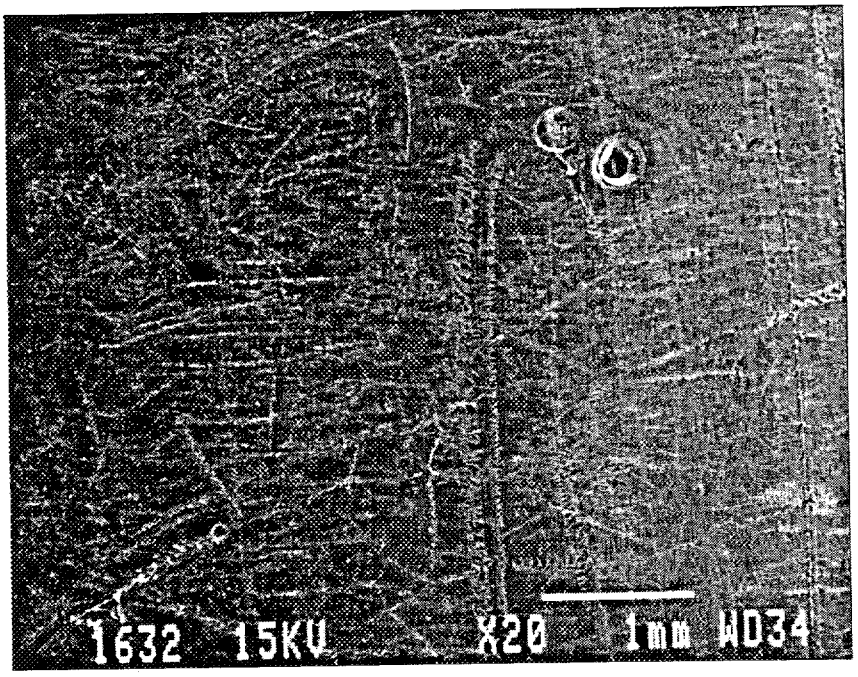

Figure 69. Outer diameter of pipe sample at low magnification (20X)

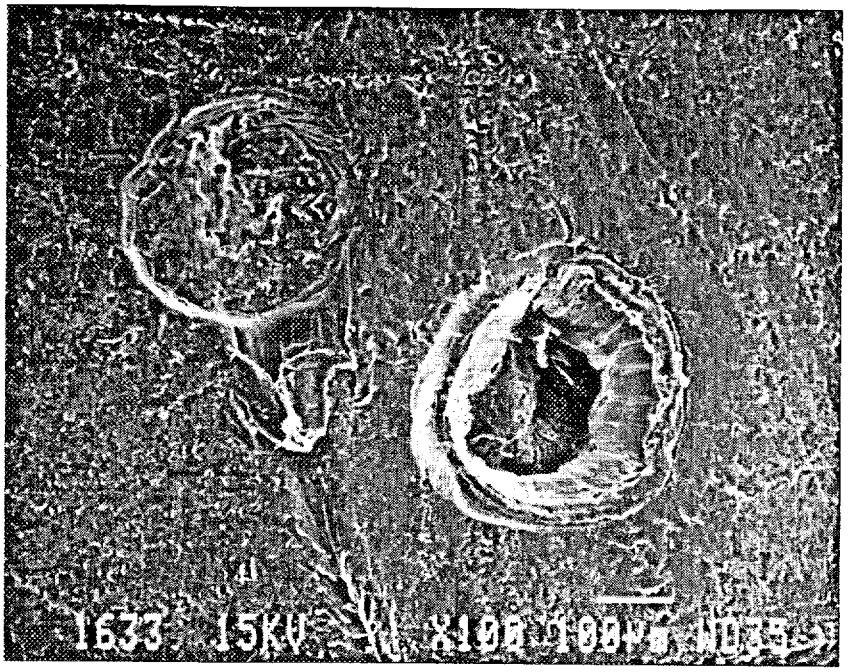

Figure 70. View of larger hole in Figure 69, magnified 100X

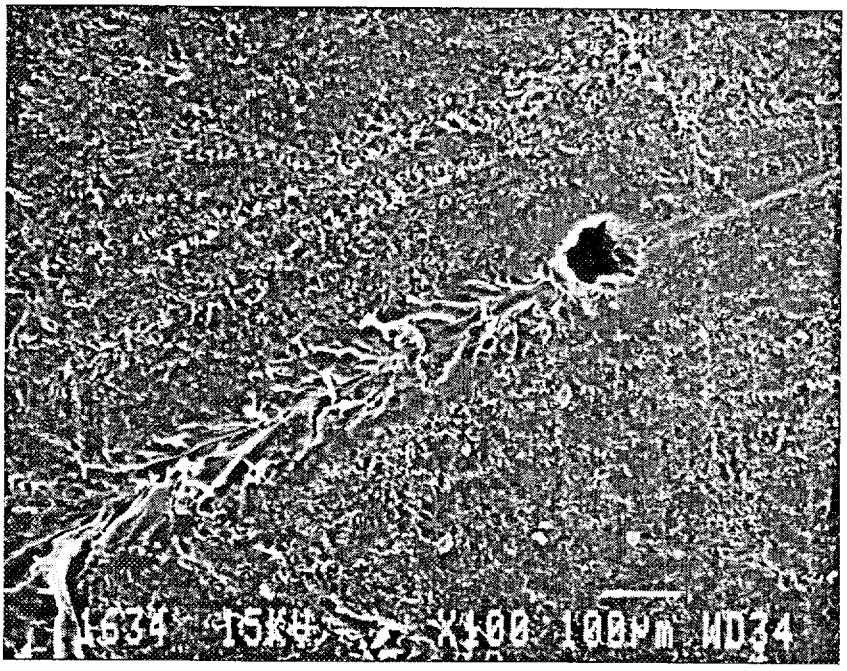

Figure 71. View of smaller hole in Figure 69, magnified 100X

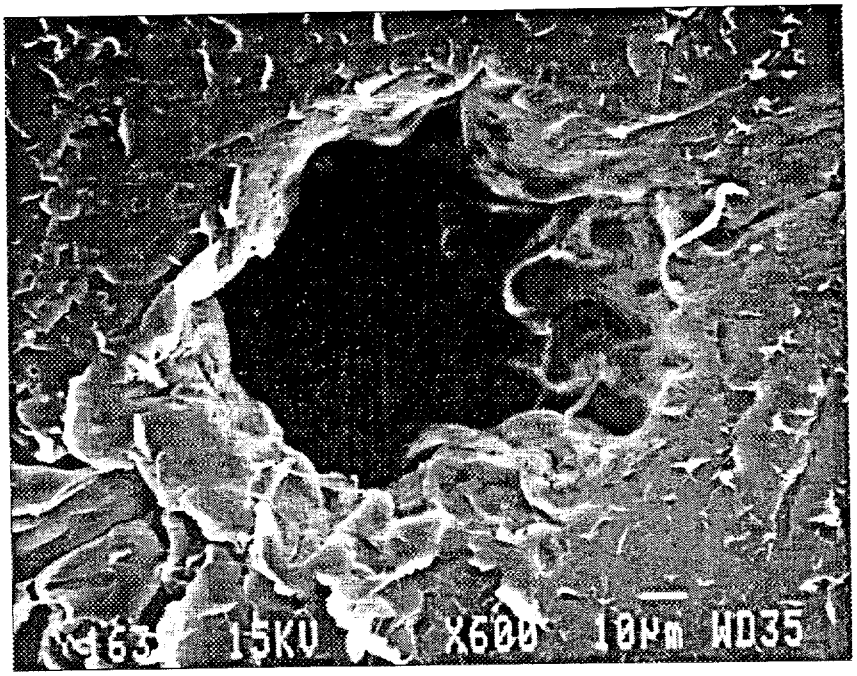

Figure 72. View A of small hole in Figure 69, magnified 600X

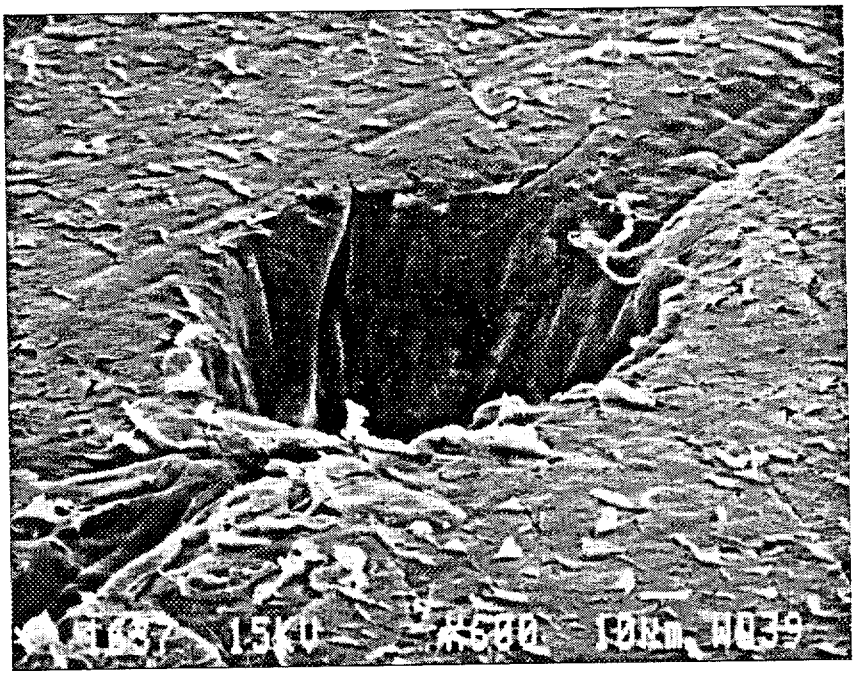

Figure 73. View B of small hole in Figure 69, magnified 600X

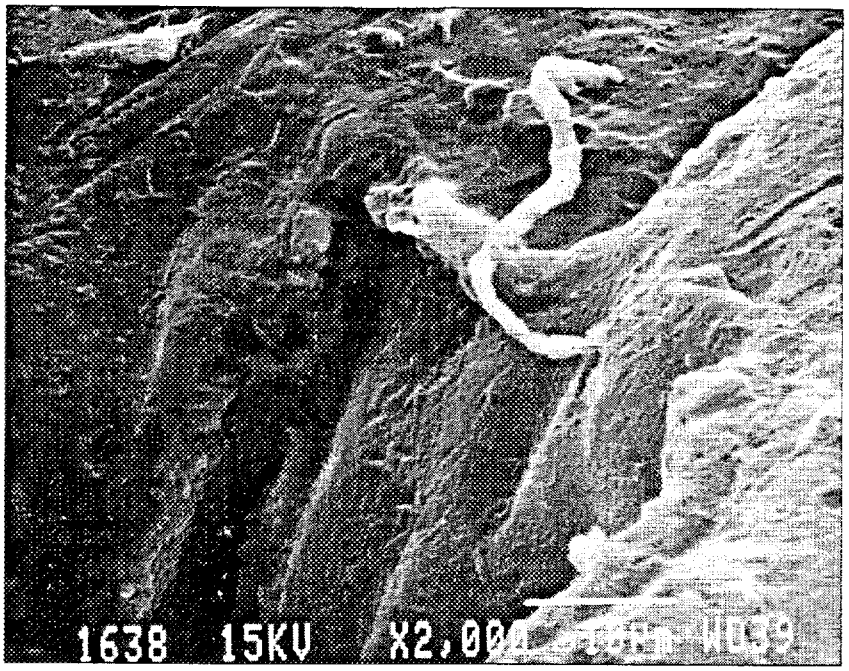

Figure 74. View of smaller hole in Figure 69, magnified 2,000X

not having fibrils covering the holes. The size of the holes is 80 to 120 micrometers. Both these characteristics are typical of high-voltage discharges and are not typical of the pinholes observed in pipe from the field. Figure 75 (photo ID 1640) shows a low-magnification (75X) view of the hole at the ID (inner diameter). The hole is surrounded by an area in which surface features are absent, as if local melting had occurred. Another view at higher magnification (350X) is shown in Figure 76 (photo ID 1641). Again, the features suggest local melting.

Published literature (e.g., Van Brunt, 1994) suggests that the dielectric resistance of a material can break down in different ways. If a high enough voltage (of the order of magnitude of 1000 volts per mil of sample thickness) is applied, immediate or instantaneous breakdown occurs. The physical character of this breakdown is manifested as a hole through the PE sample. The size of the hole varies with the energy involved in the breakdown, but typically the diameter is of the order of 100 micrometers or larger. The entry and exit holes are smooth and free of fibrils. Occasionally, branching occurs. If a smaller voltage is applied for a longer time, a progressive breakdown of the

Figure 75. Inner diameter of pipe sample at low magnification (75X)

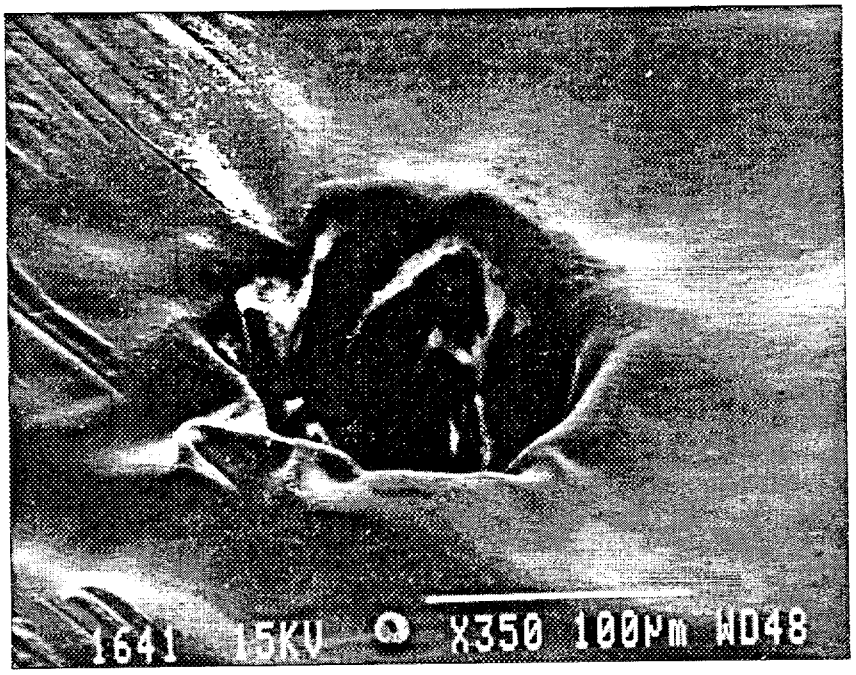

Figure 76. View of hole in Figure 75, magnified 350X

dielectric resistance occurs. The morphology of such a breakdown does not appear to have been studied for gas distribution PE pipe. Therefore, an experiment to examine this was set up at Battelle.

The physical setup of the experiment is shown schematically in Figure 77. A special circuit was set up to monitor and limit the amount of current passing through the PE. The intent was to apply a voltage to a PE sample taken from the proximity of a known visible field pinhole while restricting the power available to melt the PE. The voltages applied and their time duration are shown in Figure 78. Initially, about 10,000 volts was applied, but the sample did not fail in 40 days, so the voltage was increased to 20,000 volts. After 20 more days, the voltage was increased to a level that caused instantaneous breakdown. The sample was then removed and examined.

Figure 79 (photo ID 2058) shows a low magnification (25X) view of the OD of the sample. Three features are evident. A hole (#1) is visible within a discolored region at the top right, another hole (#2) in the proximity of a scratch appears on the upper left, while an indeterminate surface mark (#3) appears to the lower right. Figure 80 (photo ID 2064) shows another low magnification (35X) view of the hole (#1) in the region of discolored material. Another view of the same hole (#1) is shown in Figure 81 (photo ID 2062). Hole #2 is shown in Figure 82 (photo ID 2059) at 150X magnification. The hole size appears to be 50 to 80 micrometers. A view at greater magnification (500 X) is shown in Figure 83 (photo ID 2060). The hole is larger than a typical pinhole but does not have the typically clean appearance of instantaneous discharge samples. Figure 84 (photo ID 2066) shows the ID of the pipe sample at a magnification of 250 X. A greatly magnified view (1500X) is shown in Figure 85 (photo ID 2067), which shows a raised area surrounding the hole and a featureless adjacent region suggestive of local melting and resolidification. The size of the hole appears to be about 10 micrometers.

In summary, the voltages required for discharge in areas containing voids are substantially lower than those in the absence of voids. Further, if the current is limited (to replicate field conditions), the holes tend to be of smaller size with the unsmooth appearance

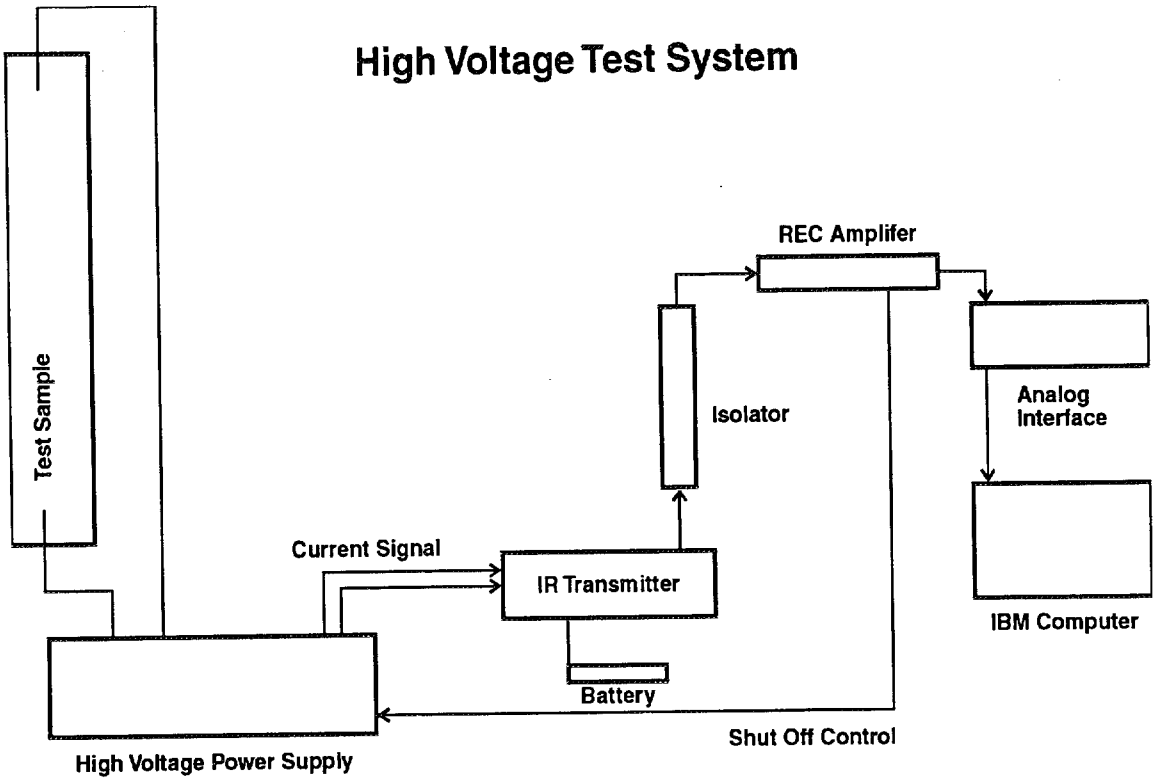

Figure 77. Schematic of experimental setup

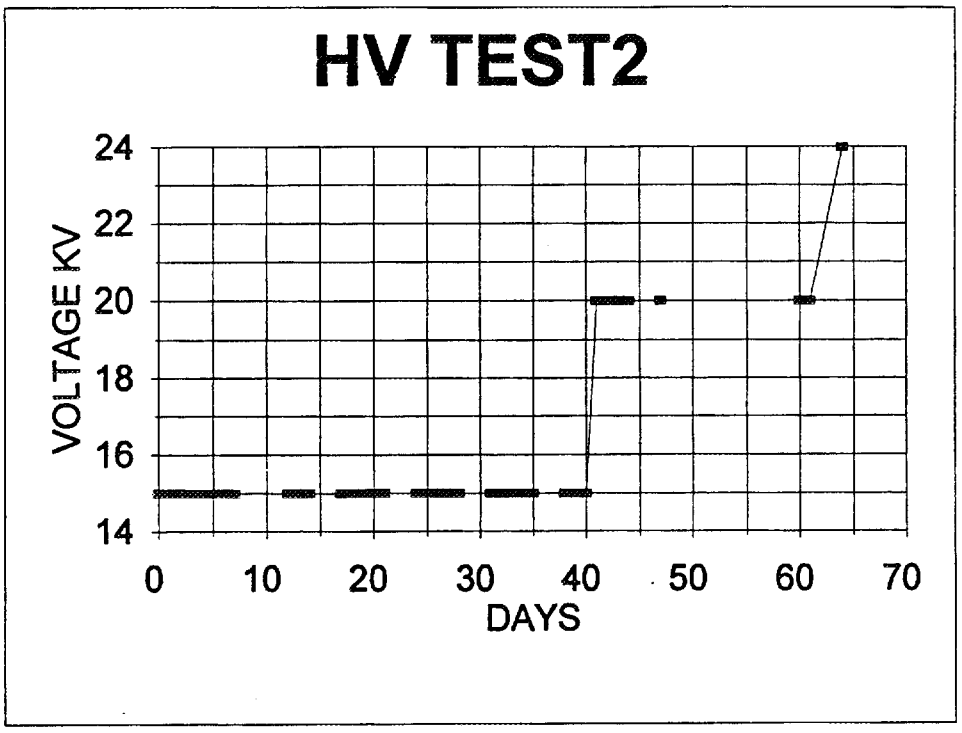

Figure 78. Voltages applied and their duration

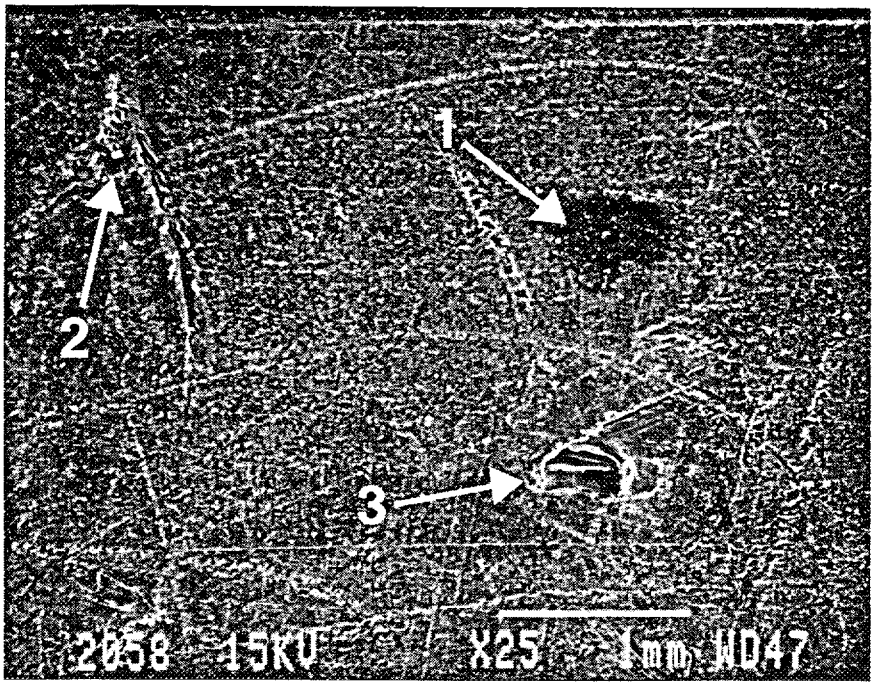

Figure 79. Outer diameter of the sample at low magnification (25X)

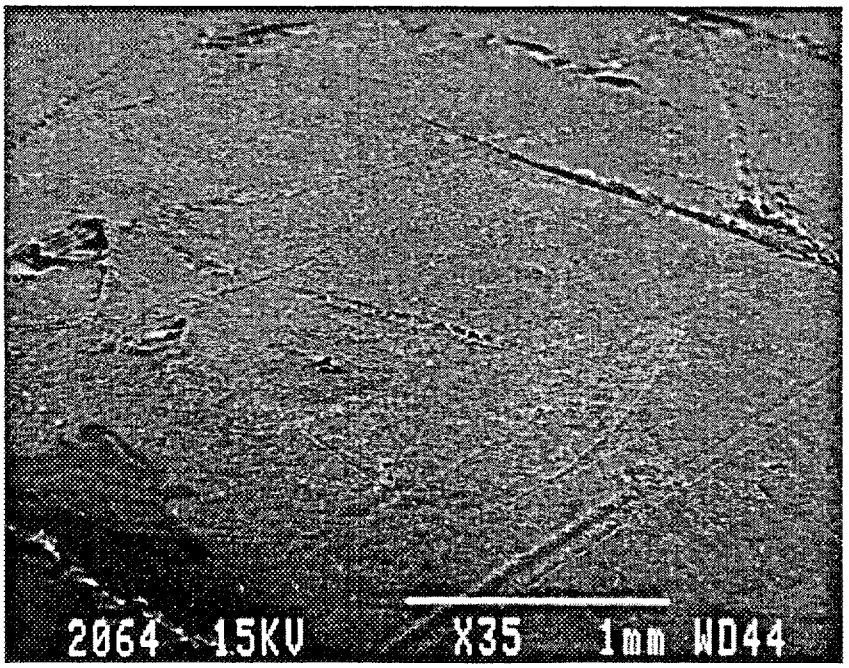

Figure 80. Hole #1 in Figure 79, magnified 35X

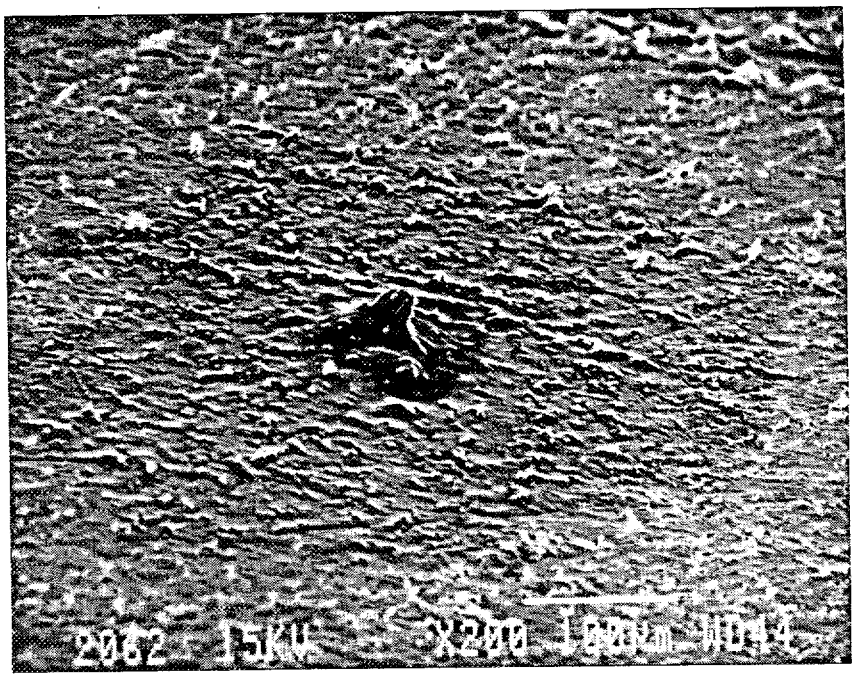

Figure 81. Another view of Hole #1 in Figure 79

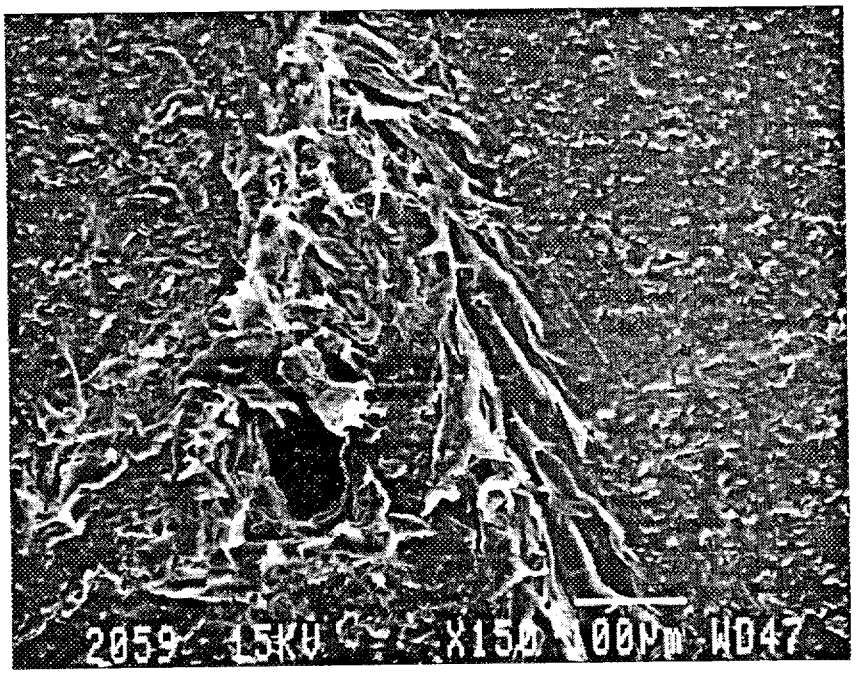

Figure 82. Hole #2 in Figure 79, magnified 150X

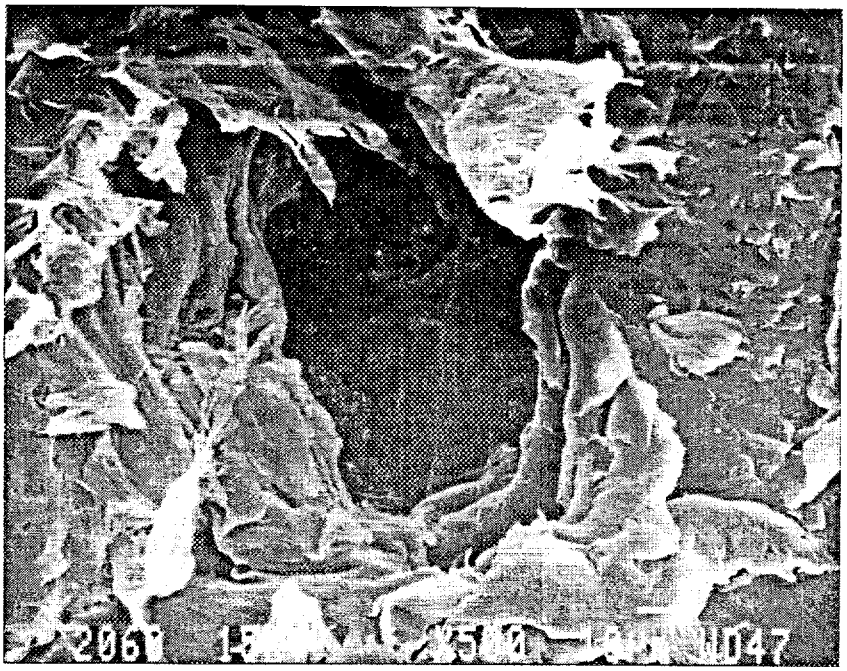

Figure 83. Hole #2 in Figure 79, magnified 500X

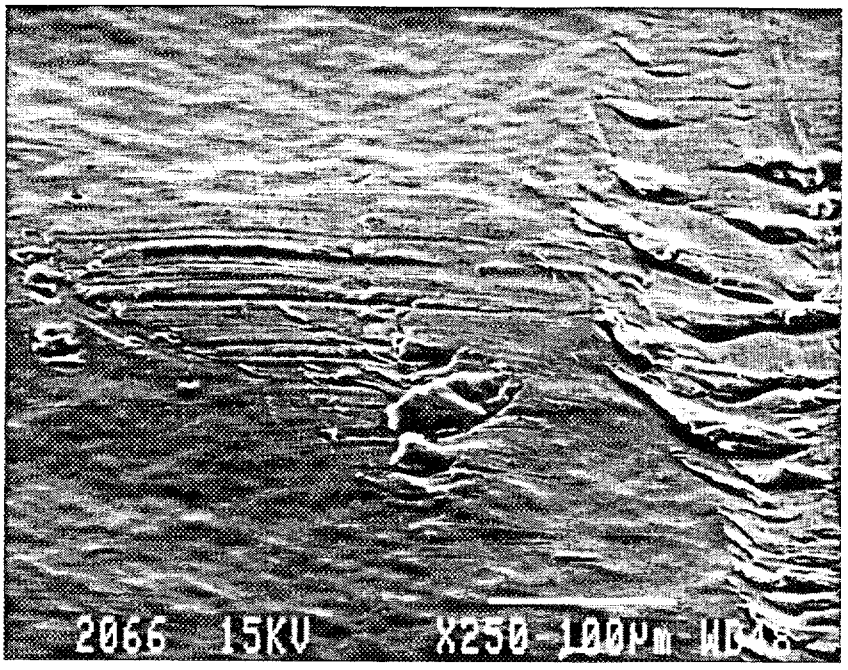

Figure 84. Inner diameter of pipe sample at 250X magnification

Figure 85. Features of pipe sample suggest local melting and resolidification

of field pinholes. The larger hole at the OD in the current-limited noninstantaneous sample may have been caused when the voltage was finally raised to cause a discharge.

Two additional electrostatic discharge tests were planned. In the first, small (about 3 mil) holes were to have been drilled axially in a PE pipe. Then a voltage gradient was to be applied between the OD and the ID. This voltage was to be sustained until breakdown occurred. The intent of this experiment was to examine the effect of known voids. The second experiment was to use a virgin pipe that had not seen service, and had no known defects. This was to be subjected to a low voltage till dielectric breakdown occurred. The test sample was to have been microtomed through the wall to see if "baby" pinholes existed. If "baby" pinholes were found, the presumption would be that the "baby" pinholes are caused at the same time as the partial discharge, and are a side-effect of it. If no "baby" pinholes were found, the presumption would be that the "baby" pinholes existed before the partial discharge, and allowed the discharge to occur more easily. These experiments were not implemented because of limited funds.

Samples Submitted by PPI Members

In January 1995, a sample of 3/4" IPS, SDR 11, PE2406 gas pipe was sent to Battelle for morphological analysis by Hugh McGee of Union Carbide at the direction of Tony Nicholas of Union Carbide and Gene Palermo of Uponor. (Mr. Palermo has since left Uponor.) There was no information given as to the antecedents of the pipe.

An optical view of the OD at 6.5X magnification is shown in Figure 86, with a scattered electron microscopy view at 10X magnification shown in Figure 87. Greater magnifications (Figure 88, photo ID 1760, 40X; Figure 89, photo ID 1761, 100X; Figure 90, photo ID 1758, 500X) show ambiguous structures that may or may not indicate hole openings. After grinding off the top surface, the holes are easily seen. There appear to be three holes as shown in Figure 90. However, additional holes may be present outside the field of view. Attempts were made to find these additional holes, but none were found in the proximity. Battelle has no specific information on how these samples were created. Visually, the surface holes look similar to field pinholes.

An optical view of the ID at 6.5X magnification is shown in Figure 91, with a scattered electron microscopy view at 10X magnification shown in Figure 92. About 9 holes are clearly visible. Close-ups of these hole openings at 75X magnification (Figure 93, photo ID 1763), at 300X magnification (Figure 94, photo ID 1790), and at 500X magnification (Figure 95, photo ID 1764) show structures that are typical of the hole openings seen in field pinholes at the ID. The hole openings appear to be within areas of discolored material, and the sizes appear to be about 100 micrometers, but this is probably more indicative of the hole "covering" than the hole diameter. Analysis of the central area in Figure 80 indicated the presence of potassium with small amounts of calcium.

Three more samples of black resin molded into Rogowski cups were sent to Battelle by Union Carbide. The samples are cup-shaped on one side and flat on the other. The samples were designated as UCLABA, UCLABB, and UCLABC. UCLABA has been analyzed. There was one hole opening on the concave surface and one hole opening on the flat surface. Figure 96 (photo ID 2283) and Figure 97 (photo ID 2284) show two views of the hole in the concave surface at low

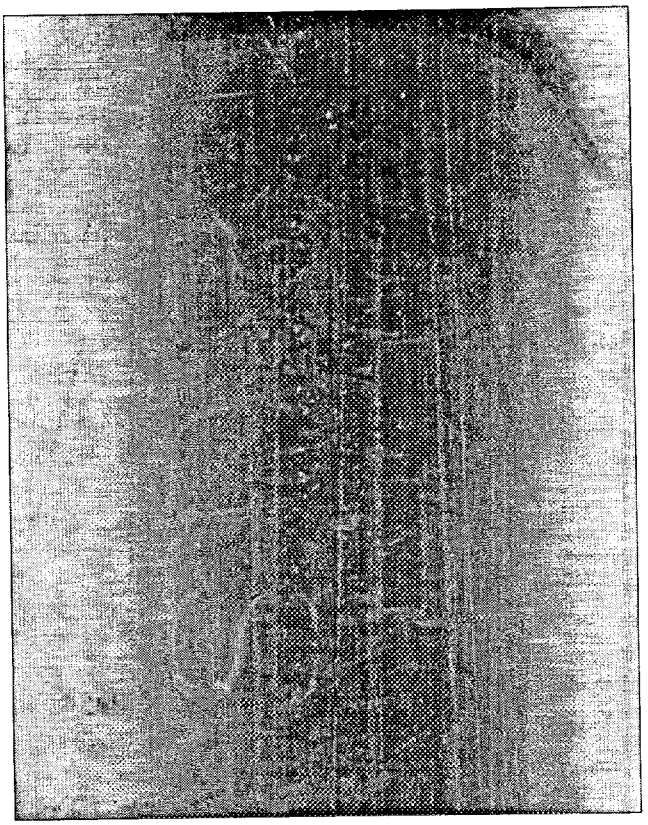

Figure 86. Outer diameter of 3/4" IPS, SDR 11, PE2406 pipe sample, magnified 6.5X

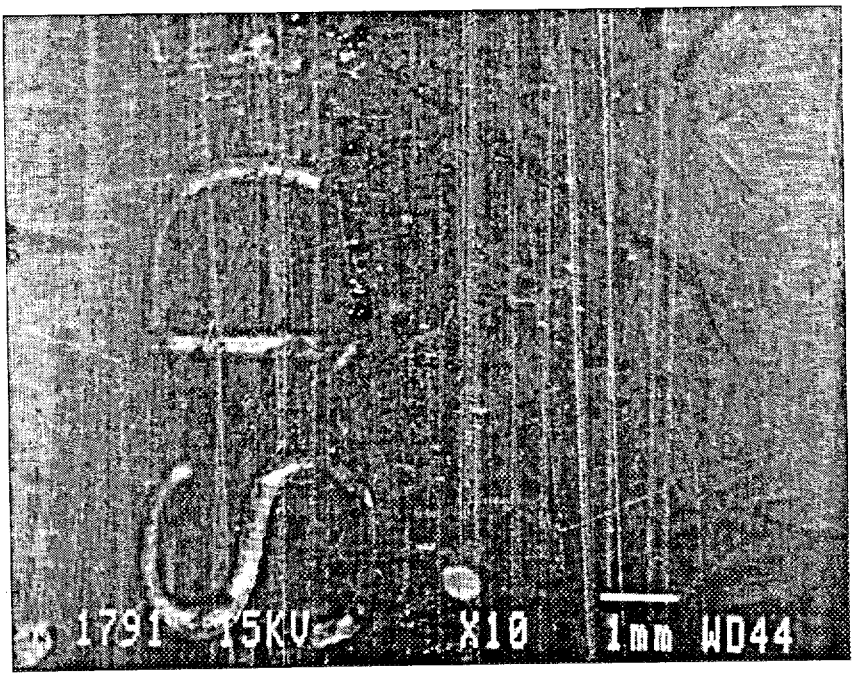

Figure 87. Scanning electron microscopic view of Figure 86, magnified 10X

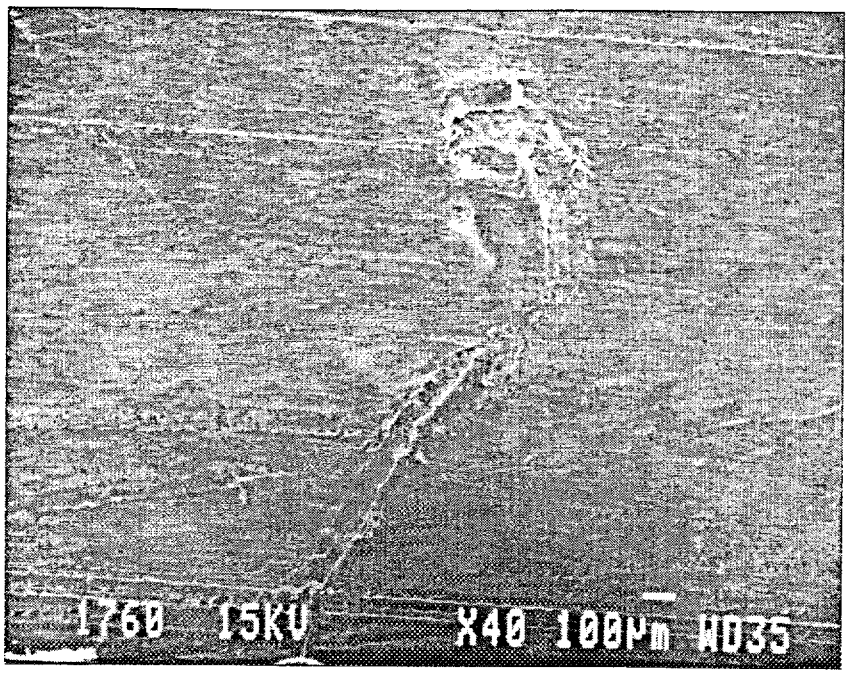

Figure 88. Figure 86, magnified 40X

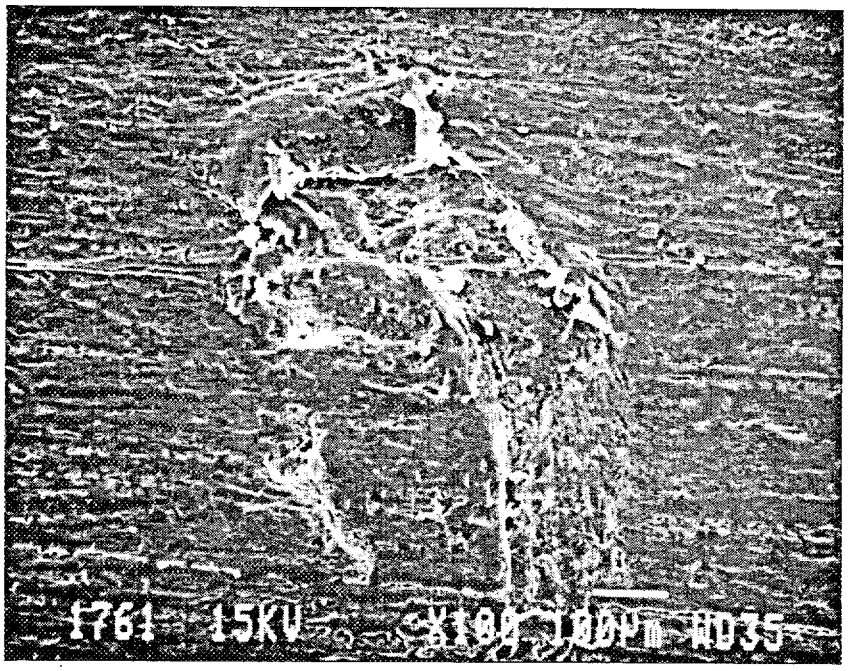

Figure 89. Figure 86, magnified 100X

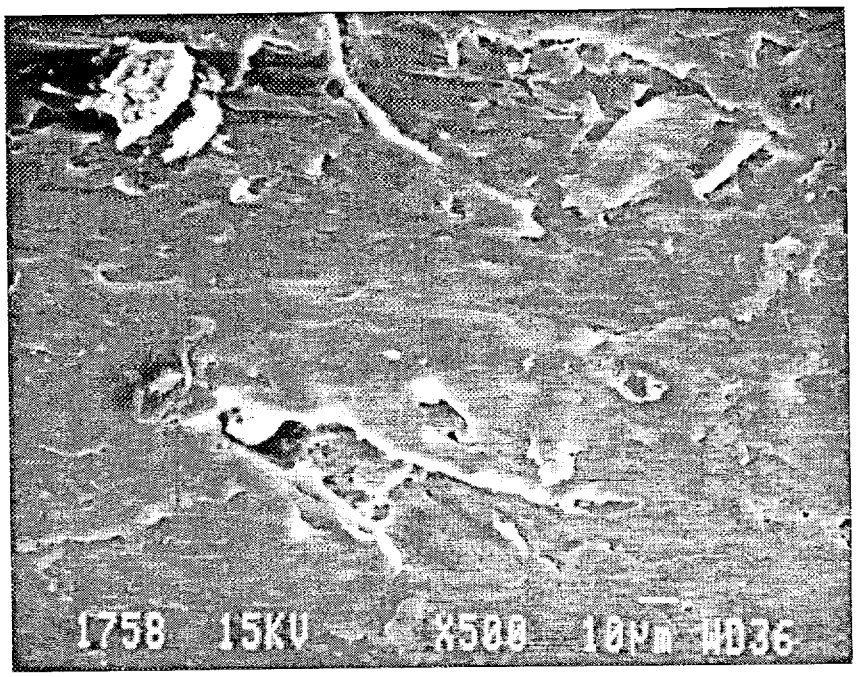

Figure 90. Figure 86, magnified 500X

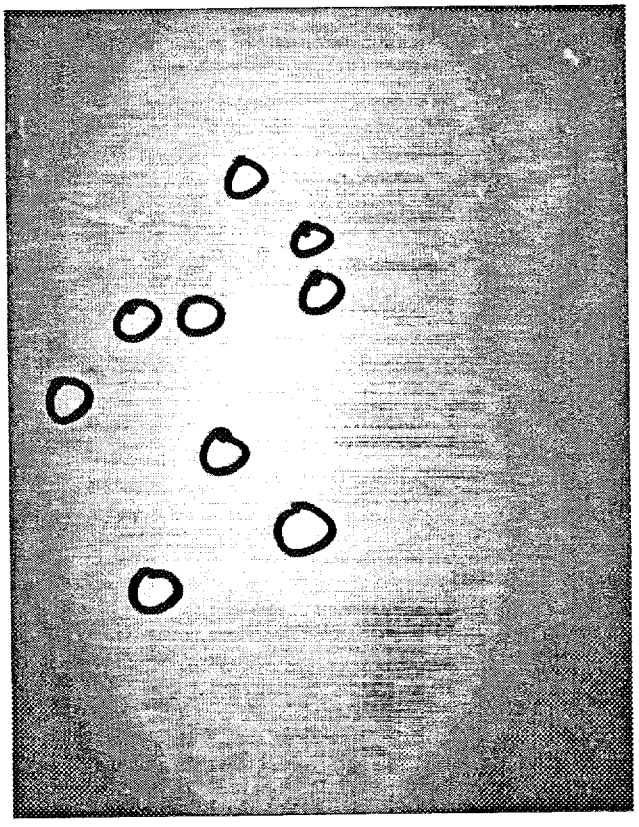

Figure 91. Inner diameter of 3/4" IPS, SDR 11, PE2406 pipe sample, magnified 6.5X

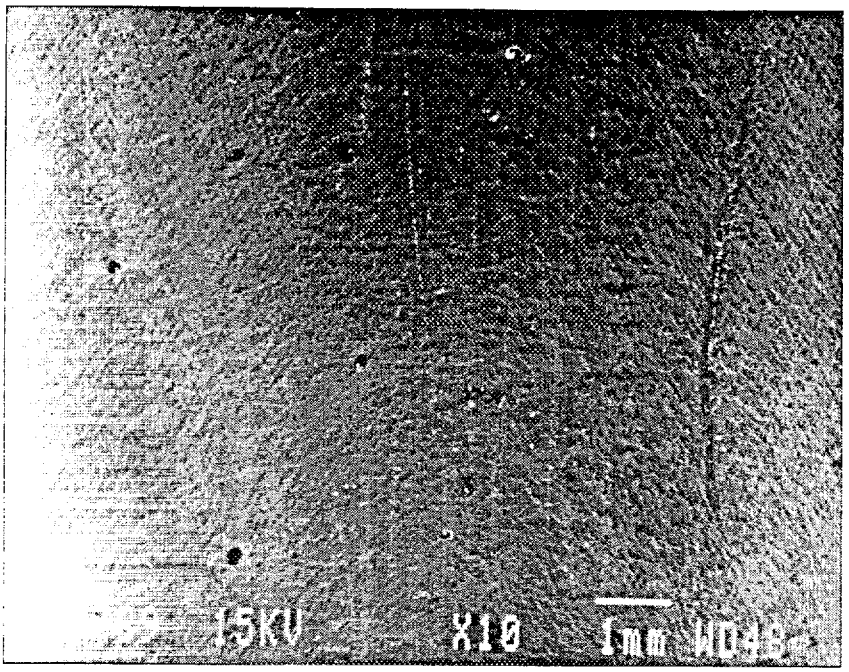

Figure 92. Scanning electron microscopic view of Figure 91, magnified 10X

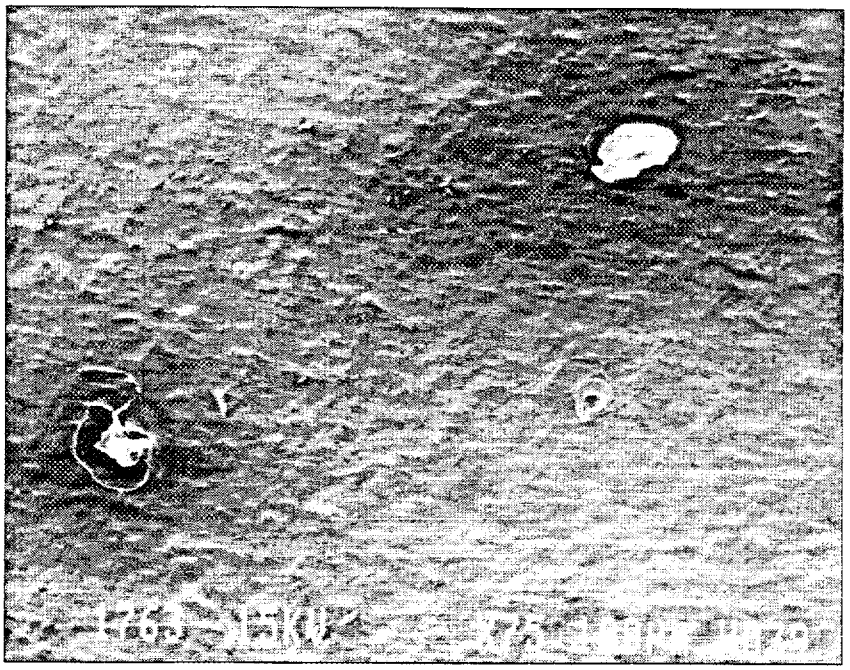

Figure 93. Figure 91, magnified 75X

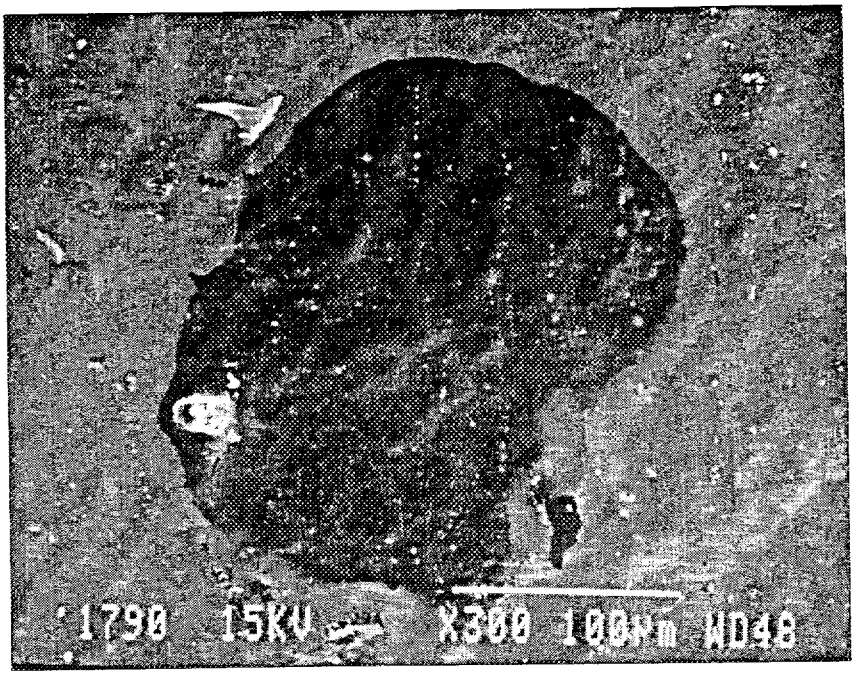

Figure 94. Figure 91, magnified 300X

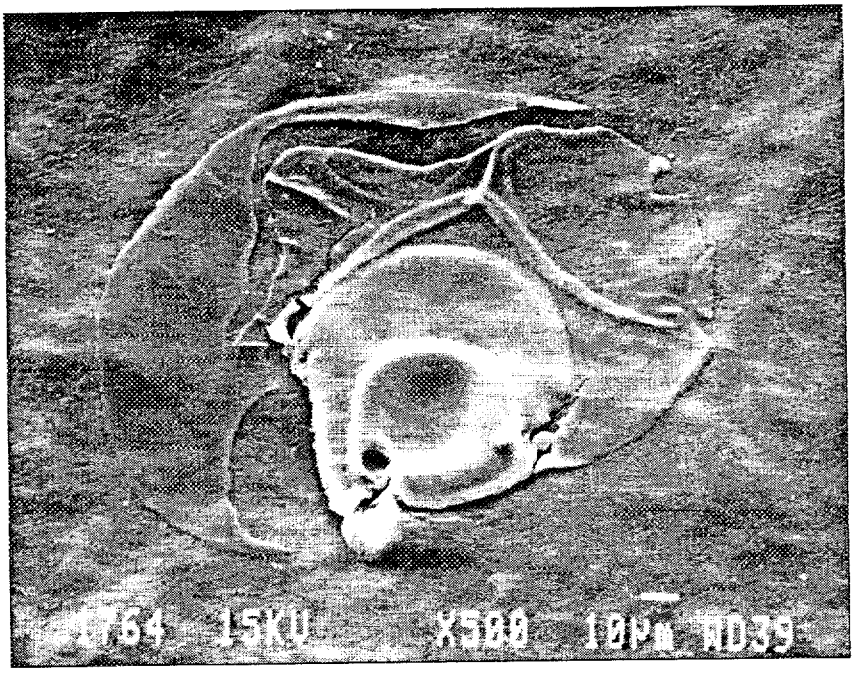

Figure 95. Figure 91, magnified 500X

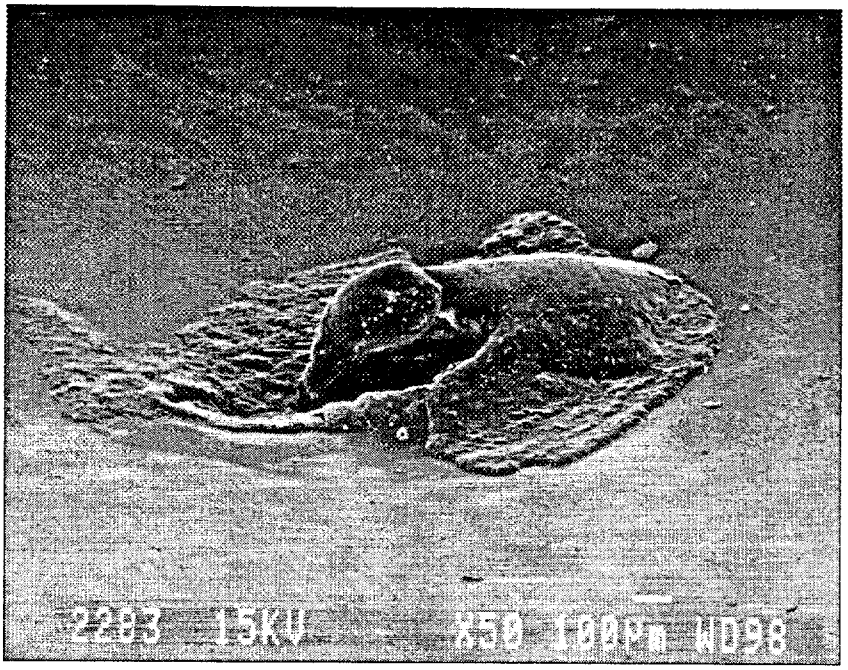

Figure 96. Hole in the concave surface of sample UCLABA, magnified 50X

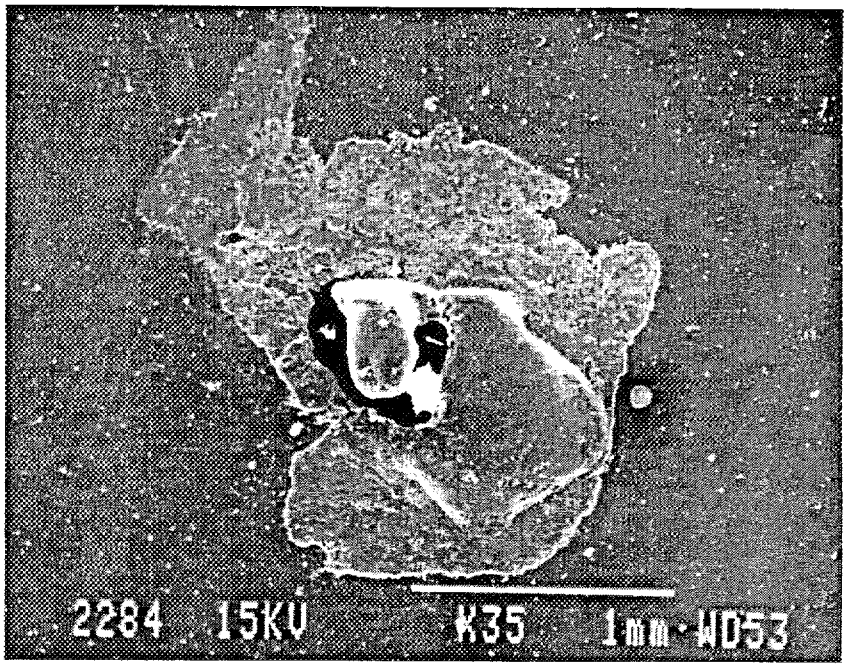

Figure 97. Hole in the concave surface of sample UCLABA, magnified 35X

magnifications (50X and 35X) respectively. The hole size appears to be greater than 200 micrometers. Two low-magnification views (50X) of the hole in the flat surface are shown in Figures 98 (photo ID 2285) and 99 (photo ID 2286). The hole looks unlike any field pinhole. It is also quite large—of the order of 200 to 500 micrometers. The same hole is shown in Figure 100 (photo ID 2288) at higher magnification (200X). The edges are smooth and characteristic of instantaneous discharge.

A third sample consisting of a 3-inch disk about 100 mils thick was also received from Union Carbide for microscopic examination. This is discussed in detail in the following section titled, "Partial Discharge Hypothesis."

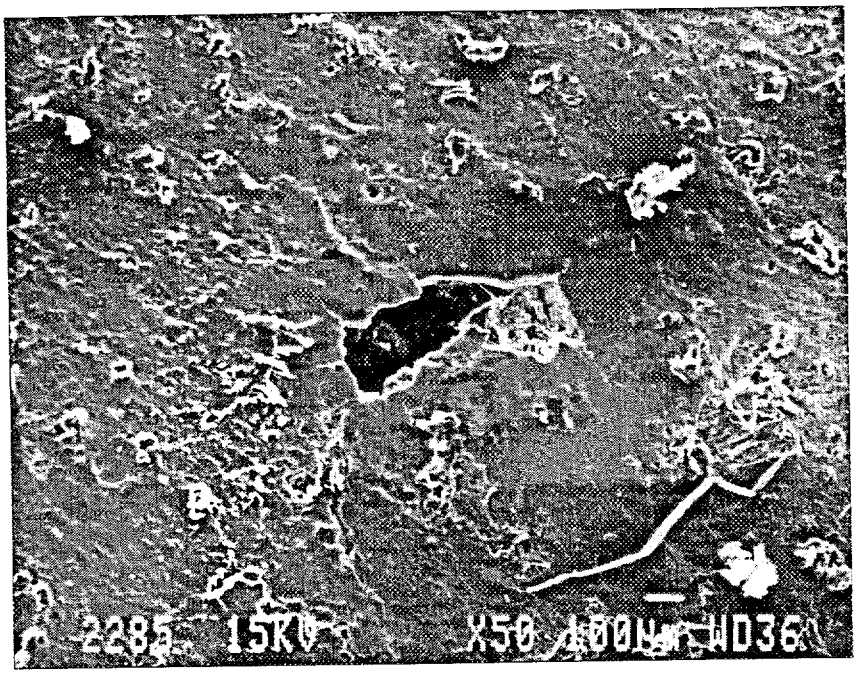

Figure 98. View A of hole in the flat surface of sample UCLABA, magnified 50X

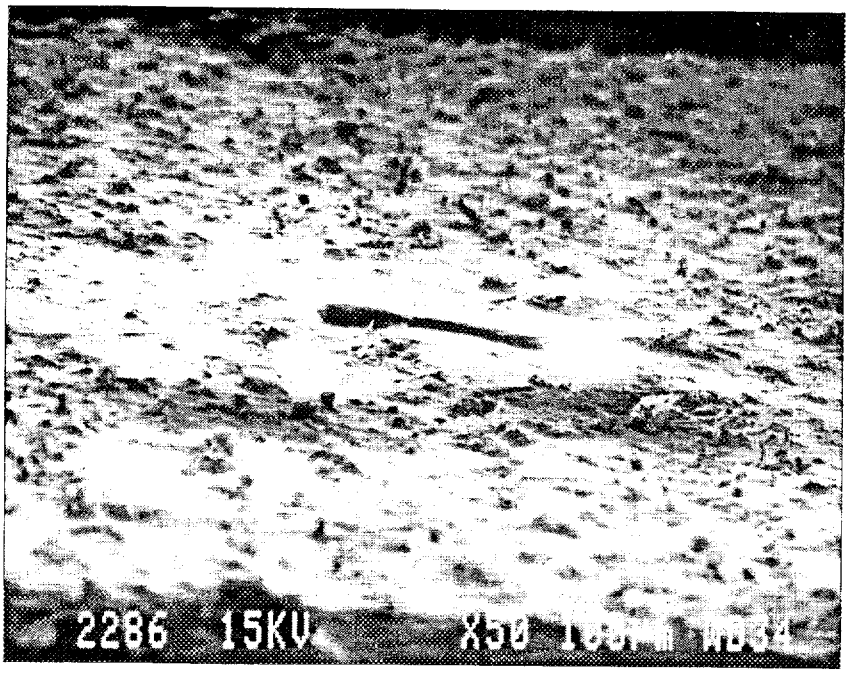

Figure 99. View B of hole in the flat surface of sample UCLABA, magnified 50X

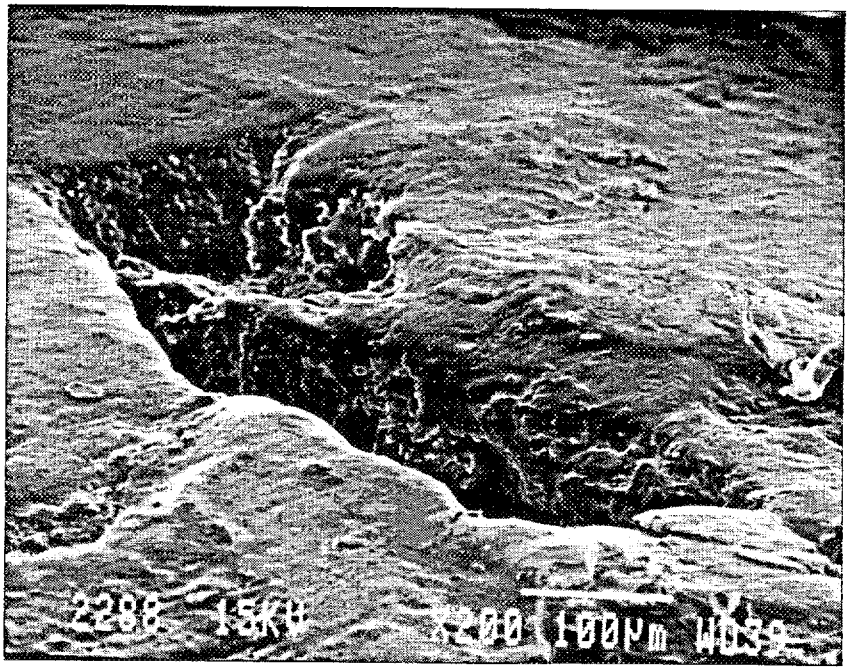

Figure 100. Hole in flat surface of sample UCLABA, magnified 200X

PARTIAL DISCHARGE HYPOTHESIS

The high-voltage cable testing group at Union Carbide, as part of the PPI-inspired activity, produced 50-micron holes in disks made from gas pipe PE material. Occasionally, these holes are said to occur in pairs. Apparently, carbon deposits are not observed, perhaps because the discharge is conducted in a dielectric fluid. One such disk containing a hole was sent to Battelle for examination.

The sample hole created by Union Carbide in a 3.5-inch diameter compression-molded medium density PE yellow gas pipe resin using the Electrical Breakdown Voltage test in accordance with ASTM D 149 was studied at Battelle. The disk was about 100 mils thick. One side contained two holes and was labeled the "exit" side. The two holes are shown in Figure 101 (photo ID 1080). The larger hole on the left appears to be about 100 microns in diameter. Its surface is also very smooth and "clean" (without overhanging or clogging fibrils) as seen in the 500X magnification in Figure 102 (photo ID 1081). There is no buildup around the rim. The other hole with the associated "trench-like" gash appears to have a 60 micron opening. An enlarged view of the smaller hole is shown in Figure 103 (photo ID 1082), and an enlarged view of the associated trench is shown in Figure 104 (photo ID 1083). On the other side, only one hole is visible as shown in Figure 105 (photo ID 1084). An enlarged view is shown in Figure 106 (photo ID 1085). Presumably one hole branched into two holes during discharge.

The disk was immersed in liquid nitrogen for about one half hour, and then fractured with the hope that the fracture plane would follow the hole for some distance. One half of the fractured disk is shown in Figure 107. The entrance surface of the disk is vertical on the right-hand side. The exit surface of the disk (with the two holes) is vertical on the left-hand side. The branching from the one entrance hole to the two exit holes can be clearly seen. The entire passage seems "clean" in the sense referred to earlier. Another view of the exit holes is seen in Figure 108.

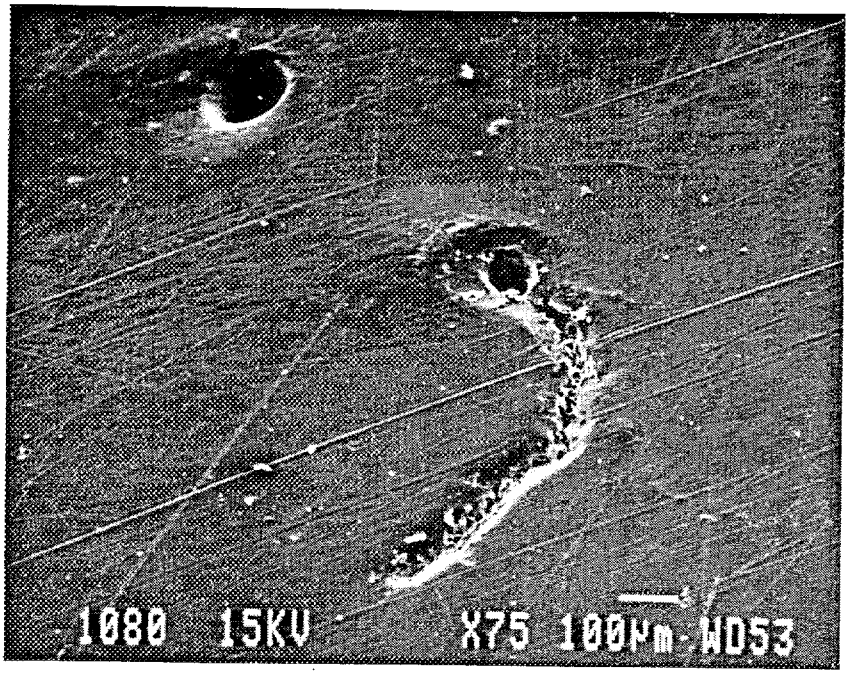

Figure 101. Holes in disk provided by Union Carbide

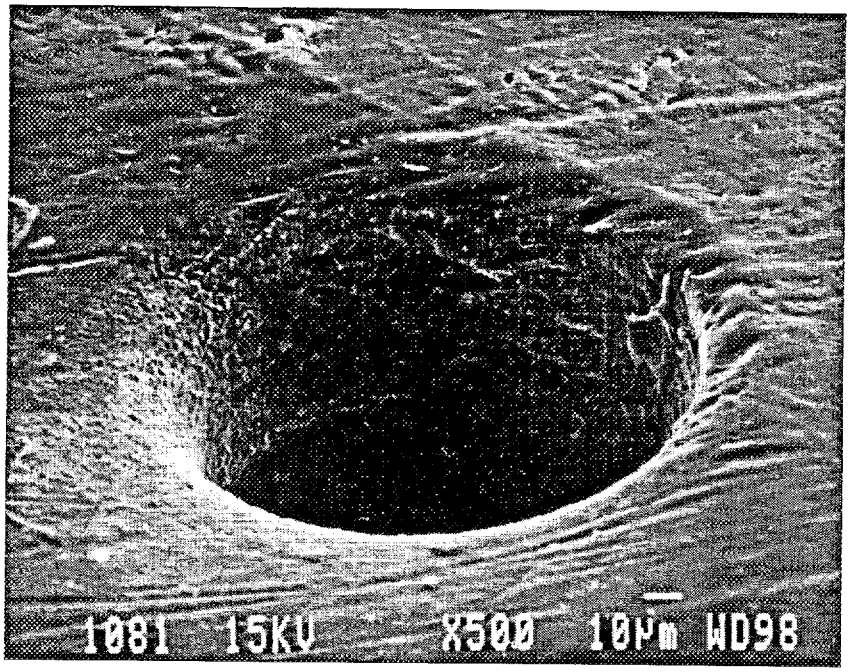

Figure 102. Magnified view of larger hole in Figure 101

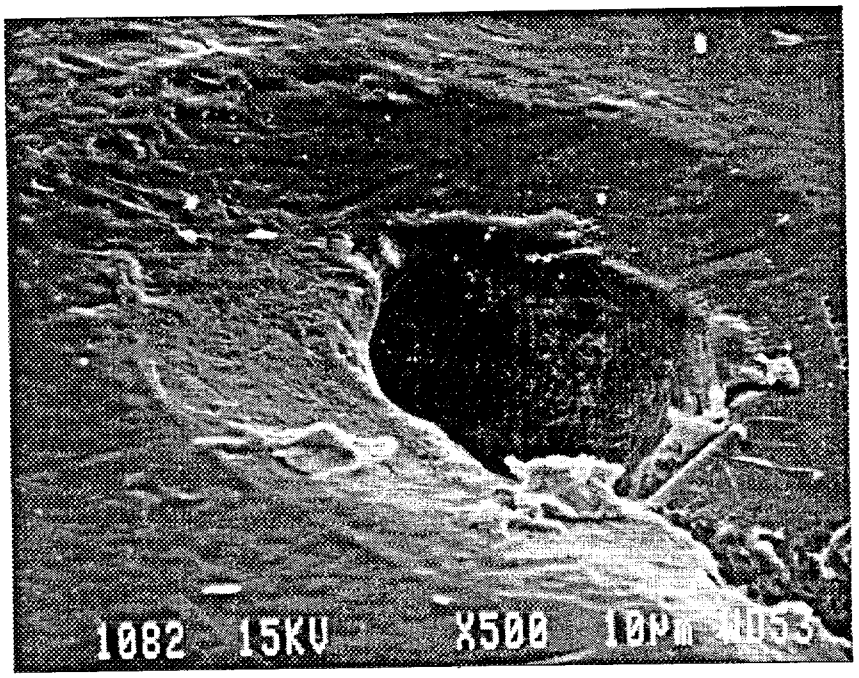

Figure 103. Magnified view of smaller hole in Figure 101

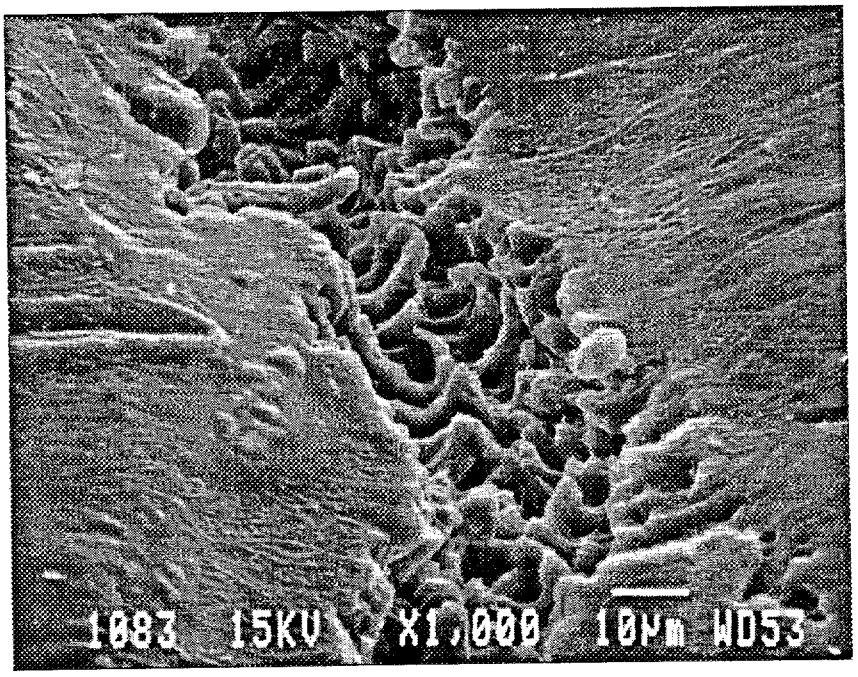

Figure 104. Magnified view of "trench" in Figure 101

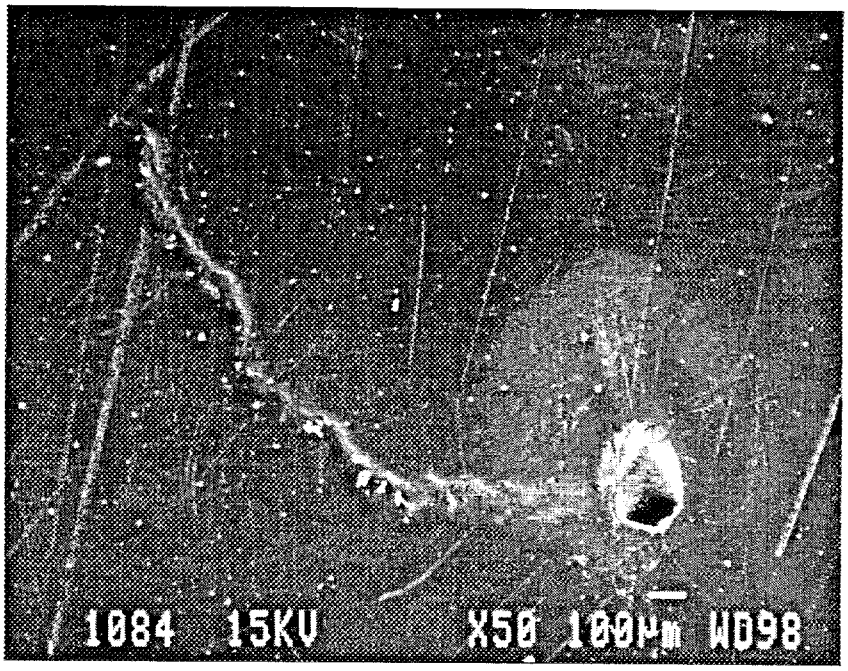

Figure 105. Hole on other side of disk provided by Union Carbide

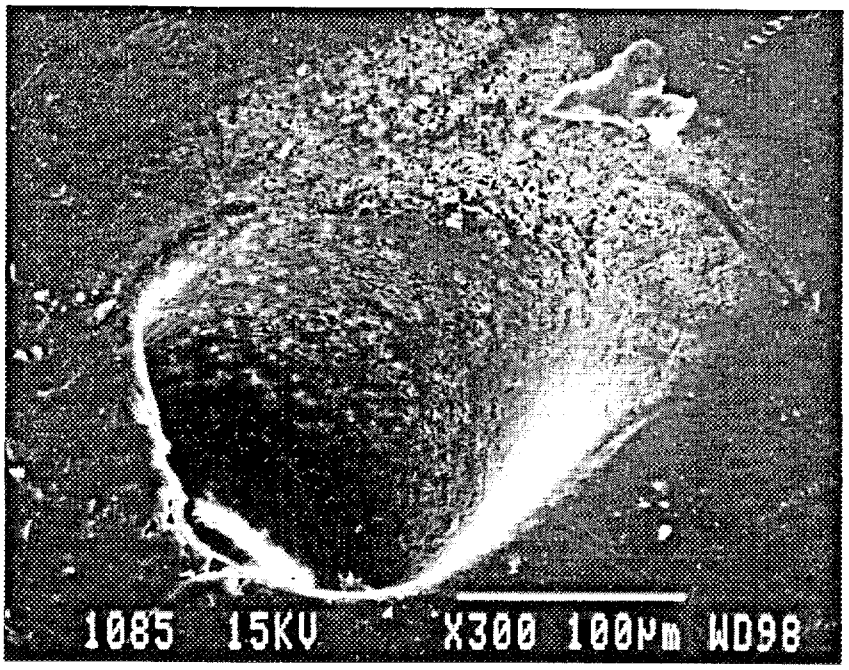

Figure 106. Magnified view of hole in Figure 105

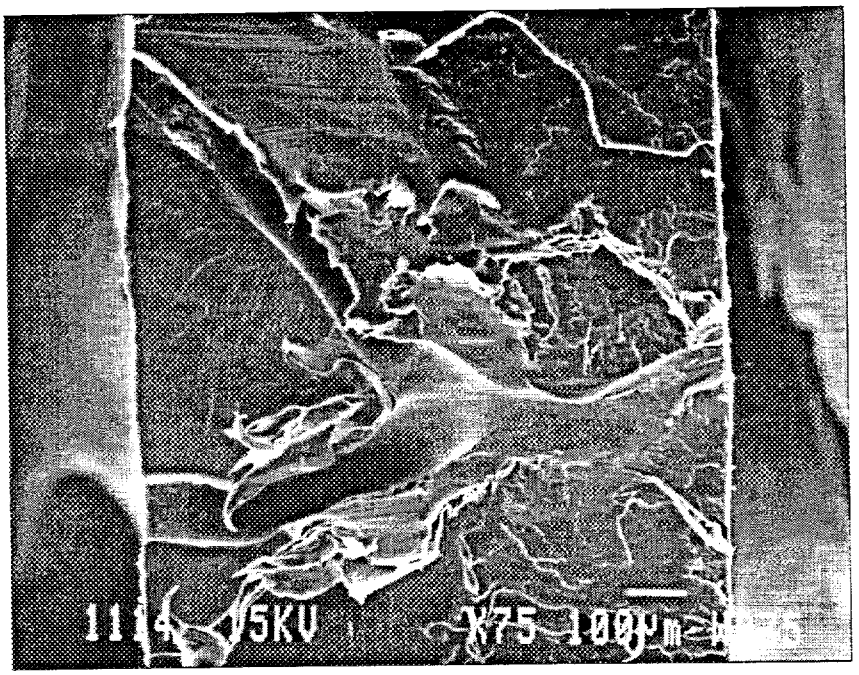

Figure 107. One-half of fractured disk from Union Carbide

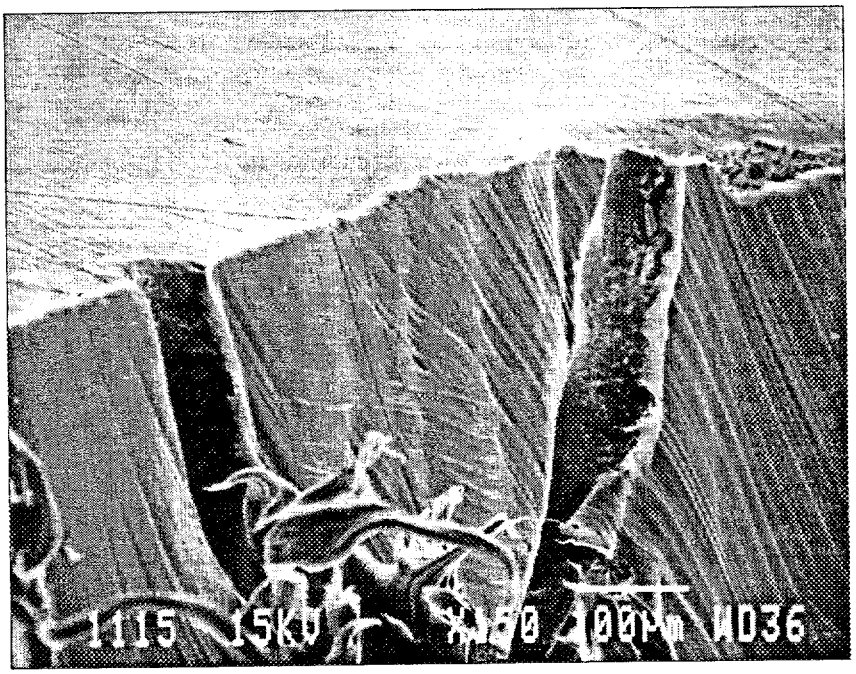

Figure 108. Two holes on exit surface of fractured disk

Clearly, the morphology of the Union Carbide disk is unlike the field pinhole morphology in four respects:

- The disk hole size is significantly larger
- The disk holes are relatively "clean"
- There is no buildup of material around the rim
- The appearance is quite unlike the typical hole at the inside diameter of the pipe in the field samples.

CONCLUSIONS AND DISCUSSION

A systematic investigation to determine the cause of the pinholes was undertaken. However, certain topics that could be relevant were not examined because of budgetary limits. In particular, the issue has been raised as to whether the causation of pinholes could be related to whether the resin was pre-compounded or blended in-plant. This was not examined by Battelle. UCG data indicate that pinholes occurred in tubing extruded from both types of materials, with a majority (about 80 percent) occurring in in-plant blended tubing.

All pinholes discovered so far have occurred in tubing sizes. The wall thickness of such tubing is quite thin (on the order of 100 mils). It has been suggested that if the wall thickness of service lines was increased, pinholes could be suppressed. This may be possible. However, deciding on the amount of increase in wall thickness is a trade-off between the desirability of suppression of pinholes, and increased material usage and cost. This decision cannot be made rationally in the absence of quantitative data demonstrating and quantifying the relationship between wall thickness and the suppression of occurrence of pinholes.

In response to the discovery of pinholes, UCG changed its specifications for purchase of tubing in 1993. In short, the new specifications require that:

- No regrind material be used,
- The resin must be a pre-blended compound,
- The resin must be pre-heated or dried before entering the extruder, and
- The manufacturer must attest to the foregoing.

"Homogeneous blending" (where the color concentrate is allowed to be added at the extruder) has been deemed to be acceptable by UCG in 1996. UCG has stated that no pinholes have been found in tubing made in accordance with the new specifications. It is noted that Plexco has categorically denied the use of regrind in tubing in which pinholes have been found.

Based on the work undertaken by Battelle, or under Battelle's direction, the conclusions are:

- No convincing explanation was found for the fact that most of the pinhole leaks have been found in Central Tennessee. Although it is true that the UCG personnel use detection equipment which have rubber "boots" that serve to trap the gas, and UCG personnel are exceptionally thorough in their inspection procedure, by itself these factors are insufficient to explain the discovery of most of the pinholes in Central Tennessee. It is possible that pinhole leaks have been found elsewhere and repaired without undue scrutiny. This, however, is conjectural. It is noted that at least one pinhole leak occurred in Missouri in the 1980s, and two pinholes were discovered in Virginia in 1996.

- Physical and chemical nonuniformities were found in the gas distribution piping material that was tested. The scale of these nonuniformities was on the order of 10 μm to 100 μm. However, these nonuniformities existed both in the proximity of the pinholes and away from the pinholes. Therefore, there is no reason to believe that these nonuniformities cause, or are associated with, the pinholes.

- Extended thermal cycling of pressurized tubing containing a pinhole, a suspect length of tubing, and virgin tubing, did not cause the formation of a pinhole or an additional pinhole. This, combined with the absence of evidence of classical service failure mechanisms such as slow crack growth, suggests that mechanical and thermal factors are not primarily responsible for the formation of the pinholes.

- The pinholes do not appear to be the result of high-voltage instantaneous discharge, which generally produces holes that are characterized by:
  - Branching of the discharge path
  - A size that is typically larger (greater than 100 μm) than that of pinholes
  - Traces of carbon
  - Absence of clogging fibrils in the discharge path.

Typically, for defect-free PE material, it takes about 1000 V/mil to cause an instantaneous discharge.

- A visible pinhole may have incomplete pinholes in its vicinity. These incomplete pinholes are radially aligned, but do not emerge at both the inside and outside surface of the pipe. It is not clear whether these incomplete or "baby" pinholes grow into visible pinholes, or whether they were present at extrusion. The difficulty in answering this question is that the "baby" pinholes are so small that they cannot be detected except by destructive microtoming. The presence of a "baby" pinhole reduces the voltage necessary to cause discharge through the pipe wall at that location.

- Voltages lower than that required for instantaneous discharge can cause dielectric breakdown of PE when the voltages are applied for a long enough time. These are termed partial discharges. The presence of imperfections in the pipe wall reduce the voltage level, or the time required, for partial discharge. Increased temperatures may hasten the discharge. The amount of data collected was not sufficient to quantify these statements.

- From the fact that the presence of "baby" pinholes reduces the instantaneous discharge voltage, and from the fact that partial discharges occur, it may be conjectured that partial discharges are likely to occur in the proximity of "baby" pinholes, thereby converting them into visible pinholes. The data collected were insufficient to validate this conjecture.

- The reason for the existence of the pinholes could not be proven statistically. However, an evaluation of the accumulated information suggests that the pinholes occur because of a progressive breakdown in the electric resistance of the PE under a static electric field which is smaller than the electric field that would cause an instantaneous discharge. It is not clear whether this progressive

breakdown and pinhole formation occur prior to the pipe being put in service, or while the pipe is in service.

REFERENCES

ASTM Standard D1238. "Standard Test Method for Flow Rates of Thermoplastics by Extrusion Plastometer," American Society for Testing and Materials, Philadelphia, PA.

Lustiger, A., Cassady, M. J., Uralil, F. S., and Hulbert, L. E. Field Failure Reference Catalog for Polyethylene Gas Piping, 1st Ed. January 1980 to December 1984, Gas Research Institute Topical Report GRI- 84/0235.1, March 1986.

Van Brunt, R. J. "Physics and Chemistry of Partial Discharge and Corona: Recent Advances and Future Challenges," IEEE Trans. on Dielectrics and Electrical Insulation, Vol 1. No. 5, October 1994.

APPPENDIX A

CHARACTERIZATION TESTS

MONTHLY PROGRESS REPORT

on

FAILURE ANALYSIS OF GAS PIPE

During February and March, work was focused on

- Extending earlier information obtained from electron microscopy and infrared investigations
- Obtaining evaluations from experts inside and outside Battelle
- Exploring the possibility of using novel techniques to obtain evidence for the causes of pinhole formation.

Electron Microscopy Investigation

A small section of yellow pipe having a pinhole was frozen in liquid nitrogen and was microtomed under liquid nitrogen perpendicular to the axis of the pipe. A Sorvall MTZ-B Ultramicrotome machine and 3/8-inch glass knives were used for slicing. Forty slices were made, starting approximately 2 mm away from the pinhole and going through the pinhole. The average thickness of the slices is approximately 40 to 50 μm. In a second series of microtoming, the slices were made at an angle (approximately 30 degrees) to the pipe axis so that the surface of the slices included a radial component and an axial component.

The sections were first examined under an optical microscope using transmitted light. Figure 1 shows a typical micrograph of the specimen oriented in the direction perpendicular to the axis of the pipe. The micrograph appears to be spotty (i.e., it has "pock marks" or "lenses") instead of being clear. The length scale of these pock marks is about 200 μm. When these sections were examined at higher magnification (200x), the pock marks appear to have distinct boundaries (see Figure 2). The regions interior to the pock marks sometimes have dark spots. The center of some pock marks has a distinct circular region. The

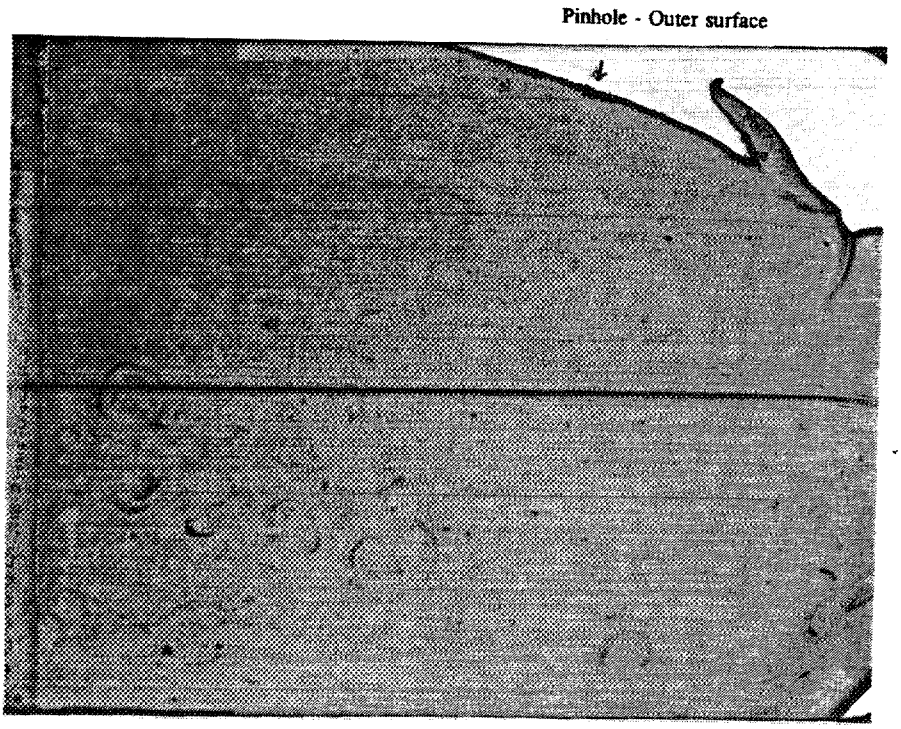

FIGURE 1. OPTICAL MICROGRAPH OF MICROTOMED SECTIONS SHOWING POCK MARKS

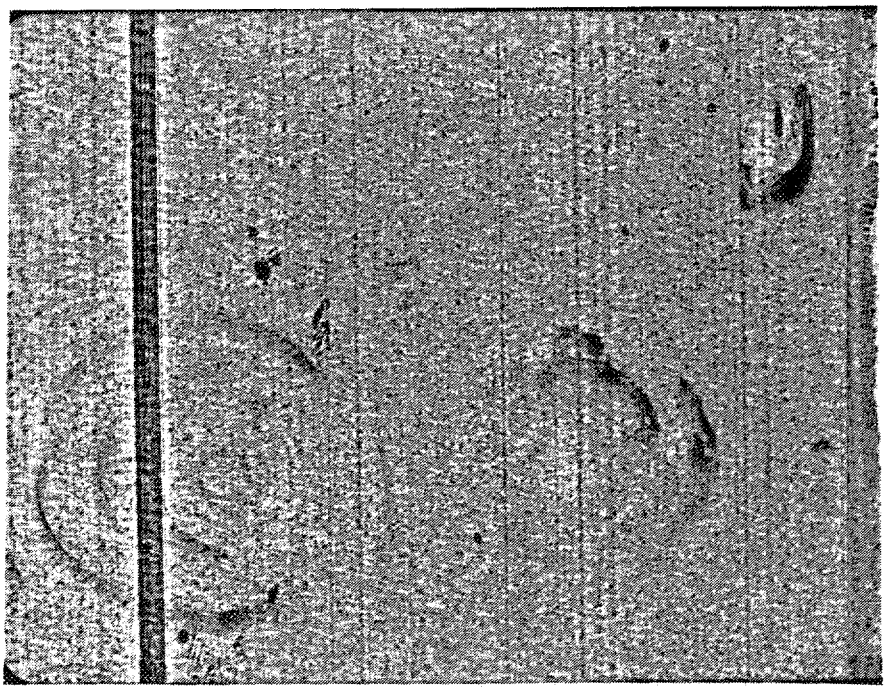

FIGURE 2. OPTICAL MICROGRAPH OF MICROTOMED SECTIONS SHOWING POCK MARKS

boundaries of the pock marks appear dark because of the transmitted light. These pock marks seem to be loosely connected to the polyethylene matrix. Occasionally, for pipe material that happens to contain a hard inclusion, microtoming shears the inclusion, leaving a hole as seen at higher magnification by SEM (Figure 3). Analysis of the inclusion using energy dispersion spectroscopy (EDS) (Figure 4), indicates that the inclusion contains mainly Si, Al, Ti, and Na (Table 1). Column 1 of Table 1 indicates the element and the spectroscopic line that were used for identification. Columns 2 and 3 present the atom percent and weight percent of each element. A scanning electron micrograph of a section (Figure 5) of the microtomed slice shows the pinhole near the left side. It looks like a crevice with an irregular edge, which indicates that the pinhole may not be cylindrical in shape. The white spots in the main body of the picture are pigments and contaminants. The scanning electron micrograph (Figure 6) of a section away from the pinhole shows a large inclusion and white spots. The white spots near the large inclusion were analyzed using EDS (Figures 7 and 8). Spot A contained mainly Ti, and spot B contained Pb and Cr. These elements occur in the pigment (Table 2). Most of the pock marks are aligned along the axis of the pipe, and are superimposable as may be seen from Figures 9, 10, and 11. This indicates that the pock marks extend over a length of at least 2 mm. Figure 12 presents a backscattered image of the pock marks in the microtomed section. Back scattering makes the heavier elements appear bright in the picture. It appears that there may be a concentration of heavier elements at the boundaries of some of the pock marks. EDS analysis shows that the white trace in Figure 12 consists of Pb, Cr, and Ti. Pb and Cr may have come from lead chromate, the pigment of the yellow pipe. Concentration of white spots at a few areas may indicate that the pigments may not be uniformly dispersed in the bulk of the polyethylene material.

The microscopic investigation is being continued to explore the geometry of the pinholes, to monitor the prevalence of the pock marks, and to examine their impact on the morphology of the pipe material.

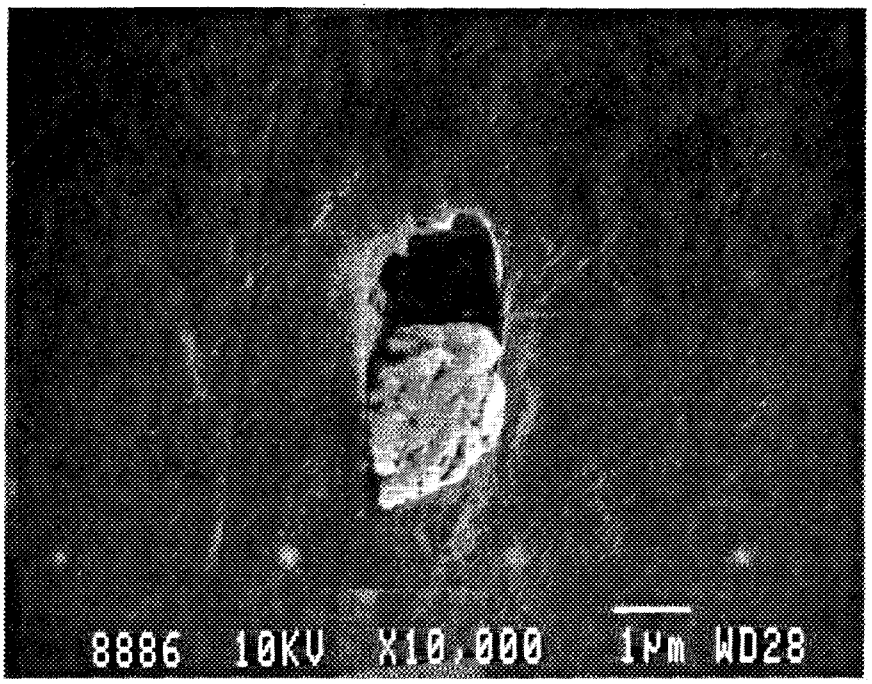

FIGURE 3. SCANNING ELECTRON MICROGRAPH OF MICROTOMED SLICES SHOWING X = 10,000

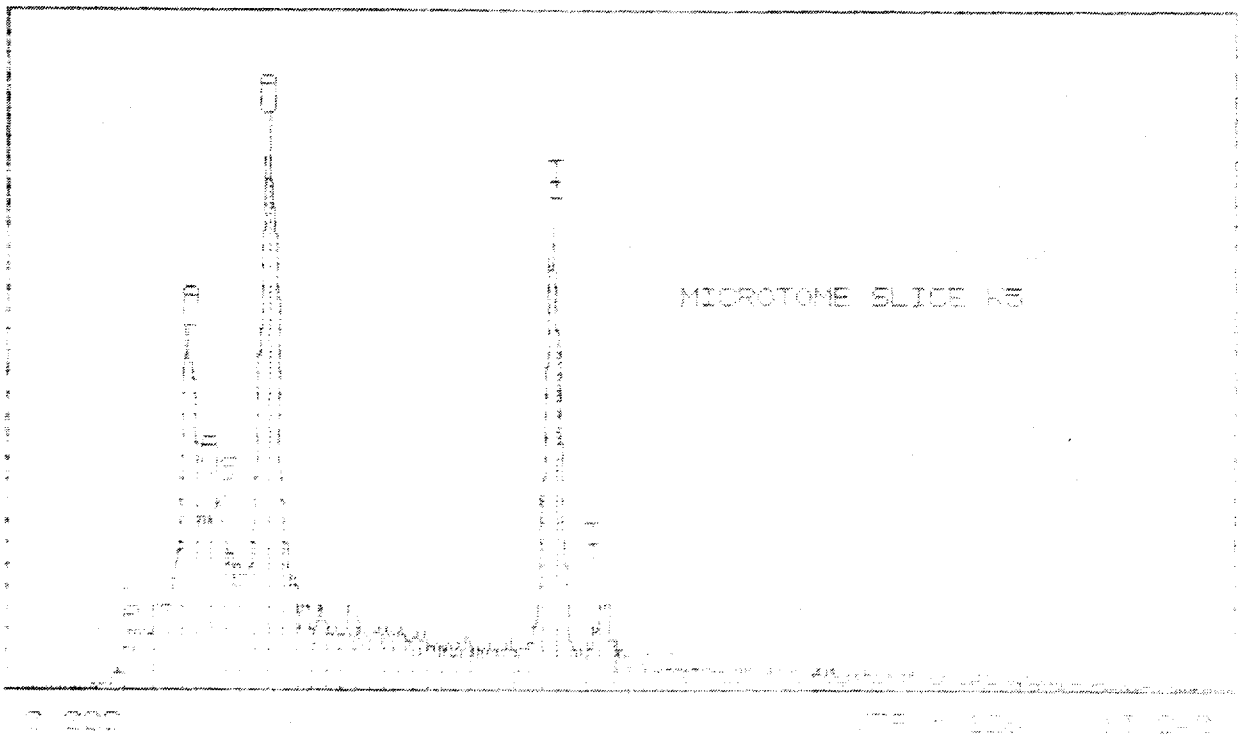

FIGURE 4. EDS OF INORGANIC INCLUSION IN MICROTOMED SLICES

TABLE 1. ELEMENTS PRESENT IN THE INORGANIC INCLUSION

Element	Atom, percent	Weight, percent
Na-K	5.73	3.34
Si-K	13.36	9.51
Ti-K	60.05	72.89
Al-K	20.86	14.26
Total	100	100

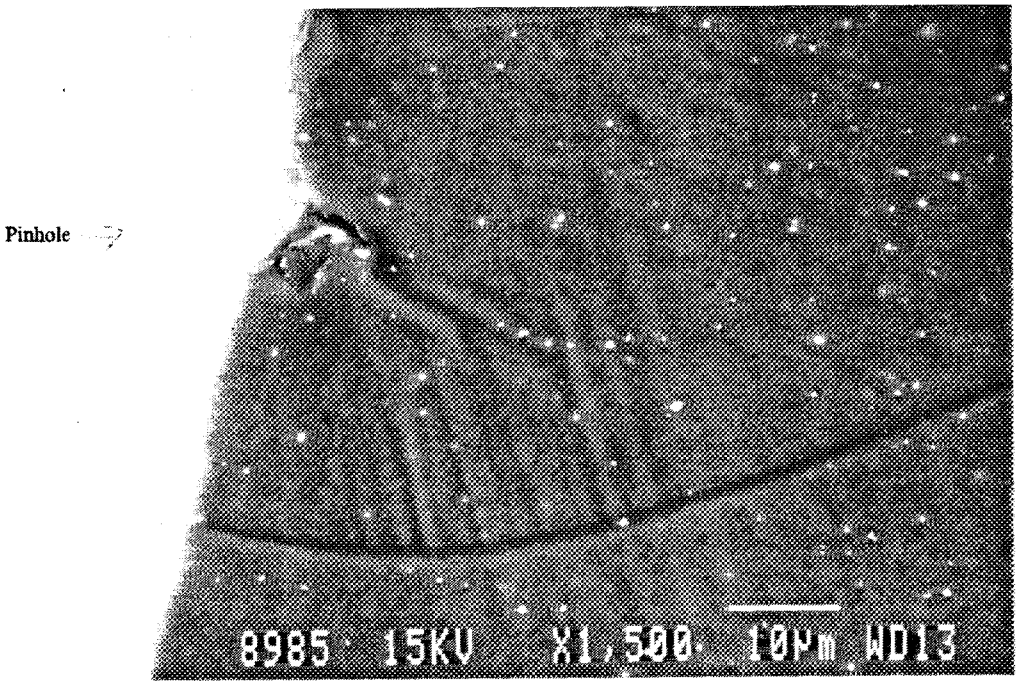

FIGURE 5. MICROTOMED SECTION SHOWING PINHOLE ON THE LEFT

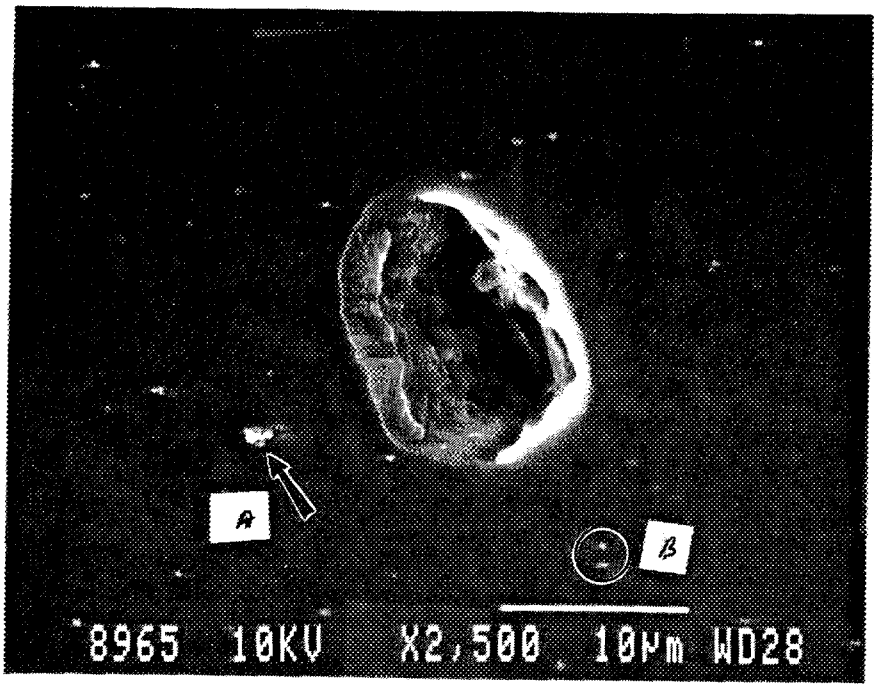

FIGURE 6. SCANNING ELECTRON MICROGRAPH OF THE MICROTOMED SECTION AWAY FROM THE PINHOLE SHOWING A LARGE INCLUSION ACCOMPANIED BY SMALL WHITE SPOTS A AND B

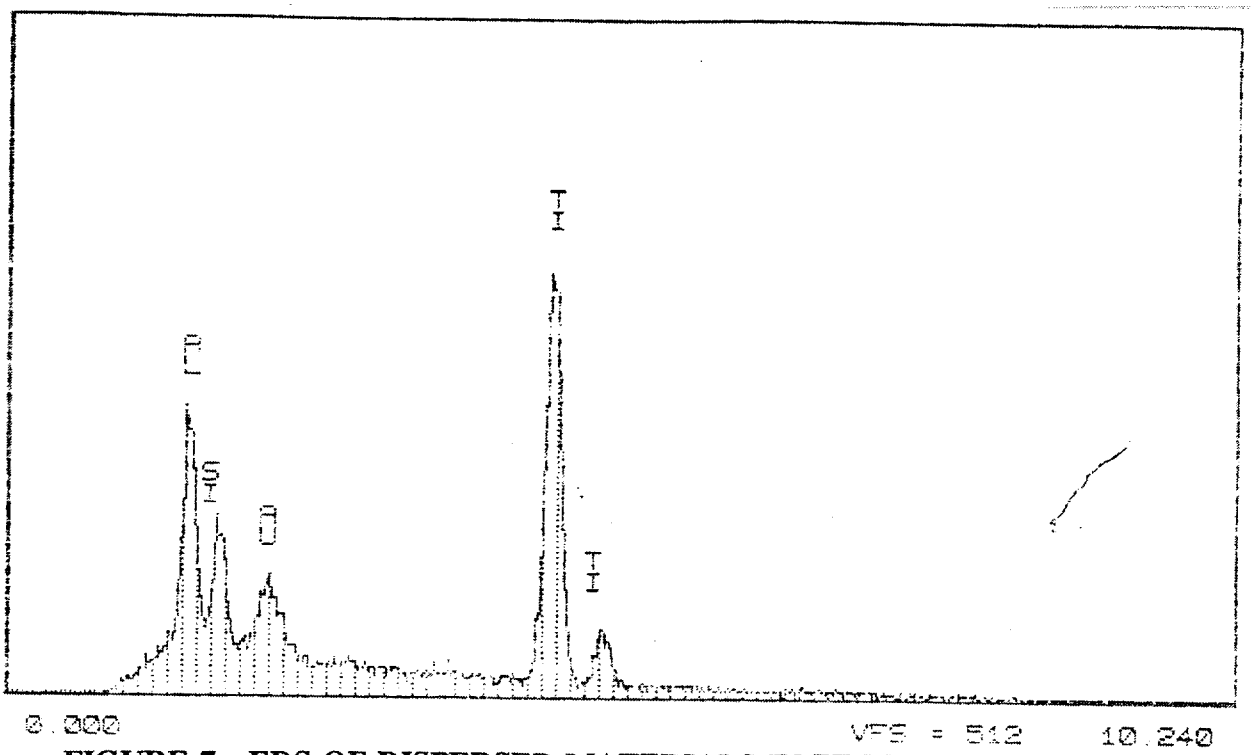

FIGURE 7. EDS OF DISPERSED MATERIALS IN PE MATRIX, AREA A

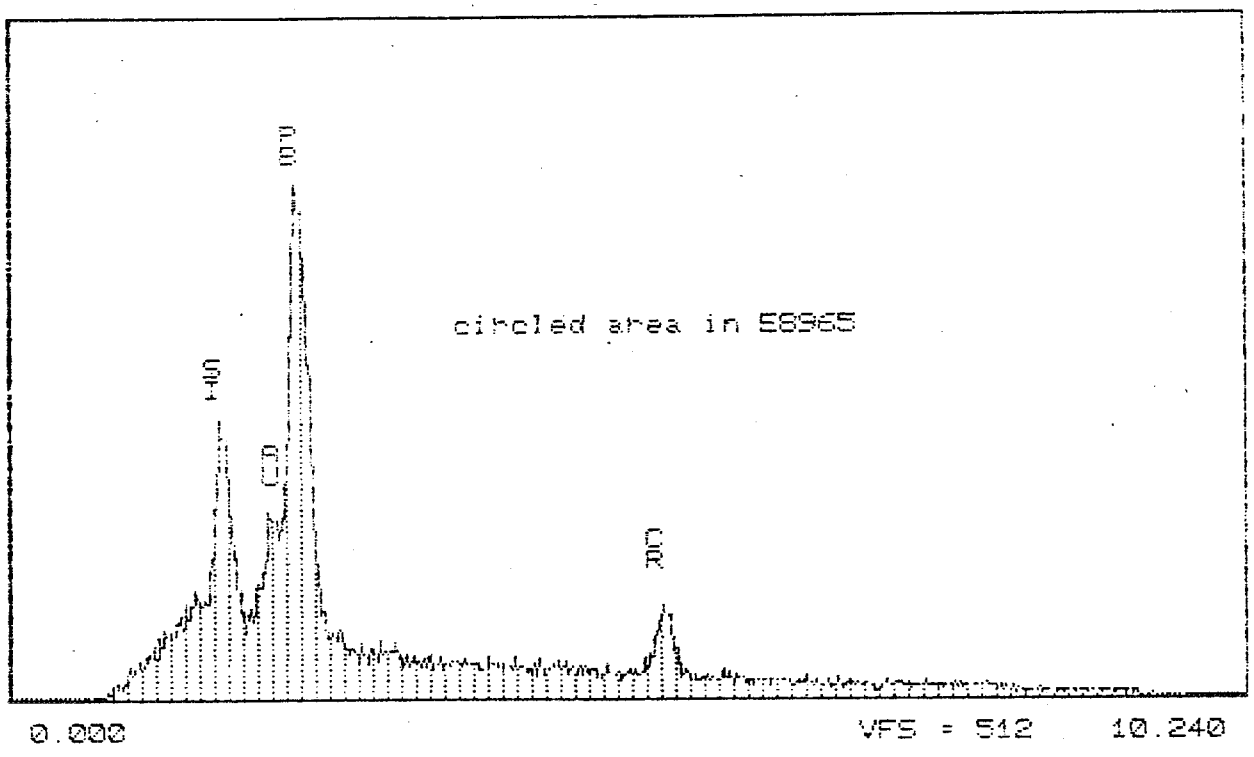

FIGURE 8. EDS OF DISPERSED MATERIAL IN PE MATRIX (AREA B)

TABLE 2. ELEMENTS PRESENT IN DISPERSED PARTICLES IN PE MATRIX

Element	Atom, percent	Weight, percent
Area A		
A1-K	18.97	12.22
Si-K	10.30	6.91
Ti-K	70.73	80.88
Area B		
Si-K	29.96	8.78
Pb-M	32.85	71.03
Cr-K	37.20	20.19

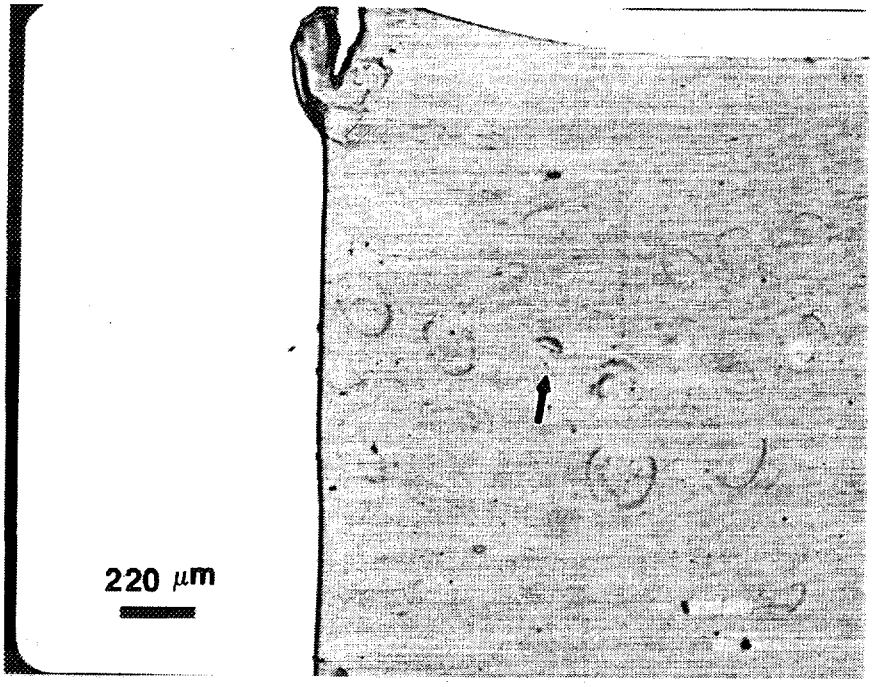

FIGURE 9. SUPERIMPOSABLE POCK MARKS FROM MICROTOMED SECTIONS OVER A DISTANCE ≈2 MM

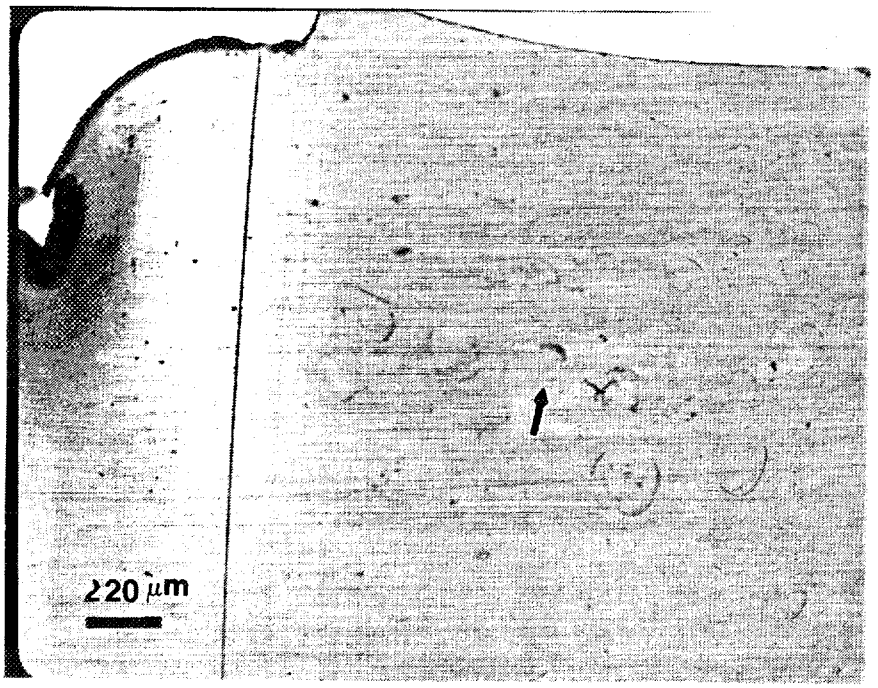

FIGURE 10. SUPERIMPOSABLE POCK MARKS FROM MICROTOMED SECTIONS OVER A DISTANCE OF >2 MM

end

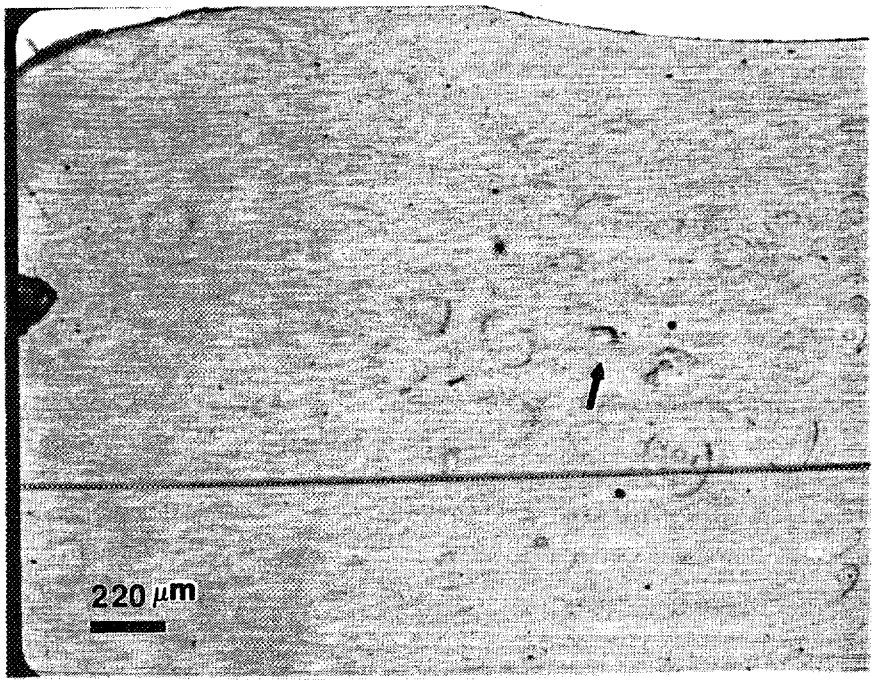

FIGURE 11. SUPERIMPOSABLE POCK MARKS FROM MICROTOMED SECTIONS OVER A DISTANCE OF >2 MM

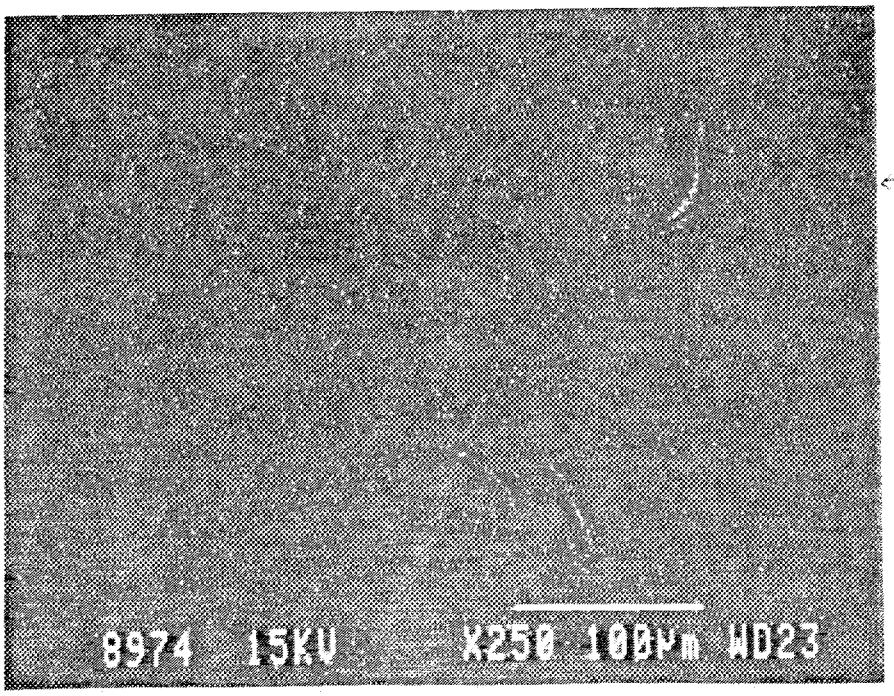

FIGURE 12. BACK SCATTERED ELECTRON MICROGRAPH OF MICROTOMED SAMPLES SHOWING WHITE STREAKS OF PIGMENT, $PbCrO_4$

Infrared Spectroscopy Investigations

Infrared spectrophotometric examination of the materials near the pinhole was continued. Figures 13 and 14 present the IR spectra of acetone extracts made from polyethylene beads (before extrusion) and pipe material away from the pinhole. Figure 15 presents the IR spectra of the acetone extract of the pipe material taken close to the pinhole. Examination of the peaks near 3,000 wave numbers shows that the ratio of the methyl ($-CH_3$) peak to the methylene ($-CH_2$) peak is small in the extract of both the bead and the material away from the pinhole, but is high in the extract of the material close to the pinhole. The combined peak area also decreases as one goes from the bead to the pinhole material. This may indicate that the proportion of paraffinic material near the pinhole area is smaller compared with the virgin pipe material, and the extracted material near the pinhole is mainly low molecular weight polyethylene. Acetone extracts are a representation of the material soluble in acetone. Therefore, additional tests are necessary to confirm these conclusions.

Expert Consultations

Twelve experts in polymeric material, polymer processing, fracture mechanics, and failure of gas pipes were consulted regarding the cause of pinhole formation. The general consensus is that the pinholes are manifestations of inhomogeneity in the pipe material. The inhomogeneity could be caused by a skewed molecular weight distribution (presence of very high and low molecular weight material), presence of gel particles (due to crosslinking and/or oxidation) or the presence of a few well-formed large crystallites. The weak interfaces between the gel particles/crystallites and the matrix material could become weaker during service. In this process, crevices are formed. A leakage path may be formed when one of these particles stretches through the entire pipe wall, or when a number of these crevices are aligned in the radial direction. Internal gas pressure and temperature cycling may accentuate the formation of the pinholes leading to gas leakage. The possibility of some

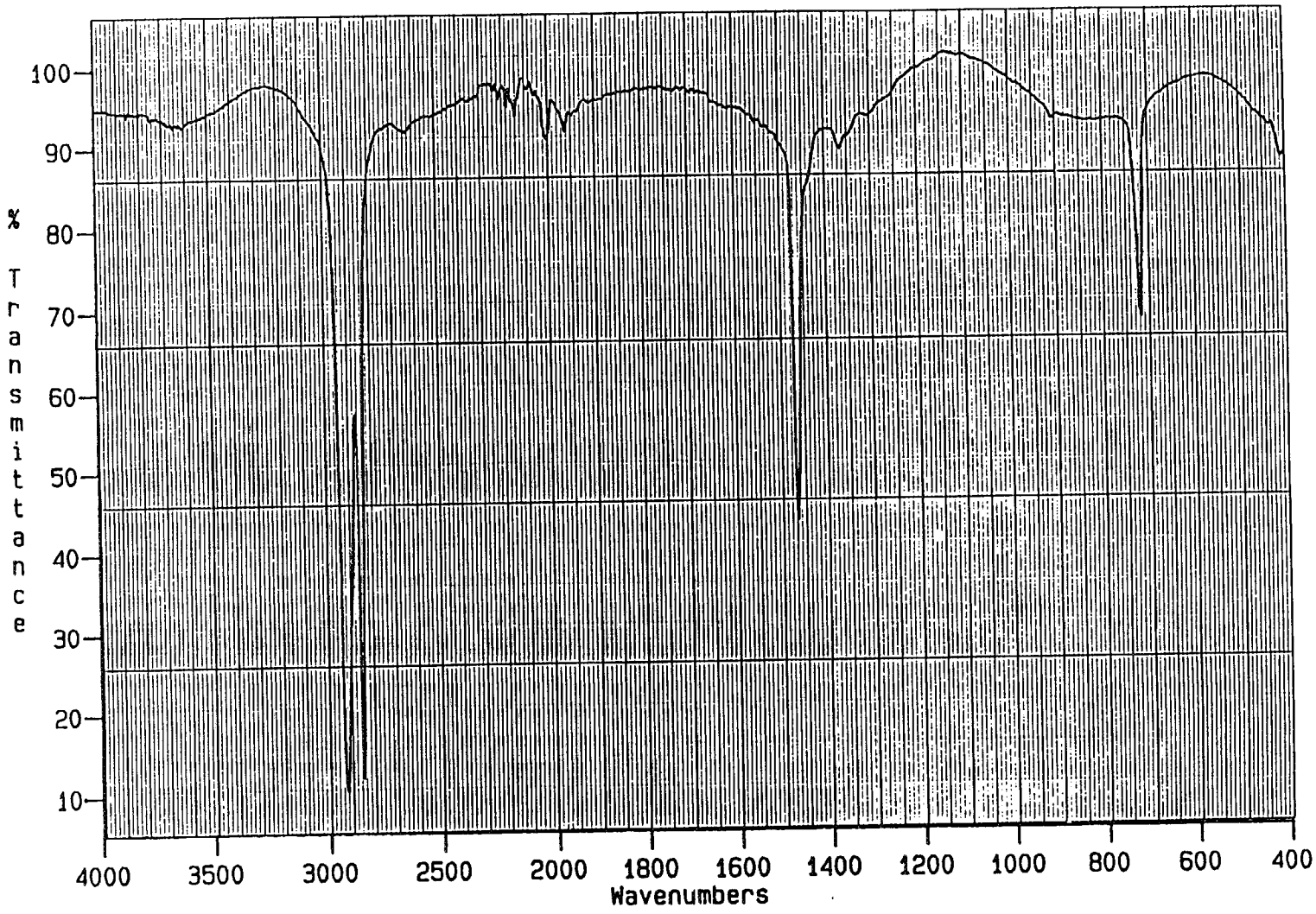

FIGURE 13. INFRARED SPECTRA OF ACETONE EXTRACT OF POLYETHYLENE BEADS PE2306-C-782 P23BC

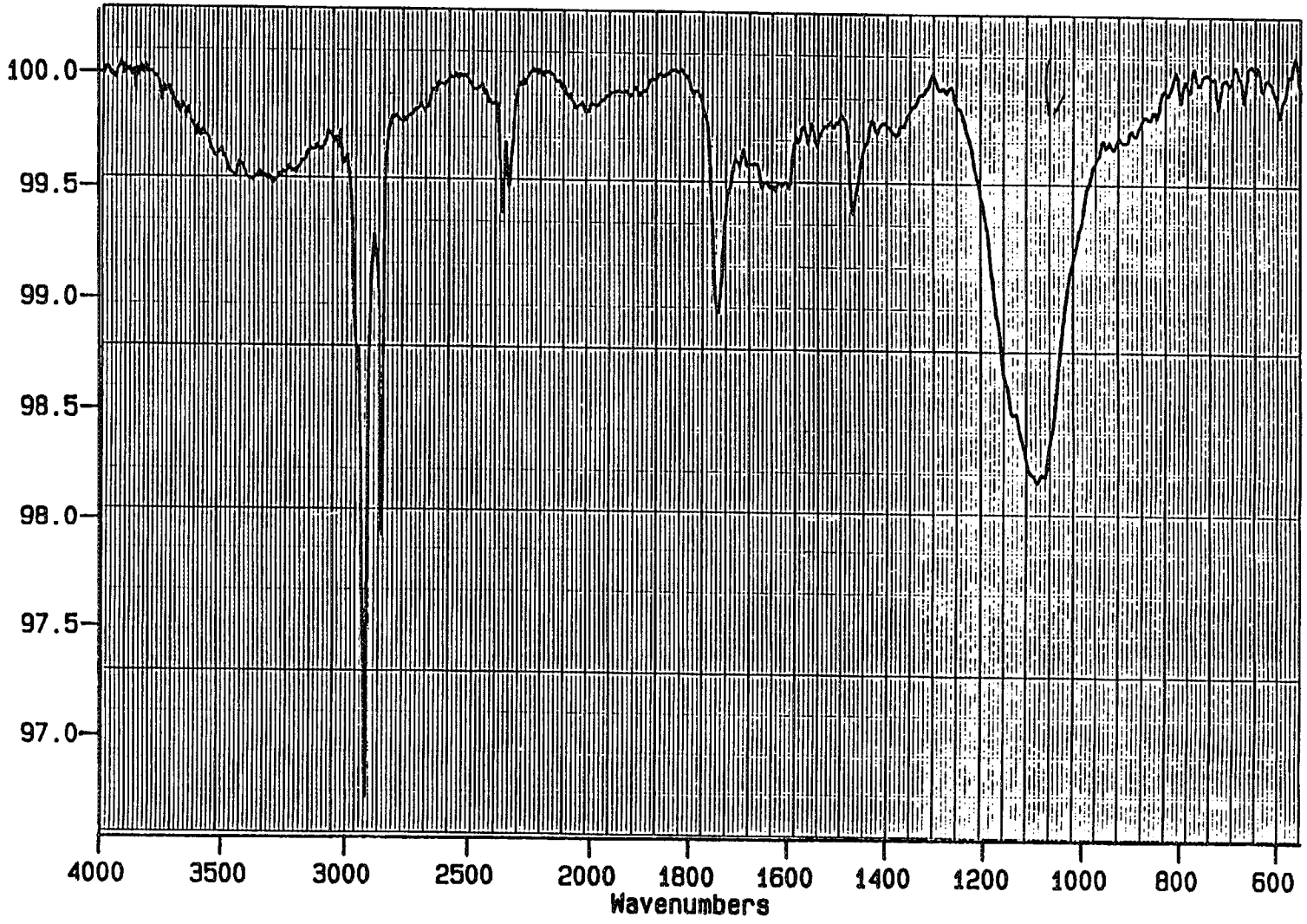

FIGURE 14. INFRARED SPECTRA OF ACETONE EXTRACT OF PE MATERIAL AWAY FROM PORE IN SAMPLE E

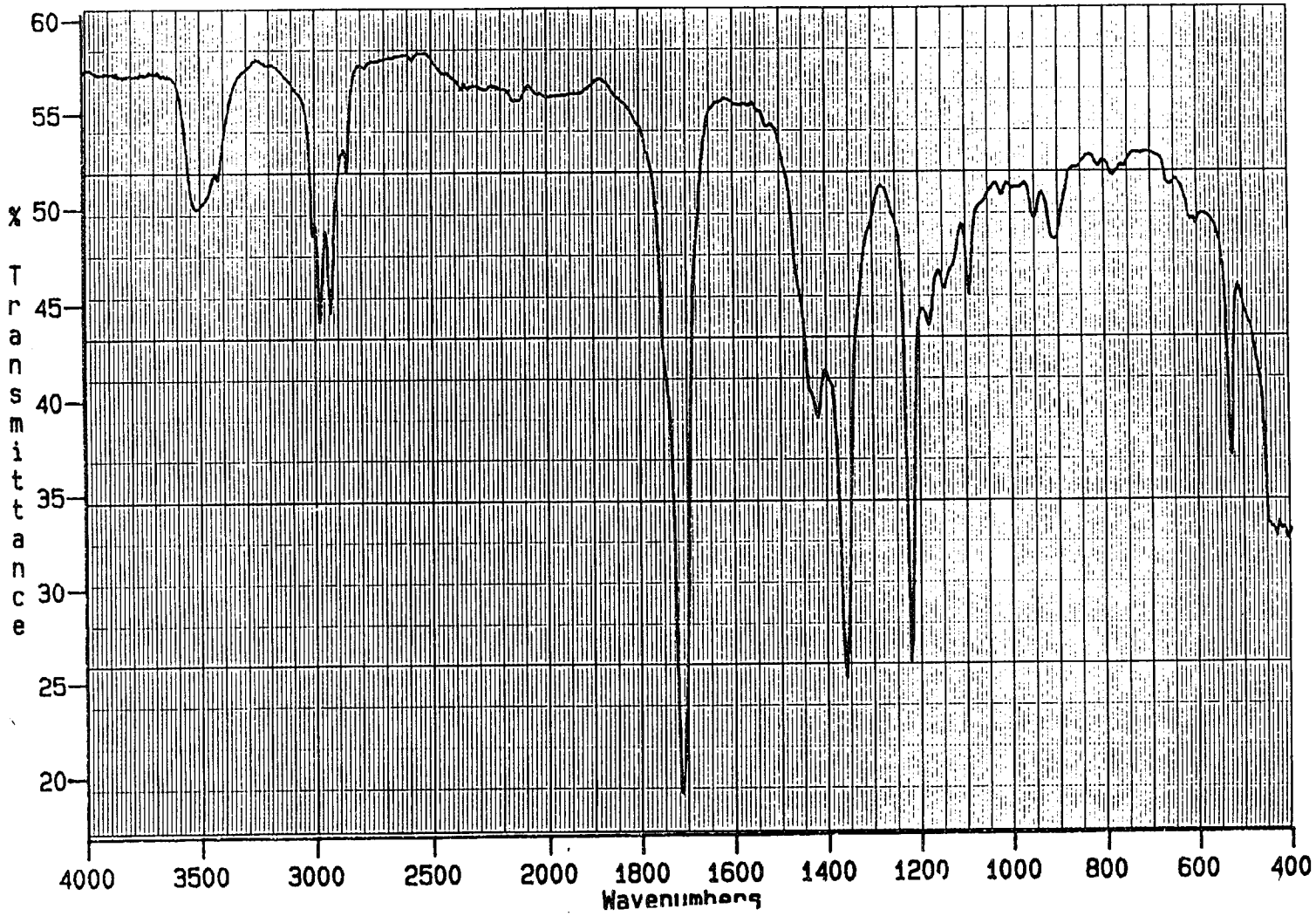

FIGURE 15. INFRARED SPECTRA OF ACETONE EXTRACT OF PE MATRIAL IN PINHOLE AREA

volatile material escaping from the pinhole area and causing a pinhole cannot be ruled out, although the chance of this happening is small.

Literature Survey

Pinholes identical to those in the present study, were examined by Battelle in the mid 1980s. They were discussed in a Battelle report, and in the *Field Failure Catalog* published by GRI. The earlier examination suggested the possibility of pinhole occurrence due to poor processing and due to the presence of contaminants. However, there is no conclusive evidence to support this contention in those reports.

Future Work

(1) **Hot stage microscopy and infrared spectrophotometry** of the pipe material near and away from the pinhole to examine the melting characteristics and crystallity.

(2) **Laser Raman Spectroscopy** of the material near the pinhole to identify fingerprints of low molecular weight species which might have escaped causing the pinholes.

(3) **Scanning Electron Microscopy and EDS** to investigate the presence of pockmarks in areas with and without pinholes. This may show that the material inhomogeneity causing pinholes is present in all parts of the pipe and is not confined to the pinhole area only.

(4) **Simulation experiments** for pinhole formation.

APPENDIX B

MOLECULAR WEIGHT MEASUREMENT DETAILS

APPENDIX B
MOLECULAR WEIGHT MEASUREMENT DETAILS

The purpose of these measurements was to determine if the material near the pinhole area differed in its molecular weight distribution from the material away from the pinhole area. A Waters 150C ALC model Gel Permeation Chromatography unit was used. Trichlorobenzene at 132 C was used as a solvent. Samples weighing approximately 25 to 30 milligrams were taken from the area close to the pinhole, and away from the pinhole.

Figures B-1 and B-2 present the gel permeation chromatograms (GPCs) of the PE material near and away from the pinhole in a yellow pipe. Broad molecular weight PE standard materials, supplied by the National Bureau of Standards (NBS), were used as a reference standard. The relative concentration of each PE fraction is plotted against the retention time, which is related to molecular weight. The longer the retention time, the smaller is the molecular weight. The numbers inserted in the chromatogram present the retention time and molecular weight of each fraction.

It is seen from Figures B-1 and B-2 that the weight fractions of high molecular weight polyethylene components are substantially lower in the pipe material near the pinhole compared to those away from the pinhole. This is further illustrated in Figure B-3, where the two distribution curves are superimposed. The polydispersity of the material away from the pinhole is 13.2, and that of the material near the pinhole is 3.3 (Table B-1). Polydispersity, B, is defined as follows:

$$B = \frac{M_w}{M_n}$$

where M_w = weight average molecular weight

M_n = number average molecular weight.

Subsequently, similar measurements were carried out with polyethylene material taken from the area close to the pinhole and away from the pinhole in an orange pipe. This time, polystyrene standards with a narrow molecular weight distribution were used as reference standard. The GPC curves are presented in Figures B-4 and B-5, respectively.

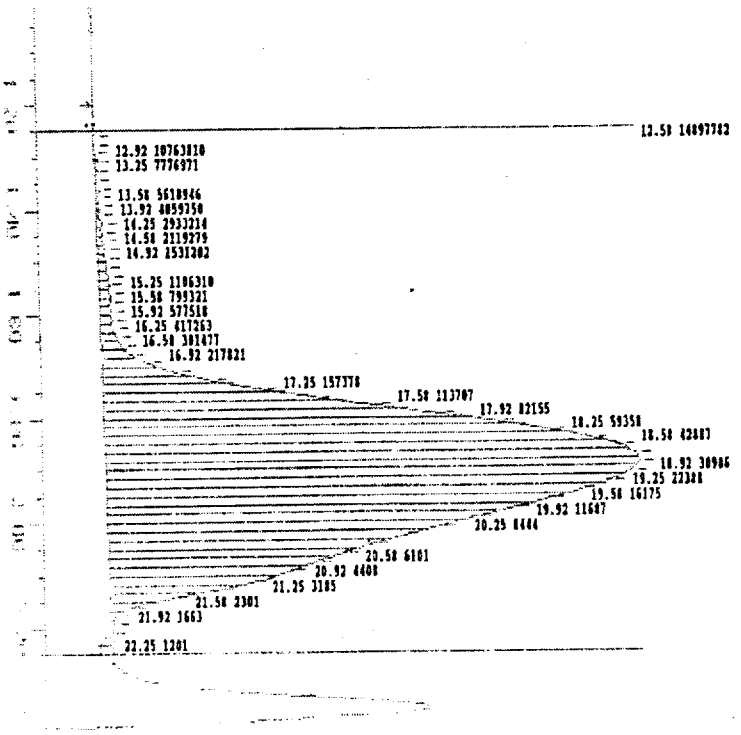

Figure B-1. GPC of PE material close to pinhole (yellow pipe)

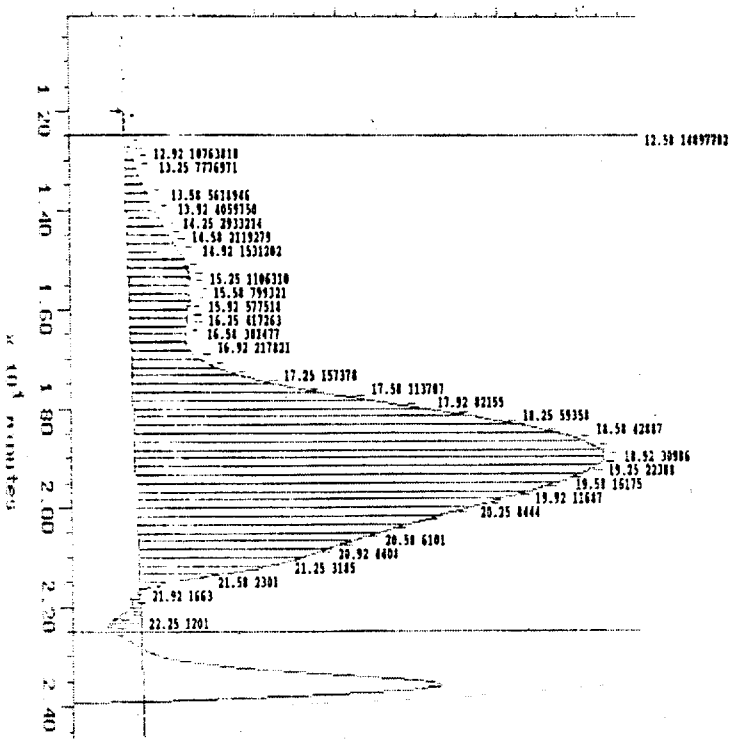

Figure B-2. GPC of PE material at a distance from the pinhole

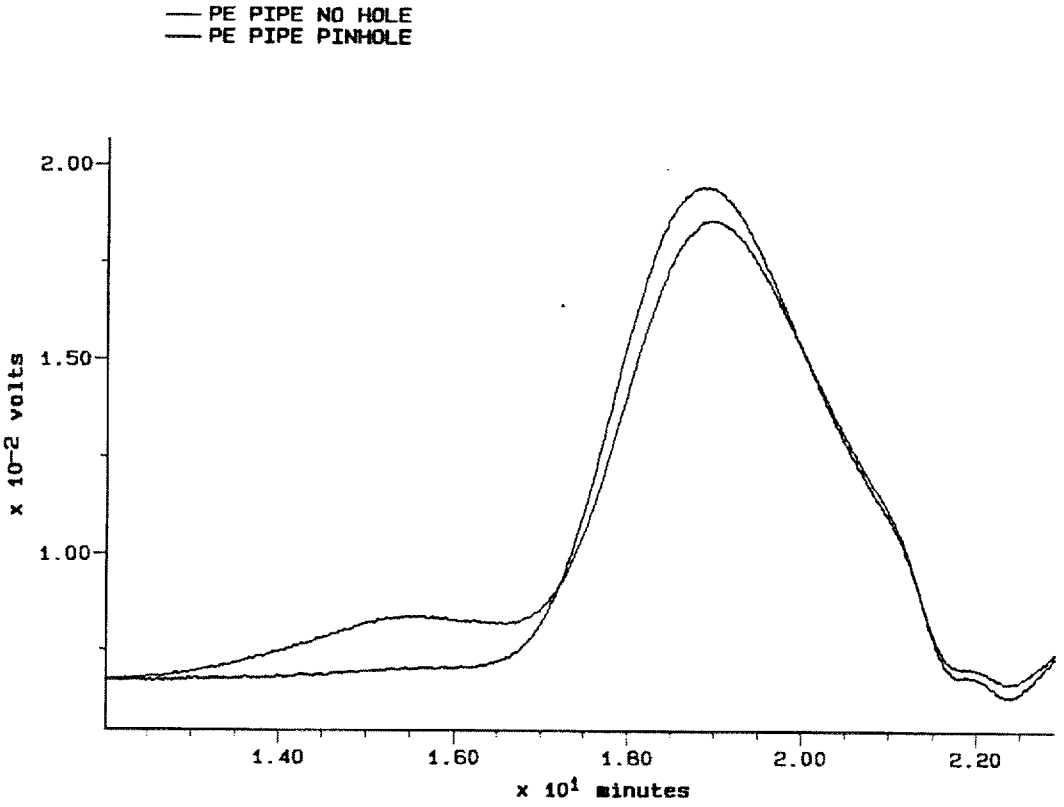

Figure B-3. Relative distribution of molecular weight of PE material close to and away from pinhole

Table B-1. Number Average Molecular Weight (M_n) and Polydispersity, B, of PE Taken from Gas Pipe

		$M_n \times 10^3$	B
Yellow Pipe	Close to Pinhole	15.7	3.3
	Away from Pinhole	16.7	13.2
	New Pipe (not in service)	21.4	14.95
Orange Pipe	Close to Pinhole	29.4	14.4
	Away from Pinhole	27.3	16.0

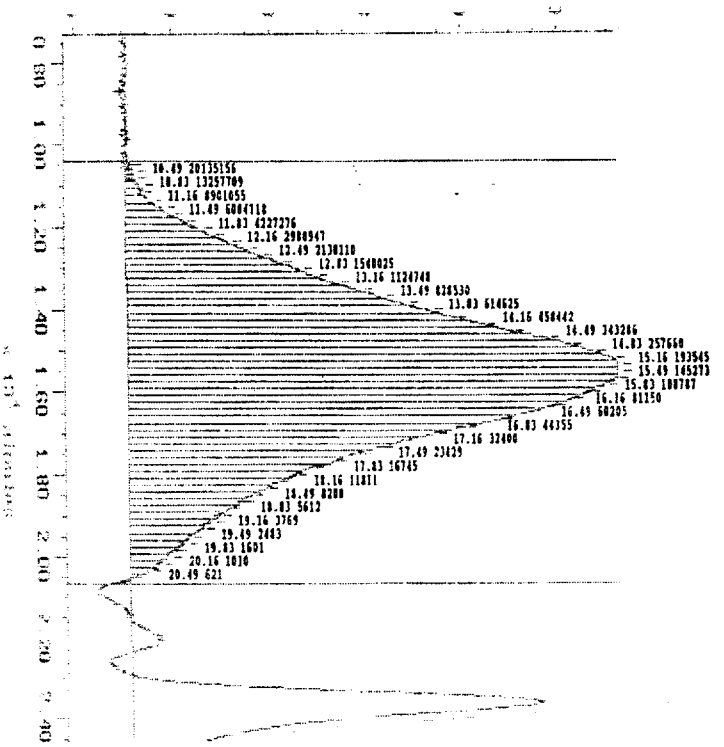

Figure B-4. GPC of PE material close to pinhole (orange pipe)

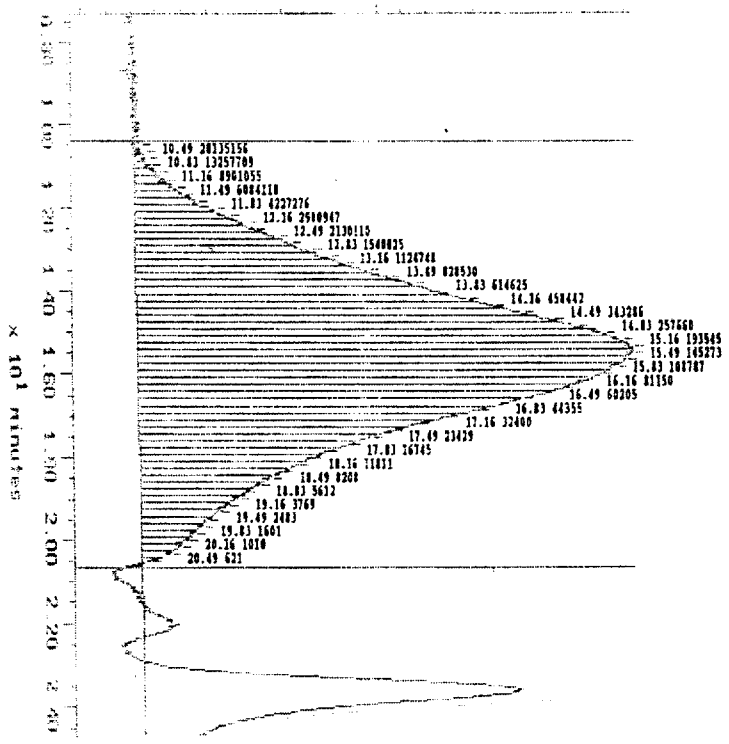

Figure B-5. GPC of PE material away from pinhole (orange pipe)

Figure B-6 presents the GPC curve of polyethylene material taken from a yellow pipe extruded in 1993 that was never put into service. The three GPC curves are compared in Figure B-7.

The GPC curves of the orange pipe material close to the pinhole, and away from the pinhole, do not show appreciable differences. They are also not very different in shape from the GPC curve for the PE material of the recently extruded yellow pipe, although the number average molecular weight of the latter is significantly smaller compared to the PE material from the old pipes as shown in Table B-1. Reprocessing of the data on a broad-distribution PE standard does not change the overall conclusion.

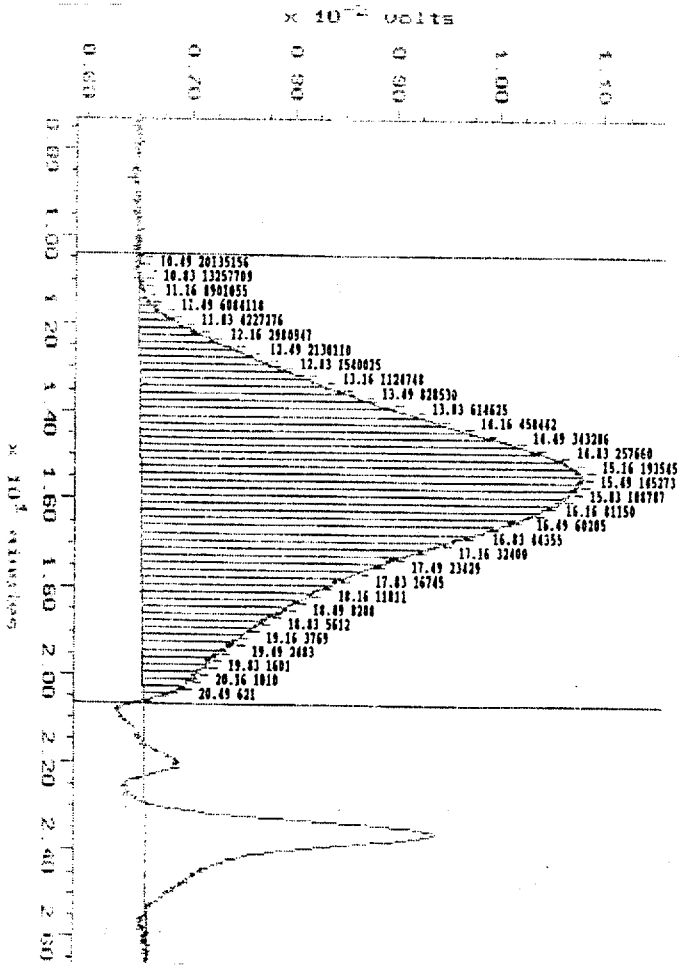

Figure B-6. GPC of PE material taken from virgin pipe (1993) (yellow)

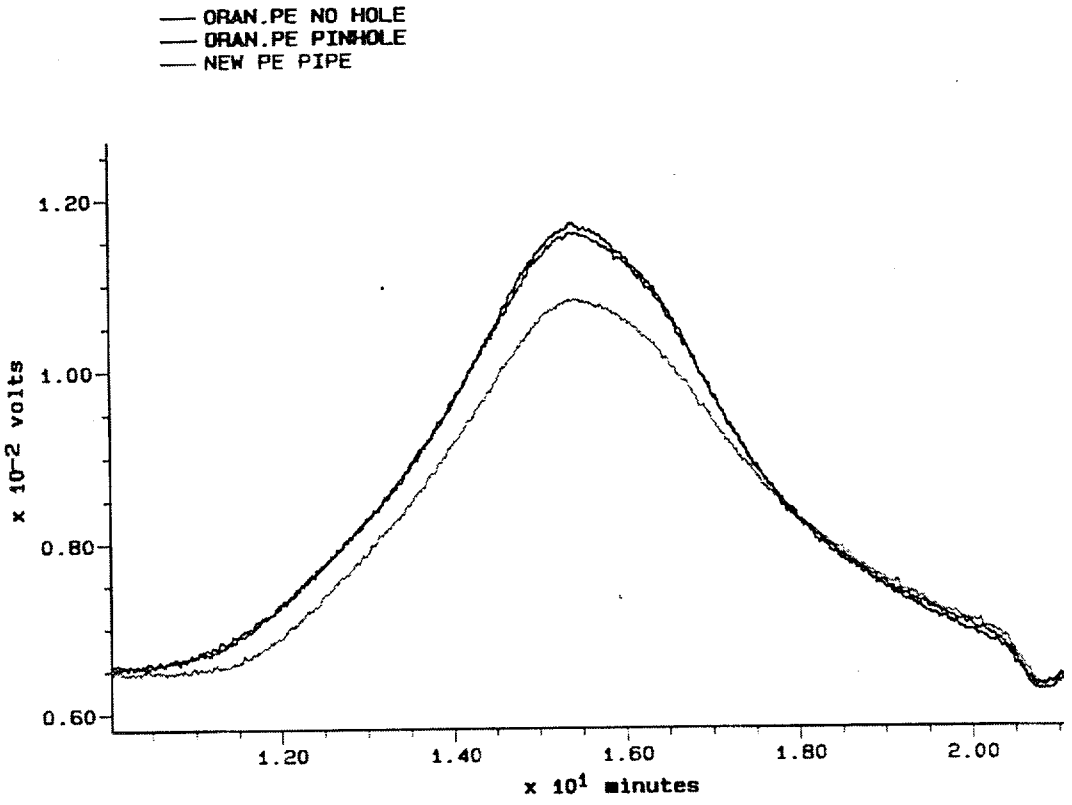

Figure B-7. Comparison of molecular weight distribution of PE material taken from orange pipe close to pinhole, away from pinhole, and virgin pipe

APPENDIX C

RAMAN SPECTROSCOPY DETAILS

APPENDIX C
RAMAN SPECTROSCOPY DETAILS

Raman spectroscopy, like infrared (IR) spectroscopy, measures vibrational transitions and provides a fingerprint of the molecular composition of the material under study. Raman spectroscopy is somewhat more sensitive to inorganic materials than IR. Micro Raman, which is a microscope to focus on specific sample locations, provides good resolution for surfaces as small as a few microns in length and as such is very suitable for studying small local differences. The objective of the Micro Raman study was to examine compositional differences of the polymeric material close to the pinhole as compared to the material away from the pinhole. Compositional differences could be due to

- Inhomogeneity in the extruded material
- Chemical changes such as polymer degradation, chain scissions, etc.
- Interaction of the organic material with the mobile phase, either gas or aqueous electrolyte.

This study was carried out at the Molecular Spectroscopy Laboratory at Miami University, Oxford, Ohio.

The samples used for analysis were microtomed cross-sections of yellow PE gas pipes having pinholes. The specimens were microtomed parallel to the length of the pipe area, close to the pinhole, and away from the pinhole. Micro Raman analysis was employed to determine if any specific material was linked to the pinholes or if any compositional changes had taken place in the tubing during normal service life. Known components of the tubing included poly-ethylene, phenolic (antioxidant), stabilizers, processing aids, and a lead chromate color concentrate.

Observation of several cross-sections at moderate to high (200 to 1000X) magnification did not show any holes. Features with a hole-like appearance were observed, however, in the form of a circular center with several halos surrounding the center. These features were on the order of 200

to 500 micrometers in diameter. Also observed in the cross-sections were yellow opaque inclusions.

Samples mounted to a microscope slide were analyzed with a Renishaw Raman scope. Excitation was by a helium neon laser with a power at the sample of approximately 12 milliwatts. A 100X infinity-corrected objective was employed to focus the laser to a diffraction-limited spot of approximately 2 micrometers. Spectra were collected with 4 cm^{-1} resolution and integration time of approximately 60 seconds per resolution element.

Preliminary analysis of the yellow inclusions in the pinhole area and a normal area of the tubing yielded Raman spectra labeled BAT081 and BAT082, respectively. A comparison of these spectra with that of polyethylene indicates that the spectrum of the inclusion having transitions with increased intensity located near 357, 443, 608, and 838 cm^{-1} are those of lead chromate.

A comparison of spectra obtained on three specimens close to the defect area and one specimen away from the defect area shows changes in the intensity of the lead chromate transitions when stepping through the defects. In addition, the transition located at 443 cm^{-1} and 608 cm^{-1} shift followed those of the lead chromate. Integrated band intensities for the chromate ion (838 cm^{-1} symmetric stretch) were normalized against polyethylene (1295 cm^{-1} CH_2 in-phase twist) and plotted as a function of position through the defect. The plots (Figures C-1, C-2, C-3, and C-4) present the variations in the chromate concentrations across the defect as well as in the non-defect area. In the normal area (away from pinhole), the chromate concentration variation has been shown over a range of 240 µm, whereas the variations in defect area are shown over 500 µm. Table C-1 presents the variation across the defect and the normal area. There is approximately a 9-fold variation in CrO_4^{-}/PE ratio in the pipe materials, ranging from 0.19 to 1.75. However, the variation for each specimen (except the first one) is smaller.

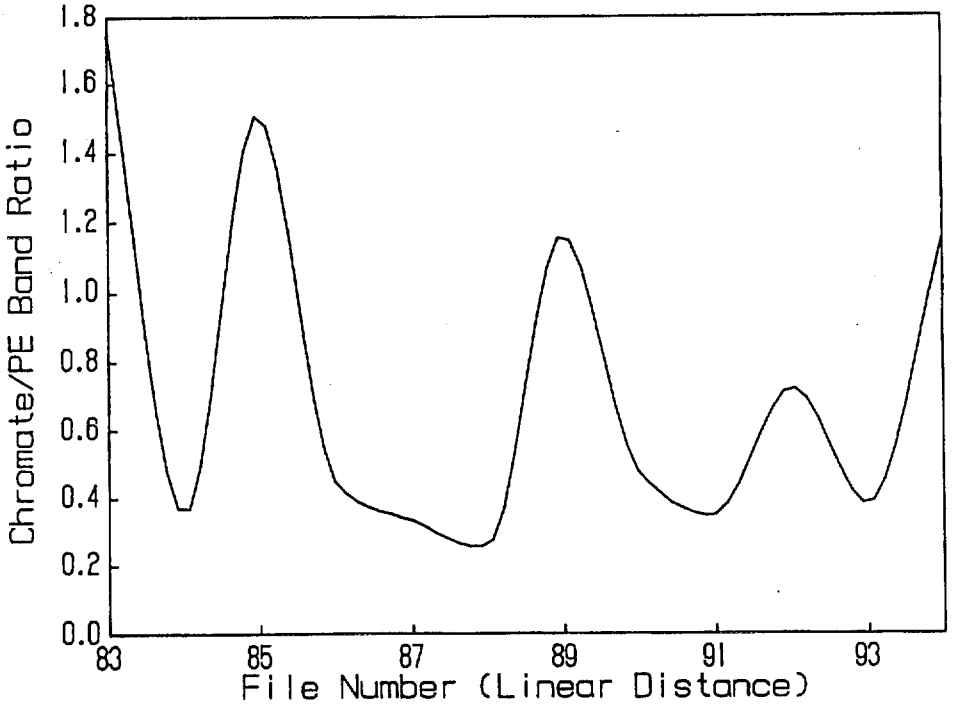

Figure C-1. Variation of chromate across defect (Sample #1)

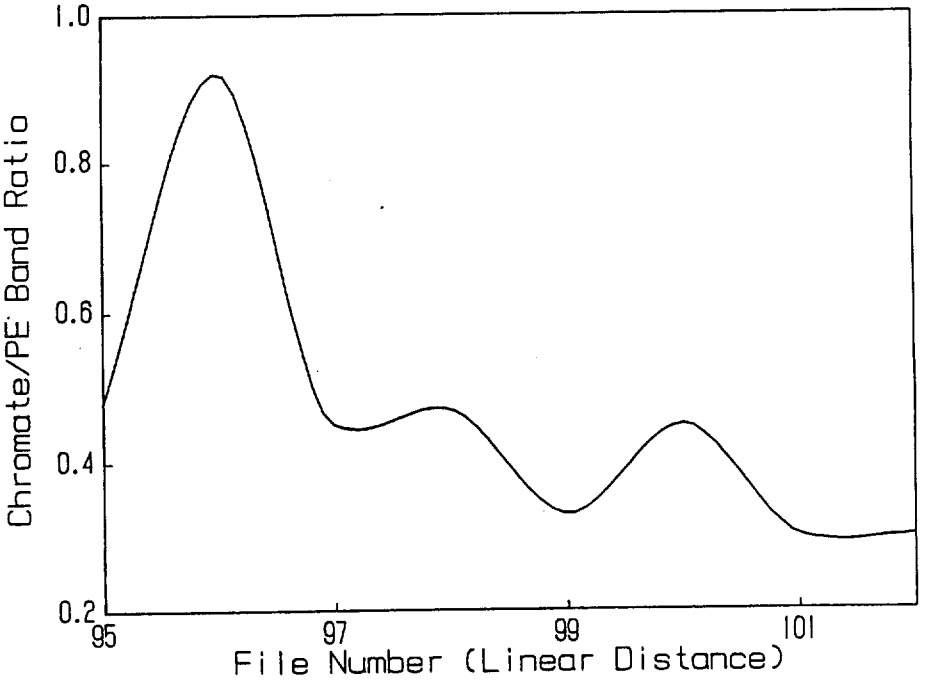

Figure C-2. Variation of chromate across defect (Sample #2)

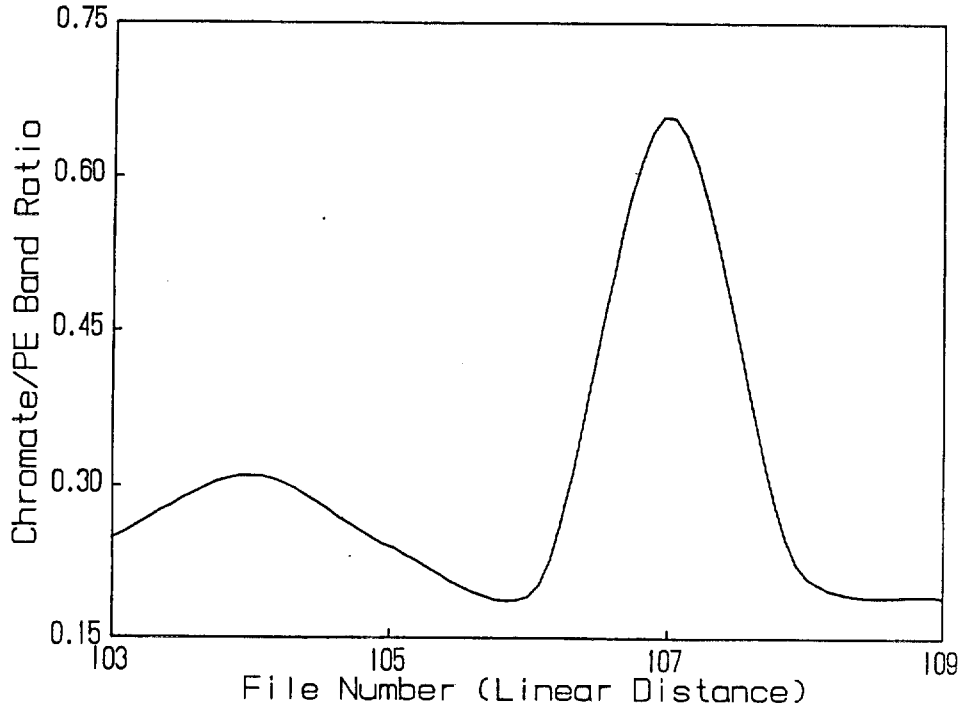

Figure C-3. Variation of chromate across defect (Sample #3)

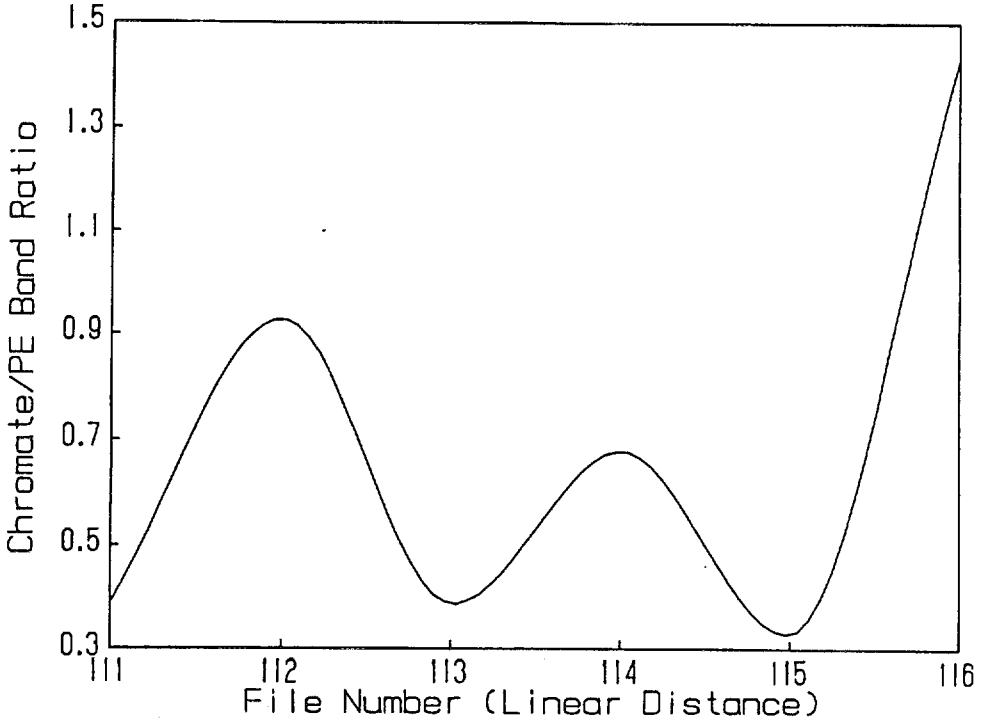

Figure C-4. Variation of chromate in normal area

Table C-1. Variation of Chromate/Polyethylene Ratio (Spectra taken at 40 micrometer intervals across three different defects and one normal area)

Spectrum Label	Chromate Area	Polyethylene Area	CrO4/PE Ratio
Sample #1			
BAT083	413380	236275	1.75
BAT084	46715	133155	0.35
BAT085	179189	118335	1.51
BAT086	56124	126552	0.44
BAT087	44881	134062	0.33
BAT088	35031	135668	0.26
BAT089	139177	120193	1.16
BAT090	59880	127705	0.47
BAT091	45188	129695	0.35
BAT092	90761	125563	0.72
BAT093	48189	127101	0.38
BAT094	140920	122656	1.15
		Average	0.74
Sample #2			
BAT095	55472	116557	0.48
BAT096	94747	103163	0.92
BAT097	54833	121489	0.45
BAT098	55826	119802	0.47
BAT099	39085	117364	0.33
BAT100	55606	123448	0.45
BAT101	37733	126283	0.30
BAT102	36814	123047	0.30
		Average	0.46
Sample #3			
BAT103	13873	56453	0.25
BAT104	19639	63864	0.31
BAT105	14701	61225	0.24
BAT106	10841	57696	0.19
BAT107	38165	57619	0.66
BAT108	13818	65323	0.21
BAT109	11600	62047	0.19
		Average	0.29
Normal Area			
BAT111	126675.00	322117.00	0.39
BAT112	306480.00	328780.00	0.93
BAT113	120761.00	312830.00	0.39
BAT114	210151.00	310503.00	0.68
BAT115	108678.00	328366.00	0.33
BAT116	463004.00	324087.00	1.43
		Average	0.69

Analysis of the circular features was conducted by producing a line scan or linear map across the defects. Three defects and one normal area were investigated with a 40 micrometer step size between adjacent areas. Table C-2 summarizes the spectra obtained for each sample and the type of information investigated.

Table C-2. Line Scan Information for Each of Three Defects

Spectra	Defect Size	Information Sought
BAT083 BAT094	440 μ	Composition across entire defect
BAT095 BAT102	500 μ	Composition across 2/3 of defect
BAT103 BAT109	500 μ	Crystallinity of polyethylene across 1/2 of defect
BAT111 BAT116	240 μ	Baseline for normal area

In the analysis of the third defect, crystallinity differences in the polyethylene were studied. An analyzer was placed in the optical train passing the Raman scattered radiation from the microscope to the spectrometer. Spectra were again collected by scanning through the defect. A comparison of spectra within the map show no significant change ongoing through the defect (i.e., no crystallinity changes). However, comparison of spectra with and without the analyzer in place show differences in the transition located near 1100 cm^{-1} which indicate that the polyethylene is oriented. As before, however, the intensity of the chromate transition was observed to change.

In conclusion, no crystallinity differences were detected in the polyethylene through the defect areas. Only compositional differences were observed, which could be attributed to the concentration of lead chromate in the pipe material. This type of compositional difference was also observed in normal areas of the pipe (without pinholes) and is therefore not uniquely related to the existence of the pinhole.

The opaque yellow inclusions within the polyethylene were identified as lead chromate whose characteristic transitions are observed at 357 and 838 cm^{-1}. Additional transitions that mimicked those of the lead chromate were observed at 443 and 608 cm^{-1}.

APPENDIX D

SOIL ANALYSES DETAILS

APPENDIX D
SOIL ANALYSES DETAILS

Samples were extracted and analyzed using EPA SW 846 Method 3550 and Method 8270. Instrument calibration and QA/QC were also carried out as specified by these methods.

Three soil samples, identified as #4, #14, and #16, were received on June 3, 1994. Samples were stored in a refrigerator until time of extraction and analysis.

Samples were extracted following EPA SW 846 Method 3550, Sonication Extraction. First, 30-g portions of each sample were mixed with 60 g of anhydrous sodium sulfate. Each sample was fortified with surrogate standards to monitor potential matrix interferences and measure extraction efficiency. Methylene chloride/acetone (50:50) was added and the sample was sonicated using a Heat Systems-Ultrasonics Sonic Cell Disruptor Model W375. The organic was then removed and dried with sodium sulfate. The extraction was repeated two more times and all extracts pooled together and concentrated using Kuderna Danish apparatus to a final volume of 1 mL. Deuterated internal standard compounds were added to the 1 mL extract prior to analysis by GC/MS.

GC/MS analysis was performed using a Hewlett-Packard 5890 GC interfaced to a 5970 Mass Selective Detector (MSD). The mass spectrometer was operated in the full scan mode from 35 to 500 amu. A Restek Rtx-5 30 m X 0.25 mm capillary column with a 1.0 µm film was used for chromatographic separation. Injections of 1 µL were made using an HP 7673 autosampler in the splitless mode. The capillary column was temperature programmed from 40 to 300°C at 10°C/minute and held for 30 minutes. EPA SW 846 Method 8270 was followed.

Method 8270 is used to determine the concentration of semivolatile organic compounds in a variety of matrices including soil. Method 8270 is able to quantify many basic, neutral, and acidic (BNA) organic compounds that are soluble in methylene chloride and capable of being eluted without derivatization from a gas chromatographic fused silica capillary column. Compounds including polynuclear aromatic hydrocarbons (PAHs), chlorinated hydrocarbons, phthalate esters, pesticides,

nitrosoamines, haloethers, anilines, aromatic nitrocompounds, and phenols can be analyzed using this method. A list of the specific analytes the mass spectrometer was calibrated for as well as practical quantitation limits (PQLs) for each analyte can be found in Tables D-1, D-2, and D-3. Each table represents a single sample. In addition to the target analytes, the 20 largest nontarget analyte peaks were library searched using the software provided with the mass spectrometer system. Only peaks yielding good library matches and not found in the method blank are reported.

Prior to analysis of the sample extracts, the mass spectrometer was hardware tuned to meet DFTPP (decafluorotriphenylphosphine) requirements specified in Method 8270. An initial five-point calibration curve containing all target analytes was also generated. An average response factor was generated for each analyte using the internal standard technique from the initial calibration curve. Concentration was then calculated by the mass spectrometer data system as follows:

$$\text{Conc. } \mu g/kg = \frac{(A_x)\ (I_s)\ (V_t)}{(A_{is})\ (RF)\ (V_o)\ (V_i)}$$

where:

A_x = Area of characteristic ion for compound being measured

I_s = Amount of internal standard injected (ng)

A_{is} = Area of characteristic ion for the internal standard

RF = Average response factor for compound being measured

V_o = Volume of sample extracted (g)

V_t = Volume of total extract (μL)

V_i = Volume of extract injected (μL).

Continuing calibration standards were analyzed and tuning checks performed every 12 hours of operation to verify the performance of the instrument.

Quality control samples included a method blank consisting entirely of sodium sulfate, a matrix spike sample, and a matrix spike duplicate sample, all processed with the samples. Recoveries of the surrogate compounds and the matrix spike compounds are reported in Tables D-4 and D-5. All of the recoveries of the surrogates and the matrix spike compounds are within the limits specified in Method 8270.

No target analytes were detected in samples #4 or #14. Tentatively identified nontarget analytes found in sample #4 include trace levels of hexadecanoic acid, a C_{20} hydrocarbon, and a C_{31} hydrocarbon. In sample #14, trace levels of a C_{30} hydrocarbon were present.

Trace levels of pentachlorophenol, phenanthrene, fluoranthene, pyrene, benzo(a)anthracene, benzofluoranthenes and benzo(a)pyrene were detected in sample #16. These compounds were present well below the practical quanitation limits of the method and thus are designated "trace." This sample also contained tentatively identified trace levels of 1,1,2,2-tetrachloroethane, hexadecanoic acid, a C_{20} hydrocarbon, and C_{28} and C_{29} hydrocarbons.

The target analytes found in Sample #16 are not naturally occurring compounds. For example, pentachlorophenol has been used to preserve telephone poles. Phenanthrene, anthracene, fluoranthene, pyrene, benzo(a)anthracene, benzofluoranthenes and benzo(a)pyrene are all PAHs. PAHs are prevalent in asphalt and roofing tars. These compounds are present at very low levels in this soil sample and we cannot draw any conclusions on how they came to be present in this sample.

Table D-1. Results for Sample #4

Compound	Amount	PQL, µg/kg
Phenol	ND	330
Bis(2-Chloroethyl)Ether	ND	330
2-Chlorophenol	ND	330
1,3-Dichlorobenzene	ND	330
1,4-Dichlorobenzene	ND	330
Benzyl Alcohol	ND	660
1,2-Dichlorobenzene	ND	330
2-Methylphenol	ND	330
Bis(2-Cl Isopropyl)Ether	ND	330
4-Methylphenol	ND	330
n-Nitroso-di-n-Propylamine	ND	330
Hexachloroethane	ND	330
Nitrobenzene	ND	330
Isophorone	ND	330
2-Nitrophenol	ND	330
2,4-Dimethylphenol	ND	330
Benzoic Acid	ND	1700
Bis(2-Cl Ethoxy)Methane	ND	330
2,4-Dichlorophenol	ND	330
1,2,4-Trichlorobenzene	ND	330
Naphthalene	ND	330
4-Chloroaniline	ND	660
Hexachlorobutadiene	ND	330
4-Chloro-3-methylphenol	ND	660
2-Methylnaphthalene	ND	330
Hexachlorocyclopentadiene	ND	330
2,4,6-Trichlorophenol	ND	330
2,4,5-Trichlorophenol	ND	330
2-Fluorobiphenyl	ND	330
2-Chloronaphthalene	ND	330
2-Nitroaniline	ND	1700
Dimethyl Phthalate	ND	330
2,6-Dinitrotoluene	ND	330
Acenaphthylene	ND	330
3-Nitroaniline	ND	1700
Acenaphthene	ND	330
2,4-Dinitrophenol	ND	1700

Table D-1. Results for Sample #4 (Continued)

Compound	Amount	PQL, µg/kg
4-Nitrophenol	ND	1700
Dibenzofuran	ND	330
2,4-Dinitrotoluene	ND	330
Diethylphthalate	ND	330
4-Chlorophenyl phenylether	ND	330
Fluorene	ND	330
4-Nitroaniline	ND	330
4,6-Dinitro-2-Methylphenol	ND	1700
n-Nitroso-di-phenylamine	ND	330
4-Bromophenyl Phenylether	ND	330
Hexachlorobenzene	ND	330
Pentachlorophenol	ND	1700
Phenanthrene	ND	330
Anthracene	ND	330
Di-n-Butylphthalate	ND	330
Fluoranthene	ND	330
Pyrene	ND	330
Butylbenzylphthalate	ND	330
Bis(2-Ethylhexyl)Phthalate	ND	330
3,3'-Dichlorobenzidine	ND	660
Benzo(a)Anthracene	ND	330
Chrysene	ND	330
Di-n-Octylphthalate	ND	330
Benzo Fluorathenes	ND	660
Benzo(a)Pyrene	ND	330
Indeno(1,2,3-cd)Pyrene	ND	330
Dibenzo(a,h)Anthracene	ND	330
Benzo(g,h,i)Perylene	ND	330

ND = not detected

Table D-2. Results for Sample #14

Compound	Amount	PQL, µg/kg
Phenol	ND	330
Bis(2-Chloroethyl)Ether	ND	330
2-Chlorophenol	ND	330
1,3-Dichlorobenzene	ND	330
1,4-Dichlorobenzene	ND	330
Benzyl Alcohol	ND	660
1,2-Dichlorobenzene	ND	330
2-Methylphenol	ND	330
Bis(2-Cl Isopropyl)Ether	ND	330
4-Methylphenol	ND	330
n-Nitroso-di-n-Propylamine	ND	330
Hexachloroethane	ND	330
Nitrobenzene	ND	330
Isophorone	ND	330
2-Nitrophenol	ND	330
2,4-Dimethylphenol	ND	330
Benzoic Acid	ND	1700
Bis(2-Cl Ethoxy)Methane	ND	330
2,4-Dichlorophenol	ND	330
1,2,4-Trichlorobenzene	ND	330
Naphthalene	ND	330
4-Chloroaniline	ND	660
Hexachlorobutadiene	ND	330
4-Chloro-3-methylphenol	ND	660
2-Methylnaphthalene	ND	330
Hexachlorocyclopentadiene	ND	330
2,4,6-Trichlorophenol	ND	330
2,4,5-Trichlorophenol	ND	330
2-Fluorobiphenyl	ND	330
2-Chloronaphthalene	ND	330
2-Nitroaniline	ND	1700
Dimethyl Phthalate	ND	330
2,6-Dinitrotoluene	ND	330
Acenaphthylene	ND	330
3-Nitroaniline	ND	1700
Acenaphthene	ND	330
2,4-Dinitrophenol	ND	1700

Table D-2. Results for Sample #14 (Continued)

Compound	Amount	PQL, µg/kg
4-Nitrophenol	ND	1700
Dibenzofuran	ND	330
2,4-Dinitrotoluene	ND	330
Diethylphthalate	ND	330
4-Chlorophenyl phenylether	ND	330
Fluorene	ND	330
4-Nitroaniline	ND	330
4,6-Dinitro-2-Methylphenol	ND	1700
n-Nitroso-di-phenylamine	ND	330
4-Bromophenyl Phenylether	ND	330
Hexachlorobenzene	ND	330
Pentachlorophenol	ND	1700
Phenanthrene	ND	330
Anthracene	ND	330
Di-n-Butylphthalate	ND	330
Fluoranthene	ND	330
Pyrene	ND	330
Butylbenzylphthalate	ND	330
Bis(2-Ethylhexyl)Phthalate	ND	330
3,3'-Dichlorobenzidine	ND	660
Benzo(a)Anthracene	ND	330
Chrysene	ND	330
Di-n-Octylphthalate	ND	330
Benzo Fluoranthenes	ND	660
Benzo(a)Pyrene	ND	330
Indeno(1,2,3-cd)Pyrene	ND	330
Dibenzo(a,h)Anthracene	ND	330
Benzo(g,h,i)Perylene	ND	330

Table D-3. Results for Sample #16

Compound	Amount	PQL, µg/kg
Phenol	ND	330
Bis(2-Chloroethyl)Ether	ND	330
2-Chlorophenol	ND	330
1,3-Dichlorobenzene	ND	330
1,4-Dichlorobenzene	ND	330
Benzyl Alcohol	ND	660
1,2-Dichlorobenzene	ND	330
2-Methylphenol	ND	330
Bis(2-Cl Isopropyl)Ether	ND	330
4-Methylphenol	ND	330
n-Nitroso-di-n-Propylamine	ND	330
Hexachloroethane	ND	330
Nitrobenzene	ND	330
Isophorone	ND	330
2-Nitrophenol	ND	330
2,4-Dimethylphenol	ND	330
Benzoic Acid	ND	1700
Bis(2-Cl Ethoxy)Methane	ND	330
2,4-Dichlorophenol	ND	330
1,2,4-Trichlorobenzene	ND	330
Naphthalene	ND	330
4-Chloroaniline	ND	660
Hexachlorobutadiene	ND	330
4-Chloro-3-methylphenol	ND	660
2-Methylnaphthalene	ND	330
Hexachlorocyclopentadiene	ND	330
2,4,6-Trichlorophenol	ND	330
2,4,5-Trichlorophenol	ND	330
2-Fluorobiphenyl	ND	330
2-Chloronaphthalene	ND	330
2-Nitroaniline	ND	1700
Dimethyl Phthalate	ND	330
2,6-Dinitrotoluene	ND	330
Acenaphthylene	ND	330
3-Nitroaniline	ND	1700
Acenaphthene	ND	330
2,4-Dinitrophenol	ND	1700

Table D-3. Results for Sample #16 (Continued)

Compound	Amount	PQL, µg/kg
4-Nitrophenol	ND	1700
Dibenzofuran	ND	330
2,4-Dinitrotoluene	ND	330
Diethylphthalate	ND	330
4-Chlorophenyl phenylether	ND	330
Fluorene	ND	330
4-Nitroaniline	ND	330
4,6-Dinitro-2-Methylphenol	ND	1700
n-Nitroso-di-phenylamine	ND	330
4-Bromophenyl Phenylether	ND	330
Hexachlorobenzene	ND	330
Pentachlorophenol	TR	1700
Phenanthrene	TR	330
Anthracene	ND	330
Di-n-Butylphthalate	ND	330
Fluoranthene	TR	330
Pyrene	TR	330
Butylbenzylphthalate	ND	330
Bis(2-Ethylhexyl)Phthalate	ND	330
3,3'-Dichlorobenzidine	ND	660
Benzo(a)Anthracene	TR	330
Chrysene	ND	330
Di-n-Octylphthalate	ND	330
Benzofluoranthenes	TR	660
Benzo(a)Pyrene	TR	330
Indeno(1,2,3-cd)Pyrene	ND	330
Dibenzo(a,h)Anthracene	ND	330
Benzo(g,h,i)Perylene	ND	330

ND = not detected

TR = trace, detected but below PQL

Table D-4. BNA Surrogate Recoveries

Percent Recovery	2FP	PHL	2CP	DCB	NBZ	FBP	TBP	TPH
Method Blank	83	84	82	80	84	85	97	71
Soil #14	64	67	64	62	61	64	77	58
Soil #14 Matrix Spike	72	73	72	70	69	68	85	62
Soil #14 Matrix Spike Duplicate	82	85	80	76	80	80	99	72
Soil #16	76	79	76	71	74	78	94	69
Soil #4	69	72	70	66	70	73	90	65

2FP - 2-Fluorophenol
PHL - Phenol-d_5
2CP - 2-Chlorophenol-d_4
DCB - 1.2-Dichlorobenzene-d_4
NBZ - Nitrobenzene-d_5
FBP - 2-Fluorobiphenyl
TBP - 2,46-Tribromophenol
TPH - Terphenyl-d_{14}

Table D-5. BNA Matrix Spike/Spike Duplicate Recoveries

Percent Recovery	PHL	2CP	DCB	NNP	TCB	CMP	ACN	4NP	DNT	PCP	PYR
Soil #14 Matrix Spike	51	50	63	66	62	50	69	64	64	41	69
Soil #14 Matrix Spike Duplicate	91	89	58	59	58	90	67	115	63	88	67

PHL - Phenol
2CP - 2-Chlorophenol
DCB - 1,4-Dichlorobenzene
NNP - N-nitroso-di-n-propylamine
TCB - 1.2.4-Trichlorobenzene
CMP - 4-Chloro-3-methylphenol
ACN - Acenaphthene
4NP - 4-Nitrophenol
DNT - 2,4-Dinitrotoluene
PCP - Pentachlorophenol
PYR - Pyrene

Headquarters
Gas Research Institute
8600 West Bryn Mawr Avenue
Chicago, Illinois 60631-3562
312/399-8100

Washington Operations
Gas Research Institute
1331 Pennsylvania Avenue, N.W.
Suite 730 North
Washington, D.C. 20004-1703
202/662-8989